

NOTICE

This document is disseminated under the sponsorship of the Department of Transportation in the interest of information exchange. The United States Government assumes no liability for its contents or use thereof. Any opinions, findings and conclusions, or recommendations expressed in this material do not necessarily reflect the views or policies of the United States Government, nor does mention of trade names, commercial products, or organizations imply endorsement by the United States Government. The United States Government assumes no liability for the content or use of the material contained in this document.

NOTICE

The United States Government does not endorse products or manufacturers. Trade or manufacturers' names appear herein solely because they are considered essential to the objective of this report.

REPORT DOCUMENTATION PAGE

Form Approved OMB No.
0704-0188

The public reporting burden for this collection of information is estimated to average 1 hour per response, including the time for reviewing instructions, searching existing data sources, gathering and maintaining the data needed, and completing and reviewing the collection of information. Send comments regarding this burden estimate or any other aspect of this collection of information, including suggestions for reducing the burden, to Department of Defense, Washington Headquarters Services, Directorate for Information Operations and Reports (0704-0188), 1215 Jefferson Davis Highway, Suite 1204, Arlington, VA 22202-4302. Respondents should be aware that notwithstanding any other provision of law, no person shall be subject to any penalty for failing to comply with a collection of information if it does not display a currently valid OMB control number. **PLEASE DO NOT RETURN YOUR FORM TO THE ABOVE ADDRESS.**

1. REPORT DATE (DD-MM-YYYY) September 2022	2. REPORT TYPE Technical Report	3. DATES COVERED (From - To) October 2019–April 2022
--	---	--

4. TITLE AND SUBTITLE Onboard Broken Rail Research and Development	5a. CONTRACT NUMBER DTFR5311D00008L
	5b. GRANT NUMBER
	5c. PROGRAM ELEMENT NUMBER

6. AUTHOR(S) David Khasenye: 0000-0003-3622-7664 Mohamad Khater: 0000-0002-1288-9906 Xu Li: 0000-0003-2777-2214 Alan Polivka: 0000-0002-6424-5846 Scott Gage: 0000-0002-8424-0479 Chase Askins: 0000-0003-2028-9473 Mathew Holcomb: 0000-0001-7799-2202	5d. PROJECT NUMBER
	5e. TASK NUMBER 693JJ619F000048
	5f. WORK UNIT NUMBER

7. PERFORMING ORGANIZATION NAME(S) AND ADDRESS(ES) Transportation Technology Center, Inc. 55500 DOT Road PO BOX 11130 Pueblo, CO 81001-0130	8. PERFORMING ORGANIZATION REPORT NUMBER
--	---

9. SPONSORING/MONITORING AGENCY NAME(S) AND ADDRESS(ES) U.S. Department of Transportation Federal Railroad Administration Office of Railroad Policy and Development Office of Research, Development, and Technology Washington, DC 20590	10. SPONSOR/MONITOR'S ACRONYM(S)
	11. SPONSOR/MONITOR'S REPORT NUMBER(S) DOT/FRA/ORD-22/35

12. DISTRIBUTION/AVAILABILITY STATEMENT
This document is available to the public through the FRA [website](#).

13. SUPPLEMENTARY NOTES
COR: Jared Withers

14. ABSTRACT
The Federal Railroad Administration (FRA) sponsored a project, performed by Transportation Technology Center, Inc. (TTCI), to research the feasibility of an Onboard Broken Rail Detection (OBRD) concept. A parallel long term track impedance characterization effort was undertaken with the objective of understanding and modelling the track as an electrical transmission line under varying environmental conditions. Between October 2019 and November 2021, TTCI carried out a series of laboratory and field experiments of the concept in two configurations over 6,000-foot and 12,000-foot sections of track.

15. SUBJECT TERMS
Alternative broken rail and rollout detection, ABRRD, full-moving block, FMB, Head-of-Train-Alternative Broken Rail and Rollout Detection, HOT-ABRRD, Onboard Broken Rail Detection, OBRD, Positive Train Control, PTC

16. SECURITY CLASSIFICATION OF:			17. LIMITATION OF ABSTRACT	18. NUMBER OF PAGES 158	19a. NAME OF RESPONSIBLE PERSON David Khasenye, Principal Investigator
a. REPORT Unclassified	b. ABSTRACT Unclassified	c. THIS PAGE Unclassified			19b. TELEPHONE NUMBER (Include area code) 719-585-1851

METRIC/ENGLISH CONVERSION FACTORS

ENGLISH TO METRIC

LENGTH (APPROXIMATE)

1 inch (in) = 2.5 centimeters (cm)
 1 foot (ft) = 30 centimeters (cm)
 1 yard (yd) = 0.9 meter (m)
 1 mile (mi) = 1.6 kilometers (km)

AREA (APPROXIMATE)

1 square inch (sq in, in²) = 6.5 square centimeters (cm²)
 1 square foot (sq ft, ft²) = 0.09 square meter (m²)
 1 square yard (sq yd, yd²) = 0.8 square meter (m²)
 1 square mile (sq mi, mi²) = 2.6 square kilometers (km²)
 1 acre = 0.4 hectare (he) = 4,000 square meters (m²)

MASS - WEIGHT (APPROXIMATE)

1 ounce (oz) = 28 grams (gm)
 1 pound (lb) = 0.45 kilogram (kg)
 1 short ton = 2,000 pounds (lb) = 0.9 tonne (t)

VOLUME (APPROXIMATE)

1 teaspoon (tsp) = 5 milliliters (ml)
 1 tablespoon (tbsp) = 15 milliliters (ml)
 1 fluid ounce (fl oz) = 30 milliliters (ml)
 1 cup (c) = 0.24 liter (l)
 1 pint (pt) = 0.47 liter (l)
 1 quart (qt) = 0.96 liter (l)
 1 gallon (gal) = 3.8 liters (l)
 1 cubic foot (cu ft, ft³) = 0.03 cubic meter (m³)
 1 cubic yard (cu yd, yd³) = 0.76 cubic meter (m³)

TEMPERATURE (EXACT)

$$[(x-32)(5/9)] \text{ } ^\circ\text{F} = y \text{ } ^\circ\text{C}$$

METRIC TO ENGLISH

LENGTH (APPROXIMATE)

1 millimeter (mm) = 0.04 inch (in)
 1 centimeter (cm) = 0.4 inch (in)
 1 meter (m) = 3.3 feet (ft)
 1 meter (m) = 1.1 yards (yd)
 1 kilometer (km) = 0.6 mile (mi)

AREA (APPROXIMATE)

1 square centimeter = 0.16 square inch (sq in, in²) (cm²)
 1 square meter (m²) = 1.2 square yards (sq yd, yd²)
 1 square kilometer (km²) = 0.4 square mile (sq mi, mi²)
 10,000 square meters = 1 hectare (ha) = 2.5 acres (m²)

MASS - WEIGHT (APPROXIMATE)

1 gram (gm) = 0.036 ounce (oz)
 1 kilogram (kg) = 2.2 pounds (lb)
 1 tonne (t) = 1,000 kilograms (kg)
 = 1.1 short tons

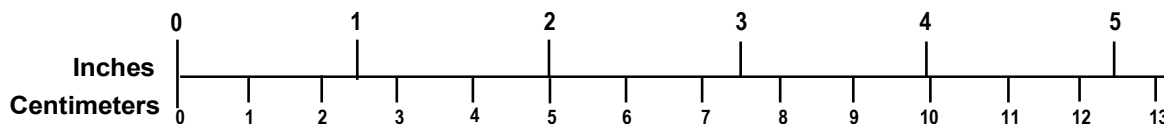
VOLUME (APPROXIMATE)

1 milliliter (ml) = 0.03 fluid ounce (fl oz)
 1 liter (l) = 2.1 pints (pt)
 1 liter (l) = 1.06 quarts (qt)
 1 liter (l) = 0.26 gallon (gal)
 1 cubic meter (m³) = 36 cubic feet (cu ft, ft³)
 1 cubic meter (m³) = 1.3 cubic yards (cu yd, yd³)

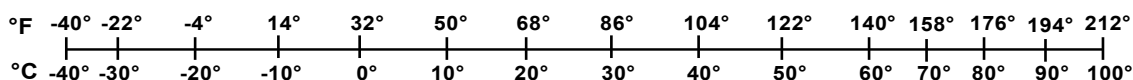
TEMPERATURE (EXACT)

$$[(9/5) y + 32] \text{ } ^\circ\text{C} = x \text{ } ^\circ\text{F}$$

QUICK INCH - CENTIMETER LENGTH CONVERSION



QUICK FAHRENHEIT - CELSIUS TEMPERATURE CONVERSION



For more exact and or other conversion factors, see NIST Miscellaneous Publication 286, Units of Weights and Measures. Price \$2.50 SD Catalog No. C13 10286

Updated 6/17/98

Acknowledgements

The authors would like to acknowledge the members of the Onboard Broken Rail Detection research and development Technical Advisory Group (TAG).

Contents

Executive Summary	1
1. Introduction.....	3
1.1 Background.....	3
1.2 Objectives	5
1.3 Overall Approach.....	5
1.4 Scope.....	7
1.5 Organization of the Report.....	7
2. Research Review.....	9
2.1 Background.....	9
2.2 Tx and Rx Coils	10
2.3 Track Impedance.....	13
2.4 Transmission Line Model	15
2.5 Summary.....	17
3. Track Impedance Characterization	18
3.1 Setup	18
3.2 Equipment.....	19
3.3 Data Collection	21
3.4 Approach.....	25
3.5 Results and Analysis.....	25
3.6 Conclusion	36
4. Evaluation of Tx and Rx Coils.....	38
4.1 Lab Testing	38
4.2 Field Testing – Static and Dynamic.....	53
5. Model Development.....	98
5.1 Track Impedance Model	98
5.2 Signal Propagation Model.....	101
5.3 Proposed System Model	102
5.4 Transfer Function Model	103
5.5 Summary.....	105
6. Preliminary Development and Migration Plan	107
6.1 OBRD Development Plan.....	107
6.2 Deployment Migration Plan.....	108

6.3	HOT OBRD Migration Plan	108
7.	Conclusion	110
8.	References.....	112
	Appendix A. Resonance Signal Generator Equipment Setup Instructions.....	113
	Appendix B. Tx Coil Specifications	117
	Appendix C. Rx Coil Specifications.....	119
	Appendix D. Supplementary Tx Coil Test Data.....	121
	Appendix E. Insulated Joints Measurements	124
	Appendix F. Measurement Equipment	127
	Appendix G. Characteristic Impedance Calculations from Sample Track Impedance Data.....	128
	Appendix H. Portable Cab Signal Tester.....	133

Illustrations

Figure 1. Illustration of the OBRD Concept.....	4
Figure 2. Project Work Breakdown Structure.....	6
Figure 3. Functional Representation of a Tx or Rx Coil.....	11
Figure 4. Functional Flow of OBRD System.....	12
Figure 5. Transmission Line	15
Figure 6. Transmission Line Distributed-Element Model	16
Figure 7. PTT Track Impedance Data Collection Zone.....	18
Figure 8. Weather Station and Trailer that Holds Desktop Node Equipment at Post P64 of the PTT	19
Figure 9. Track Impedance Data Collection and Measurement Setup	20
Figure 10. External Data Collection Hardware.....	21
Figure 11. Sample of Time Log File Raw Data.....	23
Figure 12. Sample of Sensor Log File Raw Data	23
Figure 13. Sample of LCR Meter Measurement File Raw Data.....	23
Figure 14. Sample of Part of a Weather Data File.....	24
Figure 15. Number of Data Points Recorded per Day by Each Measurement Source	24
Figure 16. Flow Diagram of Measured Track Impedance Data of Data Analysis Process	25
Figure 17. Weather and Rail Temperatures for All Data During 24 Hours of the Day.....	26
Figure 18. Weather and Rail Temperatures for a Sample of Summer Days.....	27
Figure 19. Weather and Rail Temperatures for a Sample of Winter Days.....	27
Figure 20. Weather and Rail Temperatures for a Sample of Fall Days.....	28
Figure 21. Track Impedance Variables (RLCG) vs. Frequency for 1 Day.....	29
Figure 22. Track Impedance Variables (RLCG) vs. Frequency for 9 Months	30
Figure 23. Track Resistance vs. Rail Temperature.....	31
Figure 24. Time Series for Rail Temperature, Ballast Moisture, RLCG and Open Circuit Impedance	32
Figure 25. Characteristic Impedance vs. Frequency.....	33
Figure 26. Time Series for Rail Temperature, Ballast Moisture, and Characteristic Impedance Magnitude, Phase Angle, Real and Imaginary Components	34
Figure 27. Estimated Input Impedance vs. Distances and for Different Frequencies.....	36
Figure 28. Diagram of Tx Coil and its Drivers.....	39
Figure 29. RNB Testing Setup.....	40

Figure 30. Resonance Signal Generation Equipment	41
Figure 31. Tx Coil Setup One	45
Figure 32. Tx Coil Setup Two	45
Figure 33. Track Impedance Model Used for Lab Testing.....	46
Figure 34. Lab Track Impedance Model Measurement Setup.....	46
Figure 35. Image Simulated Track Circuit	47
Figure 36. Gamma Voltage Measurements from 345–400 Hz.....	48
Figure 37. Gamma Current Measurements from 345–400 Hz	48
Figure 38. Omega Current Measurements from 345 Hz–400 Hz.....	49
Figure 39. Portable Cab Signal Tester-Rx Coils Setup.....	50
Figure 40. Signal Generator-Rx Coils Setup	50
Figure 41. Gaussmeter Testing Orientation.....	51
Figure 42. TTT Testing Zone.....	54
Figure 43. Track Resistance Measurement Setup.....	56
Figure 44. Tx Coil Setup for Static Testing.....	57
Figure 45. Test Setup for Static Testing	57
Figure 46. 6,000-foot Block Configuration for Static Testing.....	58
Figure 47. 12,000-foot Block Configuration for Static Testing.....	58
Figure 48. 18,000-foot Block Configuration for Static Testing.....	59
Figure 49. Comparison of Induced Currents at Far and Source Ends at Various Tx Coil Heights Above Rail and Distances from Far-End Shunt for Static Tests	62
Figure 50. Comparison of Induced Current at Far and Source Ends at 12,000 feet vs. Tx Coil Height at Different Frequencies.....	62
Figure 51. Comparison of Induced Current at 568 Hz to Distance from Source.....	63
Figure 52. Comparison of Induced Current at Far and Source Ends for Closed (Shunt) and Open (No Shunt) Track Circuit at Different Tx Coil Heights and Different Frequencies	64
Figure 53. Tx Coil Setups	66
Figure 54. Rx Coil Setup	67
Figure 55. Test Case 1 Setup with Rx Coil on Locomotive	67
Figure 56. Test Case 2 Setup with Rx Coil Located 30 feet from Locomotive.....	68
Figure 57. Rx Coil Setup	71
Figure 58. Case 1 Shielding Orientations	72
Figure 59. Detected Cross Talk RMS Voltage Across Rx Coil for Various Shields.....	73

Figure 60. Skin Effect Depth Variance with Frequency for Various Materials	74
Figure 61. Images of Shielded Tx and Rx Coils.....	75
Figure 62. Evolution of Tx Coil Shielding	75
Figure 63. Evolution of Rx Coil Shielding.....	76
Figure 64. Locomotive, Tx and Rx Coil Configurations for Dynamic Test Cases 4, 5, 6, 7, 8, and 9.....	78
Figure 65. TTT Section and Track Connection Diagram for 12,000-foot Block Tests.....	81
Figure 66. Test Track Section and Track Connection Diagram for 6,000-foot Block Tests.....	82
Figure 67. Illustration of Tx Coil Setup When Attached to Locomotive	83
Figure 68. Electrical and Measurement Configuration of Tx and Rx Coil for Configuration A.....	83
Figure 69. Rx Coil Configurations and Setup.....	84
Figure 70. Shunt Current at T33.5 for Dynamic Test Cases 4 and 5 vs. Locomotive Location...	86
Figure 71. Rx Coil Signal Amplitude for Dynamic Test Cases 4 and 5 vs. Locomotive Location	87
Figure 72. Shunt Current at T33.5 for Dynamic Test Case 6 vs. Locomotive Location	88
Figure 73. Rx Coil Amplitude for Dynamic Test Case 6 vs. Locomotive Location	88
Figure 74. Shunt Current at T39.5 for Combined Dynamic Test Cases 7, 8, and 9 vs. Locomotive Location	89
Figure 75. Rx Coil Amplitude for Combined Dynamic Test Cases 7, 8, and 9 vs. Locomotive Location	90
Figure 76. Phase Difference Between Tx and Rx Coils for Combined Dynamic Test Cases 7, 8, and 9 vs. Locomotive Location.....	90
Figure 77. Dynamic Test Cases 11 Showing Effects of Wet Ballast on Induced Signal vs. Locomotive Location	91
Figure 78. Dynamic Test Cases 11 and 5 Comparison Showing Effects of Wet Ballast on Induced Signal vs. Locomotive Location	91
Figure 79. Dynamic Test Case 12: Phase Difference Between Signal Generator and Tx Coil vs. Locomotive Location	92
Figure 80. Dynamic Test Cases 7, 8, and 9 Tx and Rx Overlay vs. Locomotive Location from T27–T40.....	93
Figure 81. Dynamic Test Cases 7, 8, and 9 Tx and Rx Overlay vs. Locomotive Location from T27–T33.5.....	94
Figure 82. Dynamic Test Case 6 Tx and Rx Overlay vs. Locomotive Location.....	95
Figure 83. Sample Closed Loop Track Input Impedances at Different Frequencies and Distance to a Shunt	99
Figure 84. Sample Open Loop Track Input Impedances at Different Frequencies	100

Figure 85. Functional Block Diagram of System Model.....	102
Figure 86. Development Phases of the OBRD Concept.....	107
Figure 87. HOT-ABRRD Migration path.....	109

Tables

Table 1. Relationships Between Input Signal Frequency and Track Impedance Variables	35
Table 2. Relationships Between Track Condition and Track Impedance Variables	35
Table 3. RNB Vendor Defined Jumper Settings.....	39
Table 4. Induced Signal Measurement with One Amplifier	42
Table 5. Induced Signal Measurements with Two Amplifiers	43
Table 6. Updated RNB Resonant Frequency Jumper Settings	43
Table 7. Gaussmeter Measurements	52
Table 8. Rx Coil Readings at 0 Inch from Test Loop.....	52
Table 9. Rx Coil Current Measurements at 8 Inches from the Test Loop	53
Table 10. Resistances of Three Test Track Blocks.....	60
Table 11. Summary of Executed Tests	61
Table 12. Static Test Measurements with Tx Coil at Various Heights from Rail and Distances from Far End Shunt.....	61
Table 13. Shunt at 30 feet from Tx Coil Under Test Setup 1	68
Table 14. Shunt at 6,000 feet from Tx Coil Under Test Setup 1	68
Table 15. Tx Coil Strap Mounted with Rx Coil at Various Distances from Tx Coil	69
Table 16. Maximum RNB Voltage with Tx Strap Mount Configuration.....	69
Table 17. Detected Crosstalk Voltage at Rx Coil for Various Shields.....	72
Table 18. Summary of Pre-Dynamic Test Results.....	77
Table 19. Other Devices, Equipment, and Tools	80
Table 20. List of Test Dynamic Testing Test Cases	84
Table 21. List of Conducted Dynamic Test Cases.....	85
Table 22. Summary of Proposed Models.....	105

Executive Summary

From October 2019 to May 2022, the Federal Railroad Association (FRA) sponsored Transportation Technology Center, Inc. in investigating a concept for an Onboard Broken Rail Detection (OBRD) system capable of detecting the presence of broken rails and occupancies (or lack thereof) in advance of a moving train through a series of lab and field tests at the Transportation Technology Center (TTC) in Pueblo, CO. The investigation concluded that the OBRD concept is practicable, but also noted that certain issues, such as improved receiver sensitivity and an extended detection range, are yet to be resolved. The primary application for the OBRD concept is the support of Full Moving Block (FMB) train control because the predominant broken rail and occupancy detection method (conventional track circuits) does not support the headway and capacity improvements attainable with FMB. The OBRD system analyzed and tested during this project also has the potential to reduce the life cycle cost of broken rail and occupancy detection since the system does not require any active wayside equipment and does not require insulated joints (IJs).

In the OBRD concept, alternating current (AC) electrical signals generated on board a locomotive are sent and received through the track via electromagnetic induction. This process allows a current to flow through a circuit comprised of the two running rails, the ballast, the wheels and axles of the train, and a series of passive, tuned shunts placed along the track. Electromagnetic coils attached to the locomotive just above the rail induce and pick up the signals from the rail. This method 1) provides a clear track indication from the train to the location of the tuned shunt associated with each received frequency and 2) detects occupancies and distinguishes them from rail breaks.

The detection range of such a system should be great enough to allow the train to come to a complete stop before it arrives at the location of the broken rail. To advance the understanding of the OBRD concept, two parallel research efforts, one on track impedance characterization and another on testing the feasibility of the concept, were undertaken. Key challenges identified from previous research included (Transportation Technology Center, Inc., 2013):

- A strong mutual inductance between the transmit (Tx) and receive (Rx) coils
- A weak mutual inductance between the rail and the induction coils
- The track impedance variability

During the investigation and analysis of these issues, significant progress was made regarding the ability of the system to induce a signal with a usable range. The transmission-coil-generated signal had a consistent detectable range of at least 12,000 feet. Under the conditions established, test results indicated that an induced signal of higher magnitude could achieve a range beyond 18,000 feet. The detectable range is a function of a combination of 1) the ability of the transmission (Tx) coil to induce a large enough signal, 2) the track impedance variability, and 3) the ability of the receiving coil to detect enough of the signal from the rail to discern the state of the track in advance of the locomotive. Variable track impedance data was collected, together with the testing of a receiver (Rx) coil, were used to help quantify the feasibility.

It took approximately 9 months to collect track impedance data. The following data were collected from a 650-foot section of track:

- Ambient weather
- Rail temperature
- Ballast temperature and moisture
- Resistance (R)
- Capacitance (C)
- Inductance (L)
- Conductance (G)
- Open loop impedance
- Closed loop impedance

This report details the following: 1) the processes used to collect and analyze the track impedance data and 2) the parallel lab and static testing of the transmit and receive coils that culminated in the dynamic testing of the OBRD concept in two configurations. The dynamic testing analysis indicates that non-trivial issues, such as improved receiver sensitivity and a more extended range to accommodate longer braking distances of heavy trains or trains going down a grade, need to be addressed to move the concept up the Technology Readiness Level (TRL) scale. The test results suggest that, as conceived, the OBRD concept is practicable.

1. Introduction

From October 2019 to May 2022, the Federal Railroad Association (FRA) sponsored Transportation Technology Center, Inc. in investigating a concept for an Onboard Broken Rail Detection (OBRD) system capable of detecting the presence of broken rails and occupancies (or lack thereof) in advance of a moving train through a series of lab and field tests at the Transportation Technology Center (TTC) in Pueblo, CO.

Continued interest in improved methods of train control drives a need to develop alternative methods of broken rail detection from conventional track circuit technology. Advancements in moving block and other train control methods can significantly increase traffic capacity while maintaining safe following train distances. However, a new broken rail detection method is needed to achieve Full Moving Block (FMB) capacity because conventional methods of train control use fixed block track circuits that impose excess train spacing.

There are potential advantages to onboard methods of detecting rail breaks as compared with wayside-based methods, particularly in terms of eliminating the need for extensive active track circuit hardware that is expensive to install, power, and maintain along with eliminating insulated joints (IJs). A suitable onboard approach is not yet available for use with FMB train control. This OBRD research and development (R&D) project aims to advance the knowledge and understanding of how such a system would function.

1.1 Background

From approximately 2008 to 2015, the team researched a concept for an OBRD system that sends and receives alternate current (AC) electrical signals generated on board a locomotive through the track via electromagnetic induction (Transportation Technology Center, Inc., 2013). In this system, a current flows through a circuit comprised of the two running rails, the ballast, the wheels and axles of the train, and a series of passive tuned shunts placed along the track. Electromagnetic coils attached to the locomotive just above the rail induce and pick up the signals from the rail. This method 1) provides an indication of clear track from the train to the location of the tuned shunt associated with each frequency received, and 2) detects occupancies and distinguishes them from rail breaks. The method is similar to cab signaling except that one onboard coil induces the signal while the other coil acts as a receiver. [Figure 1](#) shows an illustration of the OBRD system and concept.

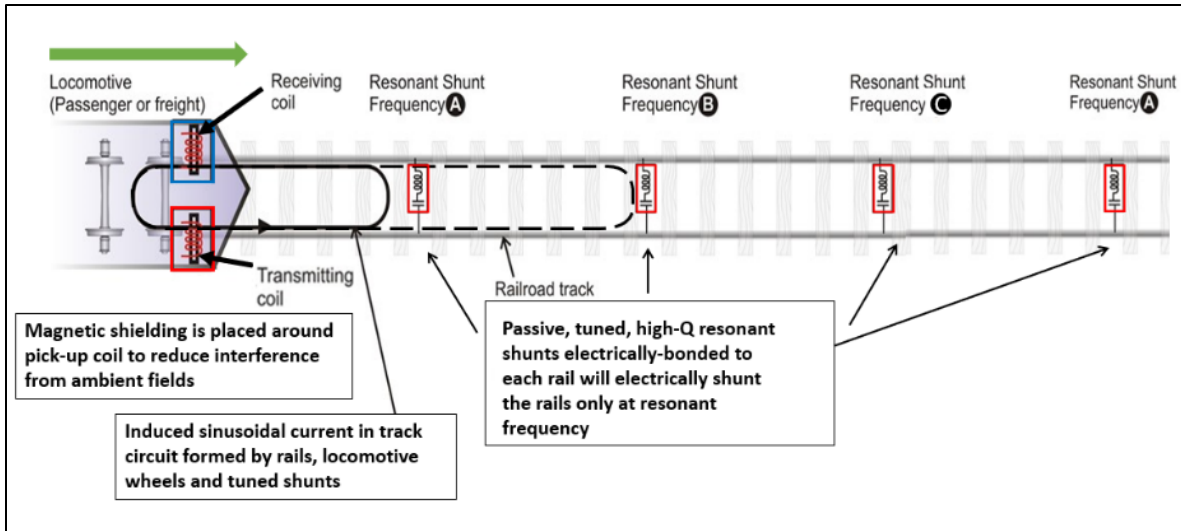


Figure 1. Illustration of the OBRD Concept

This system, as shown in Figure 1, functions as follows:

1. The transmit (Tx) coil transmits at Frequency A, onto Frequency B, then Frequency C and Frequency D (D is not used in any shunt), and keeps repeating this cycle.
2. The OBRD determines how far ahead track is clear based on which signal frequencies it receives.
3. If one or more signals is not received, then the OBRD system will assume that there is a rail break between the locomotive and the nearest shunt of that frequency ahead of the train.
4. If all frequencies are detected at the receive (Rx) coil (including D), then the OBRD system will determine that there is an occupancy ahead.
5. The locations of the shunts and their expected tuned frequencies will be stored in an onboard track database, so that the OBRD system will be able to determine which shunts and associated frequencies to expect.

This concept's ability to induce a signal in the rail and detect it was proven early on with static demonstrations using electromagnetic coils mounted above the track. Subsequently, patents were filed and granted by the United States Patent and Trademark Office (USPTO).¹

Follow-on research was conducted to further the development of the concept. This research identified three fundamental challenges:

1. Strong mutual inductance between the transmit and receive coils: Due to the proximity of the transmit and receive coils on the locomotive (both placed in front of the first axle), some of the strong magnetic field generated by the transmit coil passes through the

¹ See US Patent 9,162,691 for a more detailed description of the concept.

receive coil and induces a current in the receive coil that can mask the desired signal received through the rail.

2. Weak mutual inductance between the rail and the induction coils: To be useful for broken rail detection applications, the current induced by the system on board the locomotive must be strong enough to flow through the desired length of track and be reliably detected by the receive coil, requiring a strong magnetic field to be generated by the system.
3. Track impedance variability: Track impedance is heavily influenced by track infrastructure and ambient conditions, both of which significantly affect the system's ability to function, as revealed in previous experimentation. Track infrastructure and ambient conditions can vary significantly with time, location, and type of construction, so the system must be able to operate over a wide range of resulting track impedances.

These fundamental challenges need to be addressed to advance the concept. In addition, it is possible that variant or alternative solutions exist for an OBRD system that could bypass these challenges. These alternatives need to be explored.

The focus of the work primarily regards the use of OBRD at the front of a train to protect the train from rail breaks or occupancies on the track ahead of it. However, the OBRD concept can also be applied at the rear of a train to protect a following train, in which case, the detection range does not need to be nearly as long as the range for a front-of-train based OBRD implementation.

1.2 Objectives

This research focused on the results from tests in the reduction of the scientific uncertainty of the OBRD concept, and the development of a transmission line track model to further the development and design of a functional OBRD system.

1.3 Overall Approach

[Figure 2](#) shows the project work breakdown structure.

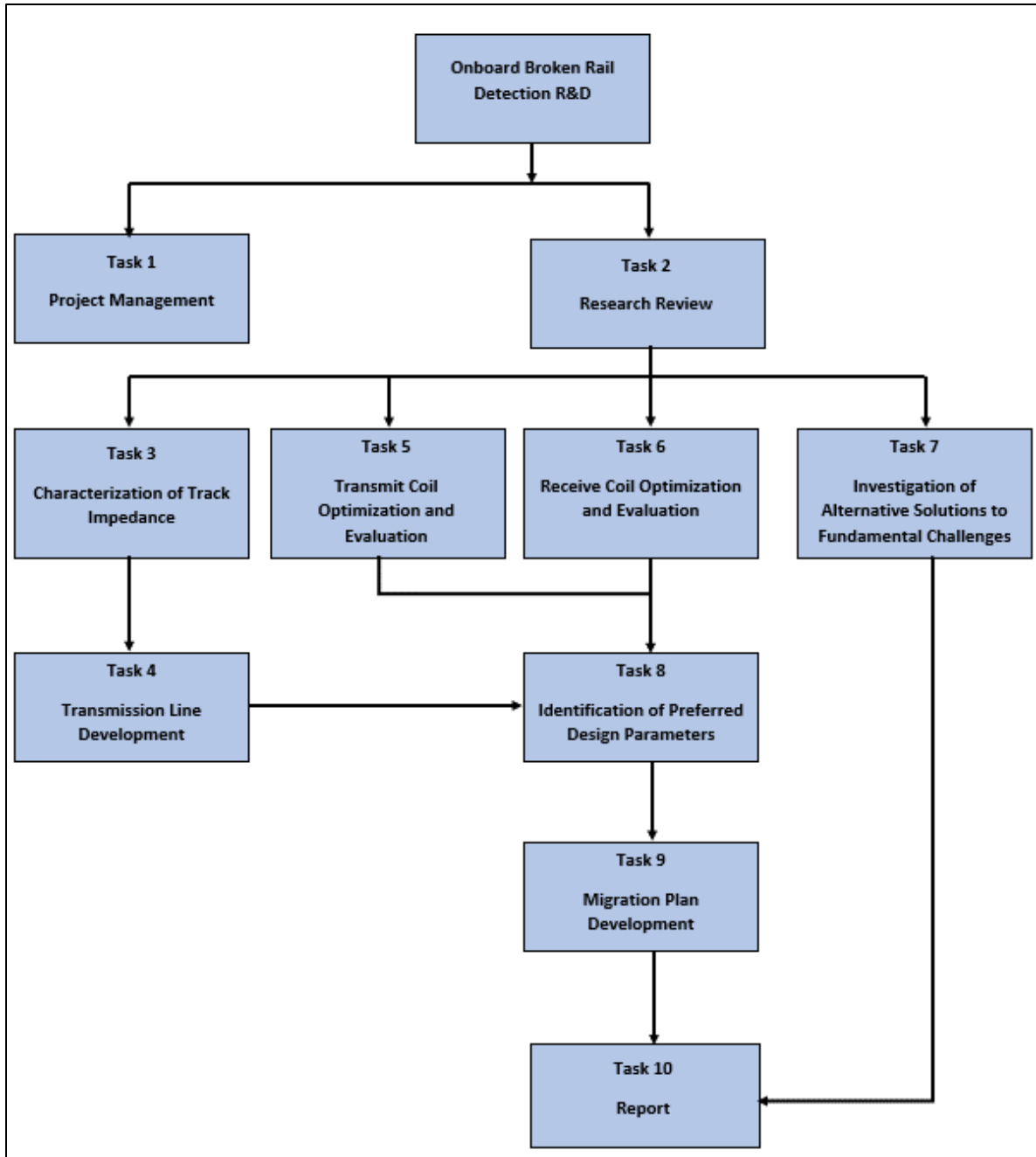


Figure 2. Project Work Breakdown Structure

The team performed a thorough review of previous research on this topic. This review was followed by the parallel track impedance characterization task that was then used, in part, to develop a transmission line model of the track. The Tx and Rx coil optimization and evaluation were done concurrently with the track impedance data collection. Potential alternate solutions to fundamental challenges, particularly the “crosstalk” issue between the Tx and Rx coils, were also investigated.

After track impedance was characterized, the findings were incorporated into the development of a transmission line model of the track. Once a working concept was developed and dynamically

tested, work was performed to identify preferred design parameters that would optimize and deconflict a system of this nature in the current field test environment.

The project was executed using an iterative approach, starting with lab testing and culminating with dynamic field testing of the Tx and Rx coils on the same locomotive. The findings from previous testing were considered in developing the subsequent tests. The laboratory and field tests followed the sequence listed below:

- Evaluation of Tx and Rx Coils
 - Lab Testing
 - Resonant Network Box (RNB) Testing
 - Tx Coil Testing
 - Rx Coil Testing
 - Field Testing
 - Static Tx Coil
 - Static Tx and Rx Coil on Locomotive
 - Shielding Testing
 - Shielding Testing II
 - Dynamic Testing

1.4 Scope

This research is a continuation of prior OBRD-related internal R&D. The objective of the current project is to advance a viable working concept for an OBRD system through the major tasks outlined in [Section 1.3](#). The project scope involved developing the OBRD system concept with a focus on the following:

- Showing 1) that an induced signal can be propagated for a distance commensurate with the train stopping distance under various track conditions, and 2) that the differences in the received signal can be detected (i.e., clear track versus broken rail versus occupancy)
- Addressing known key challenges
- Developing models that can be used to refine the design

1.5 Organization of the Report

The report is organized into eight major sections:

- [Section 1](#) introduces the importance of the work performed and provides a brief background of the OBRD R&D project.
- [Section 2](#) provides an overview of the research review task.
- [Section 3](#) includes the overview, analysis, and outcomes of the track impedance characterization task.
- [Section 4](#) consists of the overview, analysis, and outcomes of the coil evaluation task.

- [Section 5](#) presents the overview, analysis, and outcomes of the model development task.
- [Section 6](#) provides the overview, analysis, and outcomes of the migration implementation task.
- [Section 7](#) includes the project summary, recommendations, and conclusions.
- [Appendix A](#) gives RNB and Tx coil signal generation setup instructions.
- [Appendix B](#) consists of Tx coil specifications.
- [Appendix C](#) provides Rx coil specifications.
- [Appendix D](#) offers supplementary Tx coil testing data.
- [Appendix E](#) contains insulated joint measurements.
- [Appendix F](#) gives information on the measurement equipment used.
- [Appendix H](#) contains information on the portable cab signal tester.

2. Research Review

The team performed extensive research on OBRD concepts and track impedance prior to this project (Transportation Technology Center, Inc., 2013). In 2014, a preliminary data collection and modeling effort was conducted to quantify the potential impact of track impedance and the variability of track impedance on the proposed OBRD system (Transportation Technology Center, Inc., 2013). The result of earlier efforts provided insight into the factors that affect track impedance, including precipitation, relative humidity, track/ballast structure, and soil conditions. In addition, research was carried out on the Tx and Rx coils. The review of the Tx and Rx coils focused on understanding the fundamental laws of electromagnetics and their application to the OBRD concept.

2.1 Background

A railroad track has similar physical characteristics to a power transmission line and can be characterized and modeled as a transmission line as they are defined by their characteristic impedance, represented as Z_0 . The characteristic impedance is a complex value with a real and imaginary part. This complex value requires magnitude and phase to fully define the transmission line impedance.

A track impedance measurement system (TIMS) was developed to measure impedance on tracks at the TTC. The TIMS was characterized with both resistive and reactive loads, and the results were compared to a Simulation Program with Integrated Circuit Emphasis (SPICE) model. Important insights, highlighted later in this section, were gained from the TIMS data collected.

A series of track impedance measurements were taken in varying weather conditions on two different tracks, the Railroad Test Track (RTT) and the Precision Test Track (PTT), with different characteristics. Three tests were conducted on each track:

- Ballast resistance (track conductance)–Conductance (G) in the transmission line model (direct current [DC] measurement)
- Track Resistance–Resistance (R) in the transmission line model (DC measurement)
- Track Impedance–Magnitude of Impedance (Z) (AC measurement)

The test results revealed that precipitation heavily influences track impedance, which, in turn, has a dramatic effect on the ballast resistance (track conductance). The correlation between track impedance and relative humidity was also apparent (Transportation Technology Center, Inc., 2013). A comparison between the RTT and PTT results indicates the physical characteristics of the track (e.g., tie material, tie fasteners, soil condition, and ballast depth) can also significantly affect the ballast resistance (track conductance) and, as a result, the track impedance.

The track impedance results from the RTT tests were used to develop a SPICE model to characterize the track as a transmission line. The model results suggested that the OBRD system will be impacted less by track impedance and ambient conditions at frequencies at or below 500 Hz.

In addition to the RTT tests, a long-term track impedance measurement effort was conducted on a track block approximately 1,740 feet long (PTT). The data from these tests were analyzed for trends during different seasons. This analysis confirmed the relationship between the following:

- Track impedance and precipitation
- The recovery of track impedance after a precipitation period and the soil condition
 - Saturated soil recovered more slowly than dry soil
 - Frozen ground recovered even more slowly

These results 1) provide important insights and general trends between track impedance, frequency, and weather conditions, and 2) refined the test conditions for the prototype electromagnet and determined its viability in the OBRD system concept. However, the analysis was limited because the TIMS did not measure phase. It was recommended that should the OBRD system prove viable, a more detailed track impedance analysis should be conducted, to include the R, L, C, G, Z, and phase measurements over a more extended time period and in a wider variety of track conditions. This analysis will require additional instrumentation and a far more detailed effort to move the prototype system to a full production system. The above recommendations were considered in implementing the TIMS effort for this project. A full description of this effort is found in [Section 3](#).

The Tx and Rx coils focused on 1) understanding how the Tx and Rx coils function and 2) applying the laws and theories of electromagnetism (Maxwell's equations, Lenz law, Faradays law and Biot-Savart law (Dorf, R. C., 2000)) to the OBRD concept. In addition, the transmit coil design specifications were reviewed to better understand how the coil functions. The results of the review can be found in [Appendix B](#). The same approach was taken with the research review of the Rx coil, the results of which can be found in [Appendix C](#).

2.2 Tx and Rx Coils

The Tx coil is a core component of the OBRD concept. The development of this concept is anchored in the source patent (US Patent 9,162,691). The system relies on an electromotive force (emf) signal induced by the transmit coil. Electrical loops were terminated by the tuned shunts segment the track and provided paths for the signal to return to the locomotive, where a Rx coil picks it up and passes it on to a signal processor for conditioning and analysis before passing it on to the train control system for use in determining the state of the track up to each tuned shunt (up to the braking/warning distance at a minimum) in advance of the locomotive. The states of concern are clear track, broken rail, and track occupancy in advance of the train.

The primary function of the transmit coil for the OBRD is to induce a sufficient signal that can propagate at least 2 miles down the track and be detectable by a Rx coil. Because there are many possible ways to implement the sinusoid signal generators required for OBRD, this research focuses on the magnitude of the generated emf, a function of the magnetic field generated by the Tx coil and the distance of the magnetic field from the rail.

To induce a signal in the rail, the Tx coil used in this research applies fundamental laws of electromagnetic theory (Maxwell's equations, Faraday's law of electromagnetic induction and Lenz's law (Dorf, R. C., 2000)). These laws explain the relationship between a time-varying magnetic flux and the induction of an emf in a nearby conductor. The time-varying magnetic flux can happen as a result of the following:

- A changing magnetic field within a stationary circuit
- A circuit moving through a steady magnetic field

- A combination of the above

The following equation gives the induced emf a time-varying magnetic flux.

$$emf = - \frac{d\Phi}{dt} \text{ Volts} \quad (1)$$

Where:

ϕ = magnetic flux

t = time in seconds

d ϕ = change in magnetic flux

dt = change in time

Figure 3 shows a functional representation of a Tx and Rx coil. The Tx coil used for this research is one of many alternative approaches that can be used to induce a significant emf in the rail. Specifications for the Tx coil used can be found in [Appendix B](#).

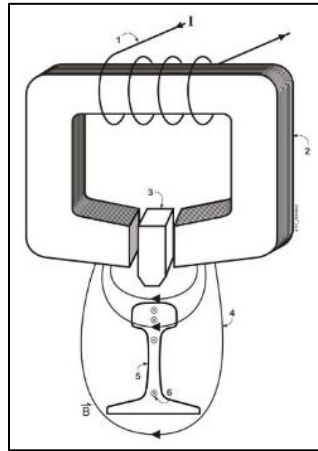


Figure 3. Functional Representation of a Tx or Rx Coil

The Rx coil takes advantage of the converse effect, i.e., it is used to detect the magnetic field generated by the induced current in the rail, that induces a voltage signal across the Rx coil. The following equation gives the magnetic field strength due to a current-carrying wire/rail at distance r .

$$H = B = \phi \mu \frac{I}{2\pi r} \quad (2)$$

Where:

H = magnetic field strength (A/m)

B = magnetic flux density (Wb/m²)

ϕ = unit vector in the positive ϕ direction in cylindrical coordinates

I = current in the wire/cable (A)

μ = permeability of the medium (H/m)

The detected magnetic field induces a voltage across the coil that is represented as an electric circuit with N turn, which transforms the equation to,

$$emf = - N \frac{d\Phi}{dt} \text{ Volts} \quad (3)$$

Where:

N = number of turns in the detection coil

ϕ = magnetic flux

t = time in seconds

d Φ = change in magnetic flux

dt = change in time

The voltage signal is passed on to the locomotive control system, as shown in Figure 4, for further processing and actions by the train control system. The control system processes the signal to infer a broken rail or occupancy by detecting a spectrum, amplitude, phase change, or other sinusoidal signal feature.

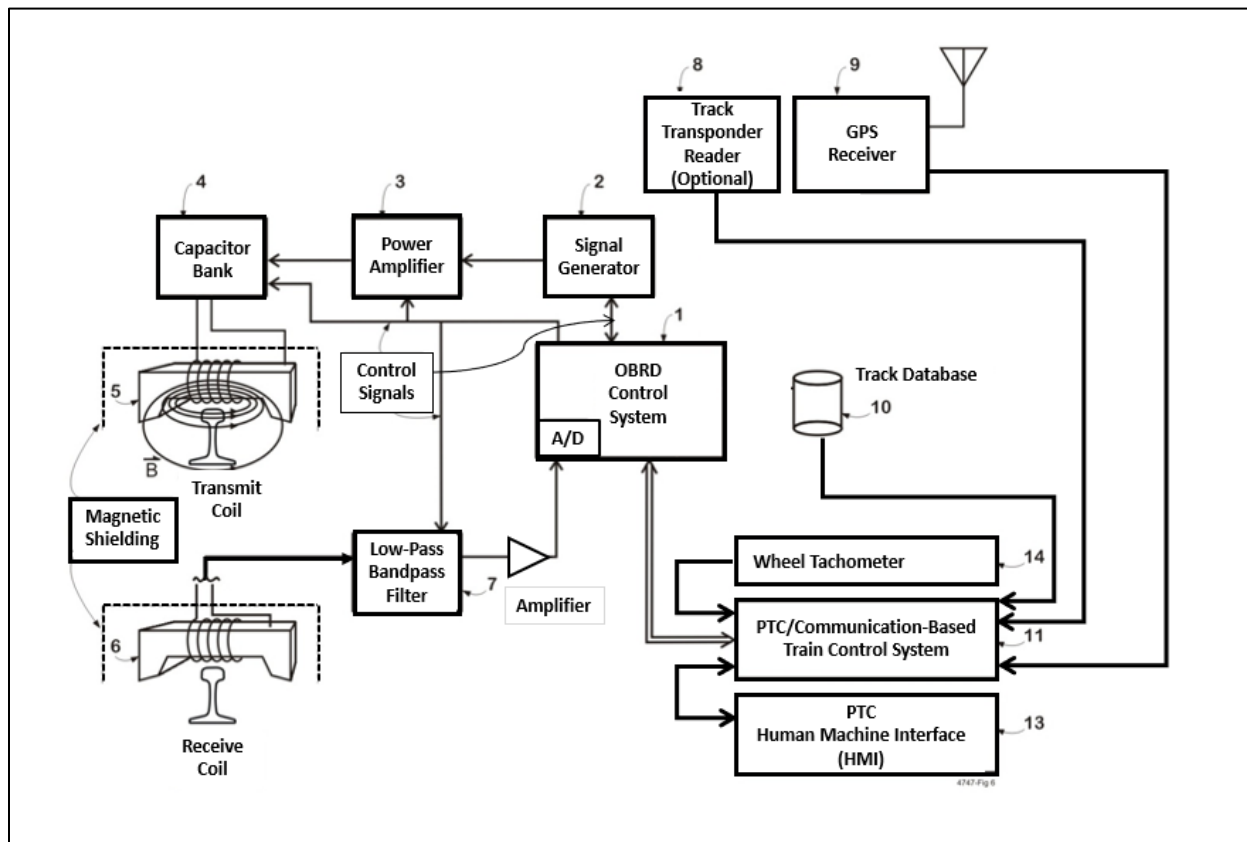


Figure 4. Functional Flow of OBRD System

The focus of this research was to answer the fundamental questions of whether a sufficiently useful signal can be induced/detected and how far the signal can propagate. Based on this focus, it was not necessary to include tuned shunts in the testing. These shunts will be incorporated in future research and testing when it becomes necessary to distinguish which shunt is closing the

circuit ahead of a train. To provide a shunt at all test frequencies, all shunts used for testing were wires or cables.

The generated signals at the Tx coil and received signals at the Rx coil are intermediated by the characteristic track impedance, affecting the quality and propagation of a signal through the (tuned) shunt loops.

2.3 Track Impedance

Conventional railroad signaling track circuits are normally constructed using a length (“block”) of railroad track that has been electrically isolated from the rest of the railroad by two pairs of IJs, with one pair of IJs installed at each end of the track circuit (i.e., one IJ per rail at each end of the track circuit). A pulsed DC or AC voltage is then applied through a track resistor to limit the current to the two rails at one end of the track circuit (the transmitter), and this signal is detected at the opposite end (the receiver) when there is no occupancy or rail break within the block. The rails of the track serve to complete the circuit between the transmitter and receiver.

A break that occurs in either rail or the conductive axles of a train being present within the boundaries of the track circuit, thereby shunting the rails to prevent the transmitted signal from reaching the receiver. This method allows conventional track circuits to detect broken rails and the presence of trains within their boundaries.

If railroad rails were perfectly insulated from the earth with no trains present, the entire current from the transmitter at one end of the track circuit would pass through the receiver at the opposite end. However, any conductive substances within or underneath the track will typically cause a portion of the track circuit’s transmitted current to flow directly from one rail to the other without reaching or passing through the receiver at the opposite end of the track circuit.

This unwanted form of conduction normally occurs when otherwise dry ionic solids beneath the rails, such as naturally occurring minerals, road salts (particularly at grade crossings in colder climates), spilled lading, and other soil contaminants are dissolved (partially or completely) by moisture from environmental sources to form conductive electrolytes. The presence of these electrolytes, both on and within railroad ties, ballast rock, soils, and other subgrade materials, increases the electrical conductivity between the rails of the track circuit.

The various leakage paths that divert the current away from a track circuit’s receiver are collectively referred to as “ballast resistance.” Unwanted “leakage” conduction between the rails of a railroad track also occur via other paths and processes, including gauge plates, gauge rods, ties, tie pads, spikes, screws, and other track hardware, especially when the insulation built into these devices becomes degraded. In properly maintained track, the rail-to-rail conduction through these “leakage” paths is minimal, and conduction through the ballast itself is the dominant factor that diverts or “shunts” some of the track circuit’s transmitted current away from its receiver.

Generally of a much lower magnitude, the “shunting” of a track circuit’s transmitted current through ballast resistance is similar in effect to the shunting action of a train’s axles. However, in severe cases of low resistance ballast, the excessively low-resistance ballast may shunt enough current away from the track circuit’s receiver to cause the track circuits to fail either intermittently or continuously.

The adverse effects of low track ballast resistance are not limited to conventional track circuits where electrical signals are transmitted from one end of a track circuit and received at the other end. Motion sensors and constant warning time crossing signal equipment can also be adversely affected, even though track circuit transmitters and receivers are located at the same end of their approach track circuits. Very low ballast resistance can prevent these types of crossing signal equipment from properly seeing a change in the electrical impedance of the track when a train enters the far end of an approach to a railroad grade crossing, resulting in shortened warning times at the grade crossing.

As the track circuit created by the OBRD system is electrically similar in many ways to those used by motion sensors and constant warning time crossing signal equipment, it is currently presumed that the OBRD system will be similarly affected by low track ballast resistance. Therefore, the research team's track electrical impedance model will need to be validated over a wide range of ballast resistance conditions.

Most railroad tracks experience a range of ballast resistance conditions that varies based on the amount of water present in the ballast. Short of sprinkling the track with copious amounts of water from a wayside water truck or an on-rail tank car, the amount of water in the ballast and subgrade materials of a railroad track at any given time is otherwise difficult to control.

The Pueblo, CO, area receives an average of approximately 12 inches of precipitation in a typical year, which is much less than many areas of North America that have railroad lines (National Weather Service Weather Forecast Office, 2021). Some of Pueblo's precipitation is also delivered in the form of snow that may sublime into the atmosphere without ever melting into the ballast and subgrade. During some of the colder parts of the year, some of the moisture present in the ties, ballast, and superficially subgrade materials of the test tracks at the TTC facility exist in the form of ice, which is largely non-conducting. All these factors are expected to combine to create a relatively low availability of liquid water in and around the test tracks at the TTC, meaning the average ballast resistance conditions at the TTC should be expected to be relatively high.

Fortunately, the expected high ballast resistance of the track at the TTC should be favorable in this instance because it is easier to lower the electrical ballast resistance of the test track artificially than to raise it artificially. Lowering the electrical ballast resistance of a railroad track circuit can be done by adding several non-inductive resistors connected across the test track at regular intervals along its length.

Adding resistors connected from rail to rail within a track circuit to simulate the effects of reduced ballast resistance works well for most types of track circuit testing. However, the polarization and "track storage effects" afflicting DC track circuits are notable exceptions. Given a sufficient electrolyte concentration and composition and enough moisture, the metal rails of a track circuit can serve as "plates," and these de facto battery components can combine to form a crude electrolytic cell (track battery). This "track battery" can generate, accept, and deliver electrical energy, which can adversely affect DC track circuits, and, to a lesser degree, pulsed DC track circuits. In extreme cases, this "track battery" may even be capable of providing enough energy to keep the track relay (i.e., the "receiver") of a simple DC track circuit energized without the transmitting source at the other end of the circuit being connected.

In addition to the above, there are polarization effects caused by the presence of these same electrolytic solutions in the ballast and subgrade materials that can interfere with the proper

measurement of ballast resistance. Such polarization effects are most noticeable when the rails are energized with DC, as in basic DC track circuits. However, polarization effects are greatly diminished when using either pulsed track circuits with pulses of alternating polarity or track circuits with AC of adequately high frequency (i.e., several Hz or higher).

As the proposed OBRD system does not use DC currents, unipolar low-frequency DC pulses or extremely low-frequency AC currents, polarization and track storage effects are not significantly affected. Consequently, the measurements of track impedance characteristics were made using AC frequencies across the full spectrum of possible frequencies used by the OBRD system.

2.4 Transmission Line Model

Track impedance characterization aims to understand the characteristics of a track modeled as a lossy electrical transmission line under varying environmental conditions. The derived track characteristic impedance would then support future system design and feasibility analysis of the proposed system which requires an AC signal to propagate for relatively long distances of approximately 2 miles or more. Signal leakage through the ties, ballast, and ground can reduce the signal's ability to propagate over a distance with weather also being a significant factor, necessitating a method to quantify the induced the transmitted and received signal.

As shown in [Figure 5](#), when modeled as a transmission line, the track has a characteristic impedance Z_0 . V_S is the driving signal, and Z_S and Z_L are the source and load impedances, respectively.

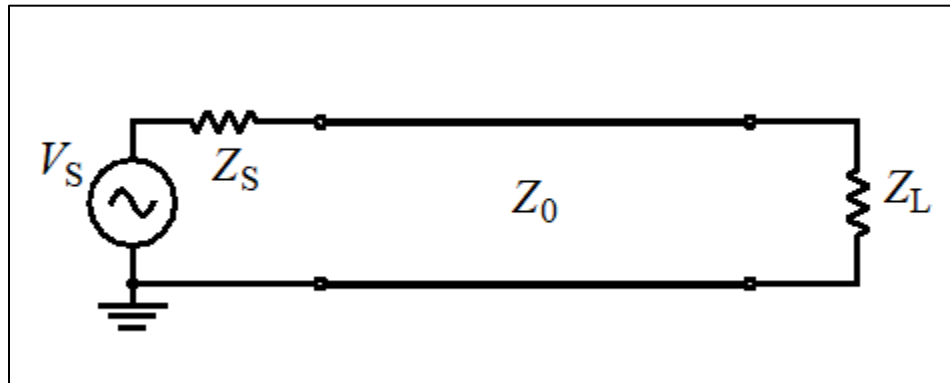


Figure 5. Transmission Line

An elemental length of transmission line can be expressed as a distributed-element model consisting of the following parameters ([Figure 6](#)):

- Series Resistance, R (Rail Resistivity)
- Series Inductance, L (Track Inductance)
- Shunt Capacitance, C (Track Capacitance)
- Shunt Conductance, G (Ballast Conductance)

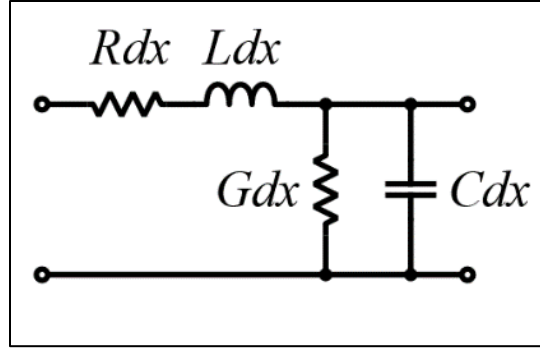


Figure 6. Transmission Line Distributed-Element Model

The parameters can be related to the characteristic impedance Z_o using the following equations.

$$Z_o = \sqrt{\frac{R+j\omega L}{G+j\omega C}} \quad (4)$$

Where:

Z_o = The complex characteristic impedance (ohms)

ω = The angular frequency (hertz)

R = Resistance (ohms)

L = Inductance (henries)

C = Capacitance (farads)

G = Conductance (siemens)

The input impedance, $Z_{in}(x)$, is the impedance a distance x from the load, Z_L , and can be expressed as:

$$Z_{in}(x) = Z_o \frac{Z_L + Z_o \tanh(\gamma x)}{Z_o + Z_L \tanh(\gamma x)} \quad (5)$$

Where:

Z_o = Characteristic Impedance (Ohms)

Z_L = Load/shunt impedance (Ohms)

$Z_{in}(x)$ = Track impedance at a distance x from the shunt (Ohms/Unit Distance)

γ = Propagation constant

Where:

γ = propagation constant and expressed as:

$$\gamma = \sqrt{(R + j\omega L)(G + j\omega C)} \quad (6)$$

By taking open circuit ($Z_L = Z_{OP} = \infty$) and closed circuit ($Z_L = Z_{SH} = 0$) input impedance measurements and substituting them into Equation (5), the characteristic impedance, Z_o , and the propagation constant γ of the transmission line can be determined.

$$Z_o = \sqrt{Z_{SH}(x)Z_{OP}(x)} \quad (7)$$

$$\gamma = \frac{1}{x} \tanh^{-1} \sqrt{\frac{Z_{SH}(x)}{Z_{op}(x)}} \quad (8)$$

The experimental measurement of the primary line parameters (R, L, C, and G) is the essential starting point of developing the transmission line model. These parameters are used to determine the characteristic impedance and propagation constants using the equations above. In addition, data was collected on the rail, ballast, and ambient temperatures, as well as on the humidity. The objective was to relate how these changing variables affect the characteristic impedance of the track and the ability to infer the state of the rail and tracks.

The detected signal is a function of the induced emf and the characteristic track impedance, both of which can be represented using Ohms law as shown in [Equation \(9\)](#):

$$I = \frac{emf}{Z_{in}(x)} \quad (9)$$

Where:

emf = Induced electromotive force by a magnetic field

I = resultant induced current in the rail (A)

$Z_{in}(x)$ = Track impedance at a distance x from the shunt

2.5 Summary

The research review was used to 1) leverage prior work and findings regarding the OBRD concept and 2) develop a framework to drive the development of a fully functional OBRD system that accomplishes the claims made in the source patent (USA Patent No. 9,162,691, 2013). The following sections further detail both the track impedance measurement setup and analysis and the laboratory and field-testing setup and analysis that was carried out.

3. Track Impedance Characterization

The OBRD project focuses on the development of an onboard electronic system capable of detecting the presence of broken rails in advance of a moving train. The detection range of such a system must be far enough to allow the train to come to a complete stop before arriving at the broken rail. To help determine the feasibility of this goal, the authors concentrated on modeling the electrical impedance characteristics of modern railroad tracks. This model was validated via a long-term study of the impedance characteristics of actual test tracks at the TTC facilities including portions of the PTT and TTT. Given the often-dry and sometimes-frozen ballast conditions prevalent at the TTC, most of the long-term test data is expected to have been collected under high ballast resistance conditions. Therefore, validating the developmental track circuit electrical model under significantly lower ballast resistance conditions required researchers to use artificial means to lower the ballast resistance of the test track(s).

3.1 Setup

A track impedance data collection system was set up on the PTT track. The test area covered P62–P59, consisting of 115-pound rail and wood ties spaced approximately 19 inches apart interspaced by relatively clean ballast. The section of track was left unoccupied for most of the data collection time. The test segment of about 650 feet (~0.1 miles) is highlighted (in dark blue) in [Figure 7](#).

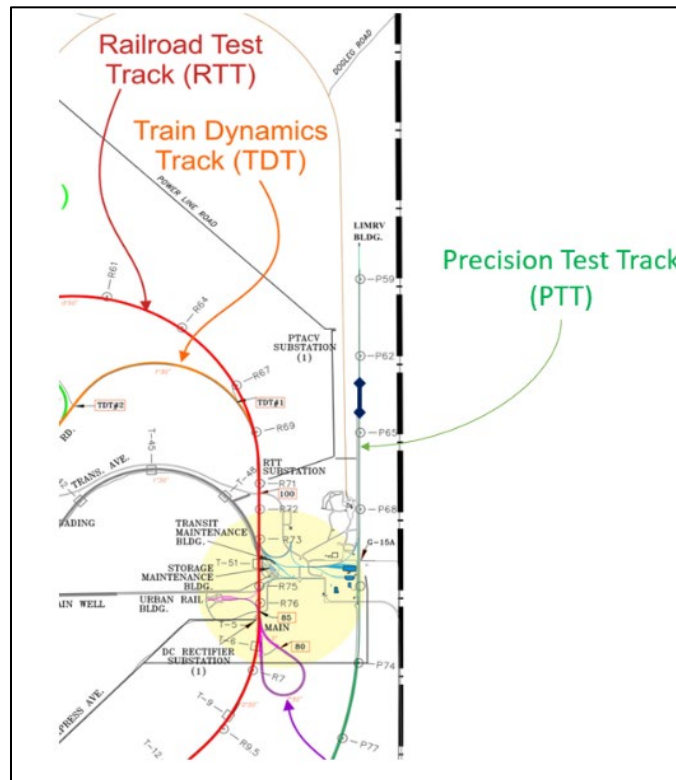


Figure 7. PTT Track Impedance Data Collection Zone

3.2 Equipment

The track impedance characterization involved building a measurement system that collects data about the track impedance variables as well as track and environmental conditions. Long-term data collection was completed over a period of 9 months (June 2021–February 2022) on the PTT using data collection equipment was set up at different nodes between P64 and P63 and covering a distance of approximately 650 feet.

The measurement system consisted of three nodes: the desktop node, the measurement node, and the relay node. The desktop node includes the desktop computer that receives and stores the measurements taken and the Inductance (L), Capacitance (C), and Resistance (R) (LCR) meter that sends the electrical signal and takes the measurements for the track impedance variables. To protect the equipment, the desktop and the LCR meter were located inside a trailer next to post P64 on the PTT, as seen in [Figure 8](#). The computer controlled the two remote nodes as well as the LCR meter, and it collected data from the weather station shown in [Figure 8](#). The weather station measured different variables such as temperature, humidity, wind direction, and UV and solar radiation.



Figure 8. Weather Station and Trailer that Holds Desktop Node Equipment at Post P64 of the PTT

The measurement node was located 363 feet from the desktop node and 287 feet from the relay node. The measurement node included a microcontroller and several sensors that took temperature and moisture readings. The relay node was 650 feet from the desktop node and includes a relay that opens and closes the circuit while taking the different measurements, and it also has another set of microcontroller sensors that take temperature and moisture readings. [Figure 9](#) shows the configuration of the track impedance data collection system.

The system uses single board computers to facilitate communication between nodes that require AC power to be run to each node. Ethernet wires, ethernet extender kits, and switches were used to establish the communication between the nodes and to avoid crosstalk.

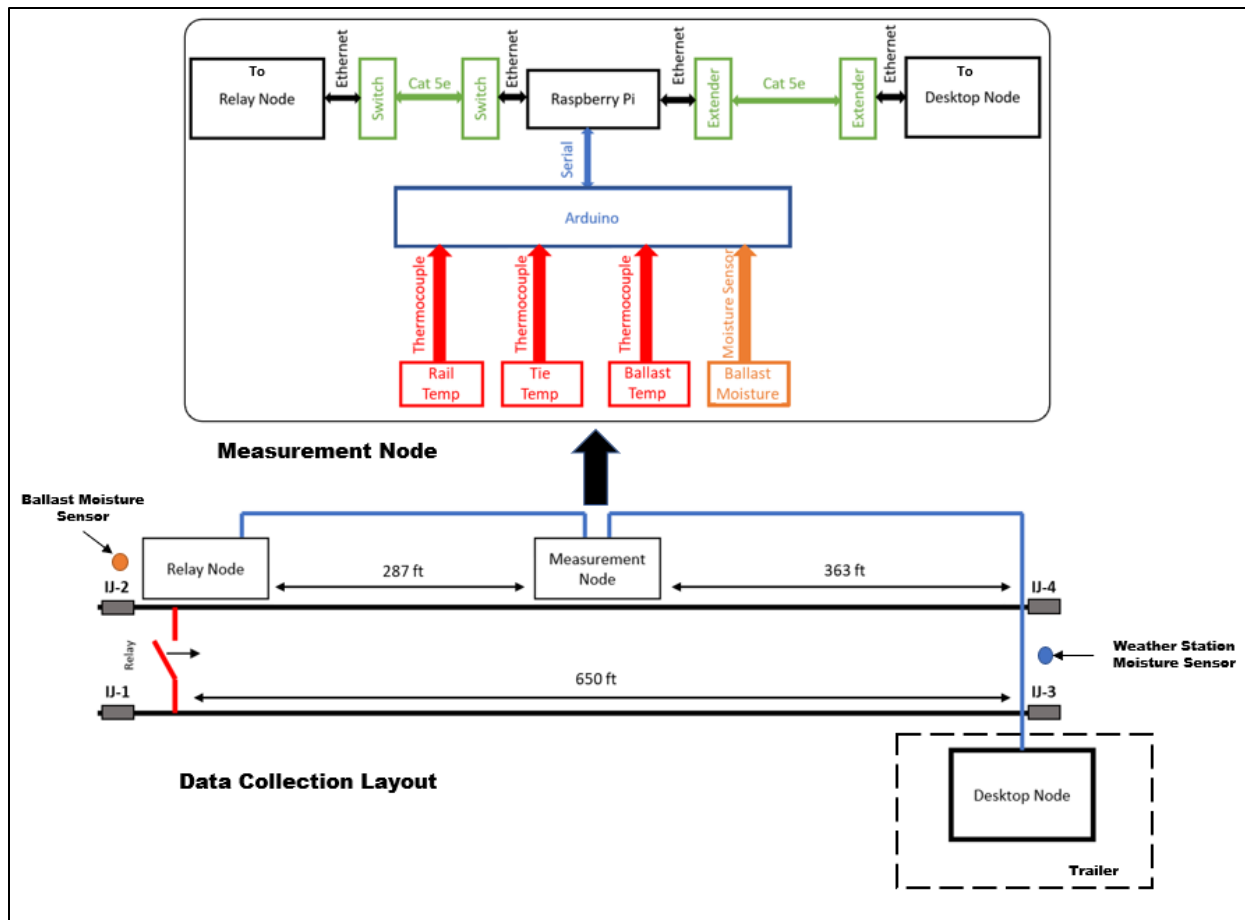


Figure 9. Track Impedance Data Collection and Measurement Setup

A single board computer was connected to the microcontroller through a serial connection to receive the measurements from the sensors. The microcontroller has three thermocouples that measure the temperatures of the rail, tie, and ballast and a moisture sensor to measure the moisture in the ballast. Information for the moisture sensor and thermocouple used are shown in Figure 10. The relay node has similar equipment with the addition of the relay switch that connects to both sides of the track to establish open and closed circuits. Figure 9 shows the organization of the measurement and the nodes, respectively. The ethernet cable was shielded and buried with the AC lines at various distances.

The use of AC power eliminated the need to work with and charge batteries. Ethernet interfaces are reliable and eliminate communication issues. The single board computers, i.e., Raspberry Pi boards, were used to facilitate communication between nodes and allow remote access and remote programming of the microcontroller Arduino. The single board computer also powered the relay using the 40 pin General Purpose Input/Output (GPIO) header, as shown in Figure 10. There are two 3.3 V-pins to power the relay, 8 ground lines, and 26 GPIO pins that can be configured to control the signal line. Because the thermocouples and moisture sensor require analog pins to take measurements, the Arduino was used to take measurements while transmitting data via a serial connection. Communication between remote nodes and the desktop node was done by sending XML packets via ethernet. A python script generates, sends, receives,

and parses messages. Pelican cases housing the Raspberry Pi, Arduino, and other equipment were used to protect the equipment, as shown in Figure 10.

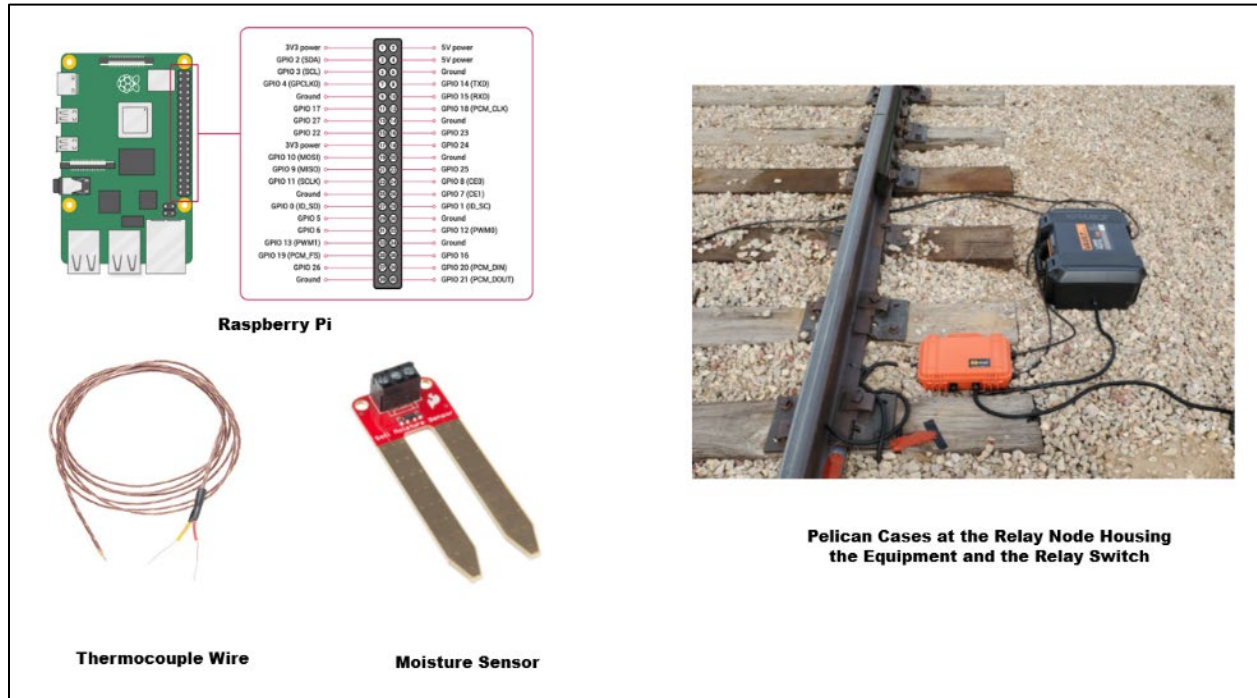


Figure 10. External Data Collection Hardware

3.3 Data Collection

To fully characterize the track impedance under varying environmental conditions, several types of data needed to be measured over a long period of time. This data serves as the foundation for determining the dominating factors that affect the track impedance and, consequently, the signal of the OBRD system. Additionally, the data can be used as a basis to construct a model intended to estimate the electrical properties of the track. Three types of data were measured as described below:

Electrical Track Impedance Data

- Open circuit impedance magnitude and phase angle
- Short circuit impedance magnitude and phase angle
- Rail resistance, R
- Rail inductance, L
- Track conductance, G
- Track capacitance, C
- Input signal frequency (30 frequencies varying between 20 Hz to 1.7 kHz)

Track Condition Data

- Rail temperature (at both relay node and measurement nodes)

- Ballast temperature (at both relay node and measurement nodes)
- Tie temperature (at both relay node and measurement nodes)
- Ballast moisture (at both relay node and measurement nodes)

Environmental

- Ambient temperature
- Relative humidity
- Precipitation
- Barometric pressure
- Wind speed and direction
- UV and solar radiation

The LCR meter was used to measure impedance magnitude, $|Z|$, and the phase angle, θ , of a selected section of electrically isolated track at predefined frequencies (i.e., 30 frequencies between 20 Hz and 1.7 kHz) as shown in [Figure 13](#). Additionally, the LCR meter was also used to measure R, L, C, and G of the track directly. These frequencies were chosen based upon known frequencies used in track circuits today.

The measurements of the impedance magnitude and phase angle ($|Z|$ and θ) were taken twice at each frequency, once when the track circuit was shorted/shunted and once when the track circuit was open. It is important to take these measurements with as little time as possible between them to minimize the effects that changing environmental conditions like weather may have on the data. When measuring R, L, C, and G directly, R and L need to be measured in a closed-circuit state while C and G are measured in an open circuit state. These measurements are repeated throughout the data collection period. The measurement process has the following sequence of events:

1. The switch is open
2. Measurements of $|Z|$ and θ are taken for all frequencies
3. The switch is closed
4. Measurements of $|Z|$ and θ are taken for all frequencies
5. Measurements of R are taken for all frequencies
6. Measurements of L are taken for all frequencies
7. The switch is open
8. Measurements of C are taken for all frequencies
9. Measurements of G are taken for all frequencies
10. Repeat

While measuring the LCR meter measurements, sensor log, time log, and weather data, four different files are generated. Samples of raw data files are shown in [Figure 11](#) through [Figure 14](#).

The sensor log includes an extra variable at each node that monitors the case inner temperature that was added in the summer days to check when the equipment could overheat.

```
*Time_Log 2022-01-19 08h15m15s - Notepad
File Edit Format View Help
Open Circuit Impedance Start Time: 2022-01-19 08:15:15
Open Circuit Impedance Stop Time: 2022-01-19 08:17:36
Open Circuit Phase Start Time: 2022-01-19 08:17:36
Open Circuit Phase Stop Time: 2022-01-19 08:20:06
Closed Circuit Impedance Start Time: 2022-01-19 08:20:08
Closed Circuit Impedance Stop Time: 2022-01-19 08:20:46
Closed Circuit Phase Start Time: 2022-01-19 08:20:46
Closed Circuit Phase Stop Time: 2022-01-19 08:21:19
Closed Circuit Resistance Start Time: 2022-01-19 08:21:19
Closed Circuit Resistance Stop Time: 2022-01-19 08:21:54
Closed Circuit Inductance Start Time: 2022-01-19 08:21:54
Closed Circuit Inductance Stop Time: 2022-01-19 08:22:28
Open Circuit Capacitance Start Time: 2022-01-19 08:22:30
Open Circuit Capacitance Stop Time: 2022-01-19 08:24:52
Open Circuit Conductance Start Time: 2022-01-19 08:24:52
Open Circuit Conductance Stop Time: 2022-01-19 08:27:15
```

Figure 11. Sample of Time Log File Raw Data

```
*Sensor_Log 2022-01-19 08h03m59s - Notepad
File Edit Format View Help
Rail RN: -2.25 degC ; Tie RN: -1.25 degC ; Ballast RN: 2.25 degC ; Case RN: 2.50 degC Moisture Sensor: 566
Rail MN: -1.25 degC ; Tie MN: -1.00 degC ; Ballast MN: 3.00 degC ; Case MN: -0.75 degC Moisture Sensor: 543
```

Figure 12. Sample of Sensor Log File Raw Data

```
LCR Meter Measurements 2022-01-19 08h15m15s - Notepad
File Edit Format View Help
Frequency (Hz)
20.30938
23.679
27.60769
32.1882
37.52868
43.75523
51.01485
59.47895
69.34737
80.8531
94.26779
109.9082
128.1435
149.4044
174.1927
203.0938
236.79
276.0768
321.882
375.2868
437.5524
510.1485
594.7896
693.4736
808.531
942.6778
1099.082
1281.435
1494.044
1741.927
Open Circuit Impedance (Ohms)
2.452031e+02
2.449260e+02
2.452979e+02
2.434885e+02
```

Figure 13. Sample of LCR Meter Measurement File Raw Data

Weather 2022-01-10 - Notepad										
File Edit Format View Help										
Date	Time	Temp	Hi	Low	Out	Dew	Wind	Wind		
		Out	Temp	Temp	Hum	Pt.	Speed	Dir		
01/10/22	12:01 a	18.4	18.5	18.4	84	14.4	4.0	ENE		
01/10/22	12:02 a	18.2	18.4	18.2	84	14.2	4.0	NE		
01/10/22	12:03 a	18.1	18.2	18.1	84	14.1	3.0	NE		
01/10/22	12:04 a	18.0	18.1	18.0	84	14.0	3.0	NE		
01/10/22	12:05 a	17.9	18.0	17.9	84	13.9	3.0	NE		
01/10/22	12:06 a	17.8	17.9	17.8	84	13.8	4.0	NE		
01/10/22	12:07 a	17.7	17.8	17.7	84	13.7	3.0	NE		
01/10/22	12:08 a	17.6	17.7	17.6	83	13.3	3.0	NE		
01/10/22	12:09 a	17.5	17.6	17.5	83	13.2	4.0	NE		
01/10/22	12:10 a	17.6	17.6	17.5	84	13.6	4.0	NE		
01/10/22	12:11 a	17.6	17.6	17.5	84	13.6	4.0	NE		
01/10/22	12:12 a	17.6	17.6	17.5	84	13.6	4.0	NE		
01/10/22	12:13 a	17.6	17.6	17.6	85	13.9	3.0	NE		
01/10/22	12:14 a	17.6	17.7	17.6	85	13.9	3.0	NE		

Figure 14. Sample of Part of a Weather Data File

Weather data is taken every minute while the other files take around 10 minutes on average to complete the impedance measurements as well as the sensor readings in the measurement and relay nodes. The number of data points from each measurement source is shown in Figure 15 where:

- *Freq_Measurement* denotes the number of data points recorded from the track impedance data
- *Freq_Weather* denotes the number of data points recorded from the weather station
- *Freq_Sensor* denotes the number of data points recorded from the temperature and moisture sensors at the relay and measurement nodes

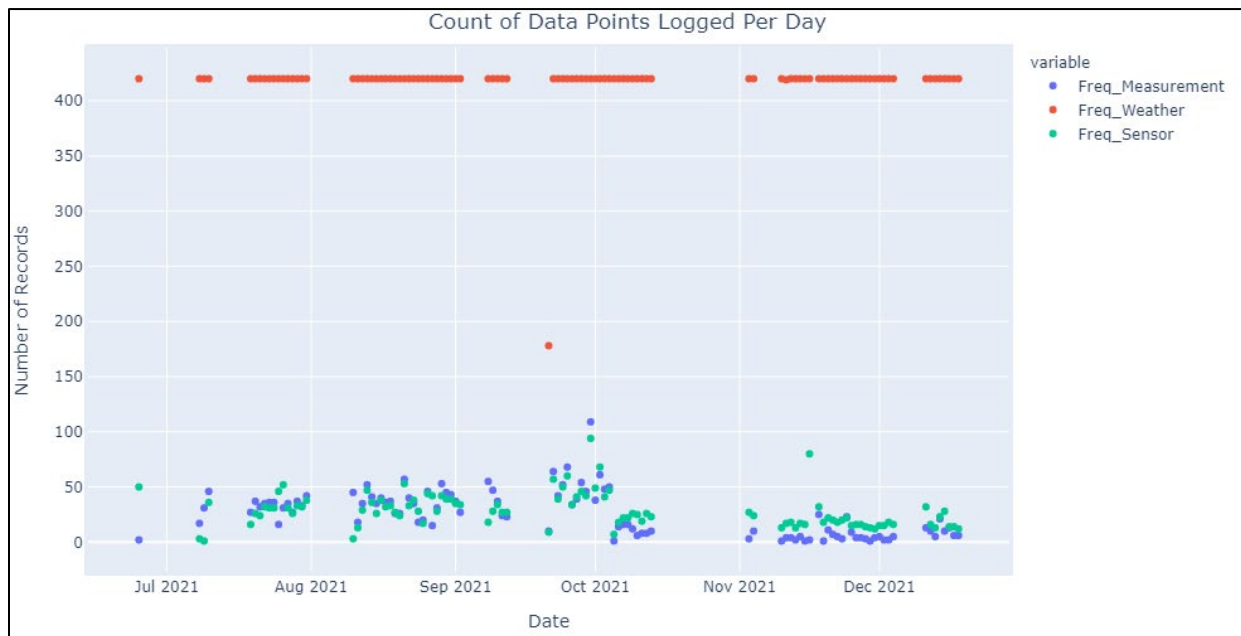


Figure 15. Number of Data Points Recorded per Day by Each Measurement Source

The collected data was saved on the desktop computer at the desktop node as well as uploaded periodically to a database on a server belonging to the researchers. The database serves as a backup for the desktop computer, and it allows analyses to be performed on the acquired

impedance and environmental data. A flow diagram in Figure 16 shows how the data moves from the different sources taking data measurements to the data analysis platform.

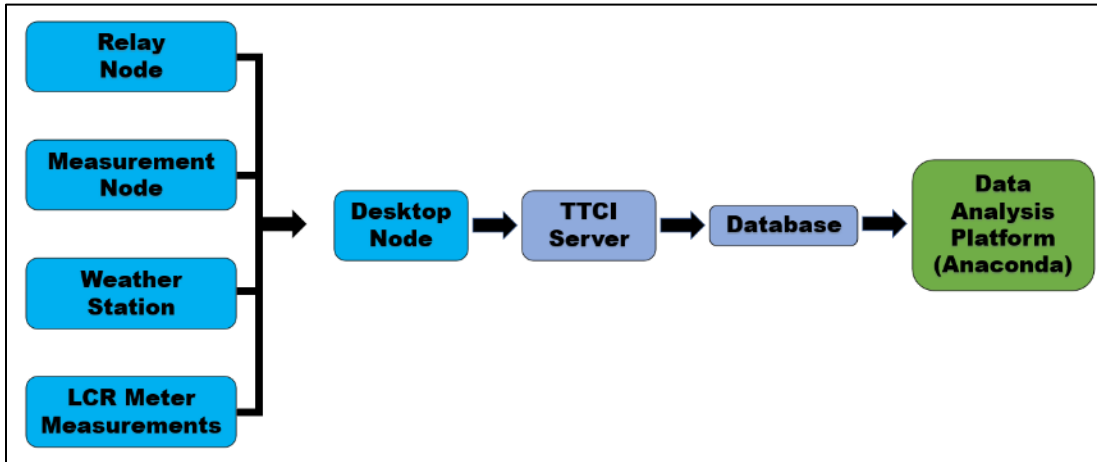


Figure 16. Flow Diagram of Measured Track Impedance Data of Data Analysis Process

3.4 Approach

Exploratory data analysis was performed to acquire general observations about the environmental and track impedance data. Graphs showing the relationship between different variables were produced to give an overview of the behavior of different variables and to investigate the trends and the relationship of importance for the analysis objectives. The Resistance (R), Inductance (L), Capacitance (C), Conductance (G) (RLCG) variables were analyzed to explore their relationships with various frequencies and weather conditions. Also, the track condition measurements were compared to weather variables to explore the correlation between them.

The collected data was used to calculate the characteristic and input impedance of the track based on the transmission line theory equations given in Section 2.4. The characteristic impedance Z_0 and the propagation constant γ can be calculated using the RLCG measured data and the frequency. Once the characteristic impedance and the propagation constant are known, the input impedance of the track can be calculated for a given distance and a load impedance Z_L . Since a standard resistive test shunt was used, the load impedance can be assumed to be 0.06 ohms. It is worth noting that, due to the parallel shunts of the locomotive wheel sets, the effective load impedance would be a much lower value. The characteristic impedance was analyzed to see the effects of varying frequencies and specific track or weather variables. In addition, estimate of the input impedance at different track distances was calculated and compared for different frequencies.

3.5 Results and Analysis

The first part of the analysis focused on investigating how much the changing weather affects the track conditions, e.g., the relationship between varying weather temperatures and the corresponding changes in rail temperature. This part of the analysis also explored the electrical impedance variable relations with changing the frequency of the input signal, as well as some environmental or track conditions. The second part of the analysis focused on the results of the calculated characteristic impedance of the track, based on the transmission line theory and how it changes with the frequency of the input signal, as well as with varying environmental and track

conditions. In addition, an estimation of the input impedance of the track based on different track distances was demonstrated and compared at different frequencies.

3.5.1 Exploratory Data Analysis

Figure 17 indicates that weather temperature affected the rail temperature, but, because there are other parameters that can affect rail temperature, this relationship is not linear. Figure 17 further shows an aggregate for all weather and rail temperature data, and Figure 18 focuses on summer days where the rail temperature readings increase reach 130 °F compared to a maximum weather temperature of approximately 100 °F. The rail temperature increase can be attributed to the fact that rail steel takes time to heat up and, as metal, can retain more heat. On fall and winter days, the rail temperature still has higher peaks compared to weather temperature, but there is almost no lag between rail and weather temperatures, as shown in Figure 19 and Figure 20, respectively. The lag between rail and weather temperatures occurred on summer days where sun exposure is longer, and temperatures are higher. A model that predicts the rail temperature based on weather temperature was developed on previous FRA research and shows a similar pattern (Al-Nazer, L., 2008).

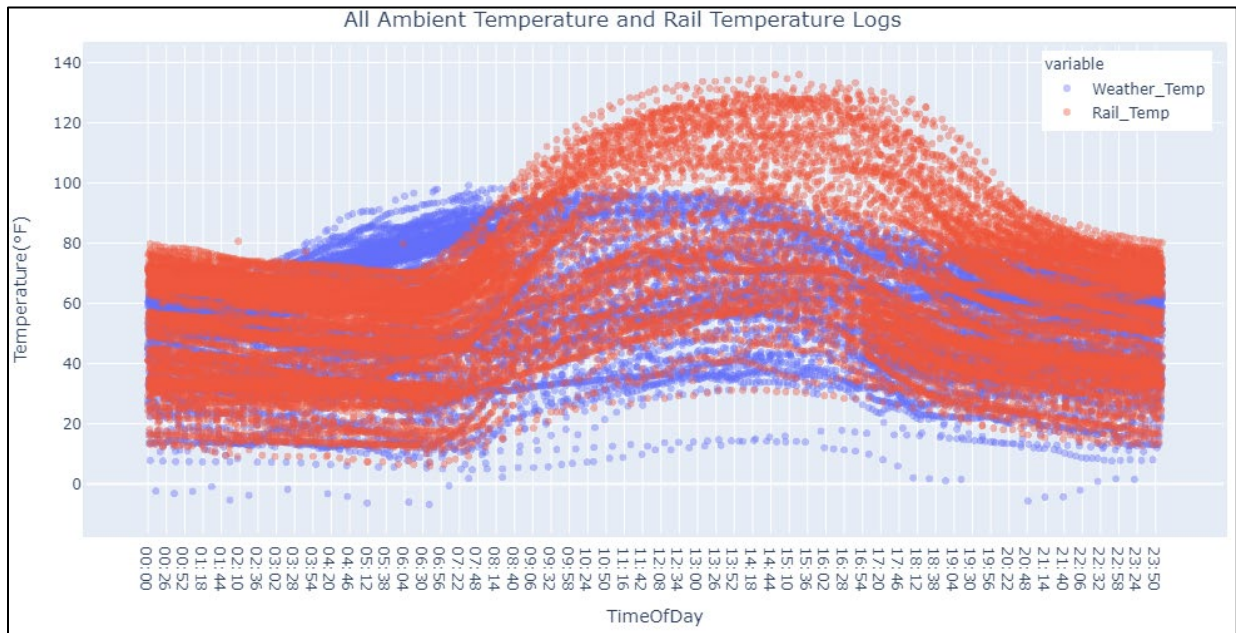


Figure 17. Weather and Rail Temperatures for All Data During 24 Hours of the Day

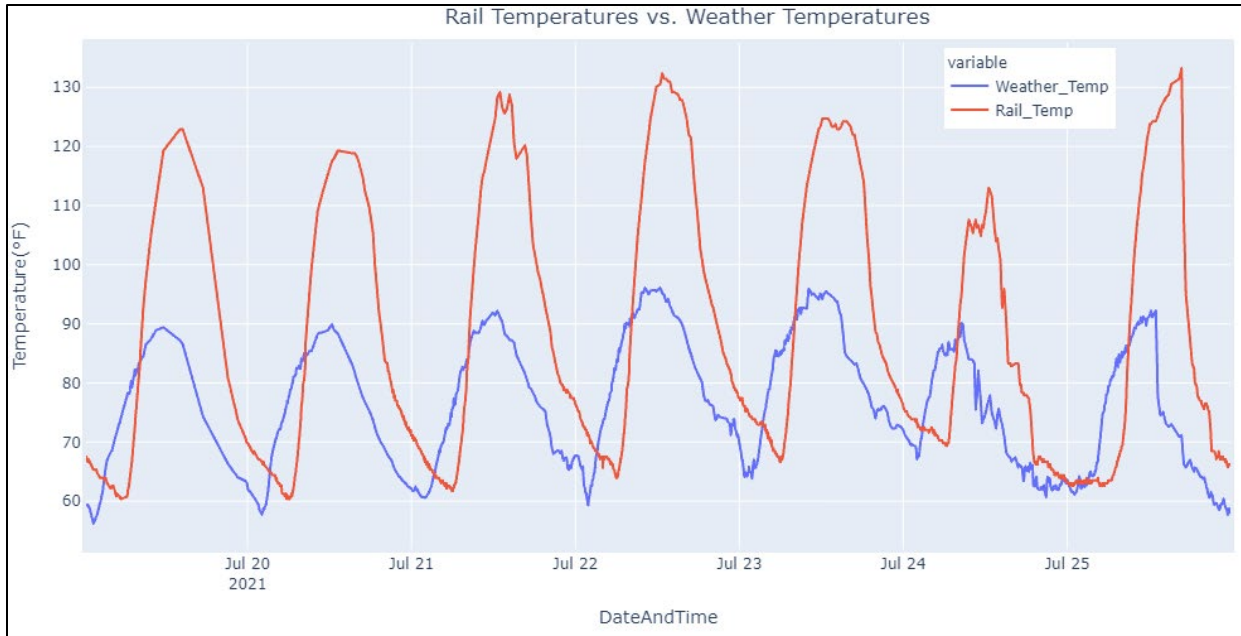


Figure 18. Weather and Rail Temperatures for a Sample of Summer Days

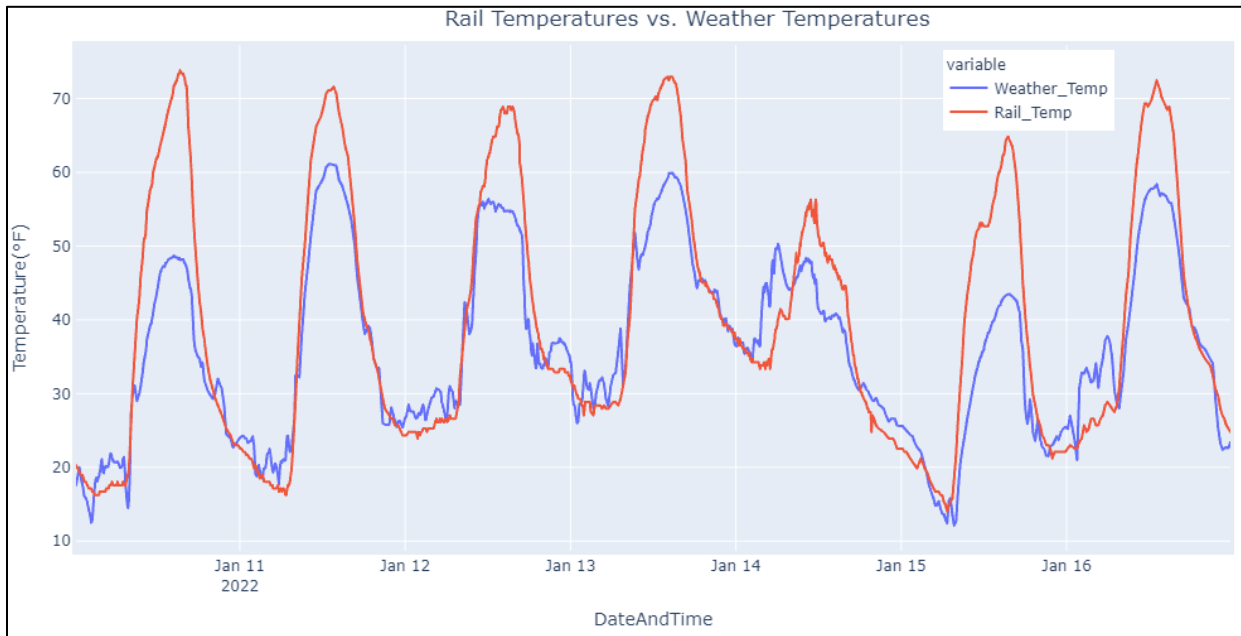


Figure 19. Weather and Rail Temperatures for a Sample of Winter Days

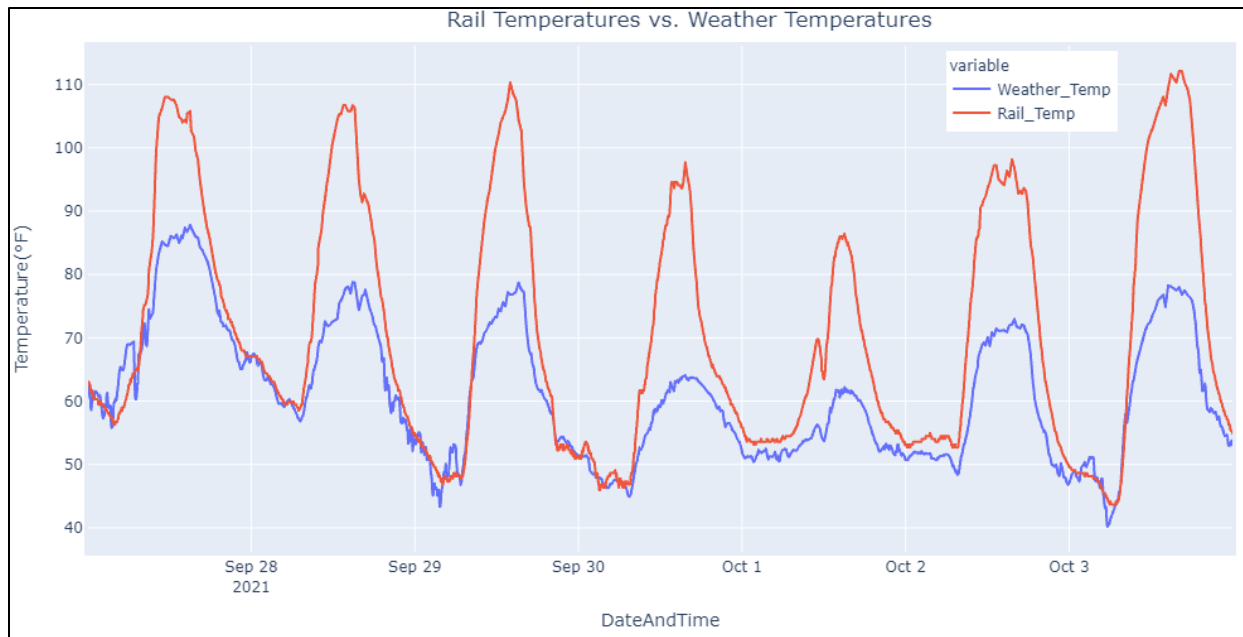


Figure 20. Weather and Rail Temperatures for a Sample of Fall Days

For the observations mentioned above, the rail temperature was used for further analysis instead of the weather temperature because the rail temperature more accurately reflects the track condition. A model can be used to estimate the track temperature based on the weather temperature as stated in Al-Nazer (2008).

The track impedance variables were measured at 30 different frequencies between 20 Hz and 1.7 kHz. The graph in Figure 21 shows the RLCG variables across the frequency range for 1 day while Figure 22 shows the RLCG variables trends for all the data. The thick lines around the C and G plots indicate the 95 percent confidence interval range the measurements fall within. In the case of R and L, the confidence interval range lines are very close to the fitted line for the R and L, and therefore, are not visible in the plots.

As shown in Figure 21, on a regular day, track resistance increases as the frequency increases while G between rails decreases. The same resistance pattern across all data is shown in Figure 22 where the resistance is still collectively increasing by the frequency. The conductance across all data measurements shows a similar pattern where it is first decreasing and then slightly increasing at 1.5 kHz.

The L and C values show an increase at low frequencies but are not affected much as the frequency increases to higher values. However, it is well known that their characteristics affect the circuit due to the frequency dependent component of the reactance (B&K Precision, 2020). Inductance and capacitance readings both have negative values that might be due to the circuit having both capacitance and inductance components. Due to the limitations of the LCR measurement equipment, the inductance measurement can have a negative value at low frequencies when the circuit contains a capacitance component while having positive readings at high frequencies (B&K Precision, 2020). Some of the readings had a positive inductance reading at relatively high frequencies around 1.5 kHz. The same effect happens for the capacitance readings when inductance exists in the circuit and causes the capacitance measurements to be negative at low frequencies.

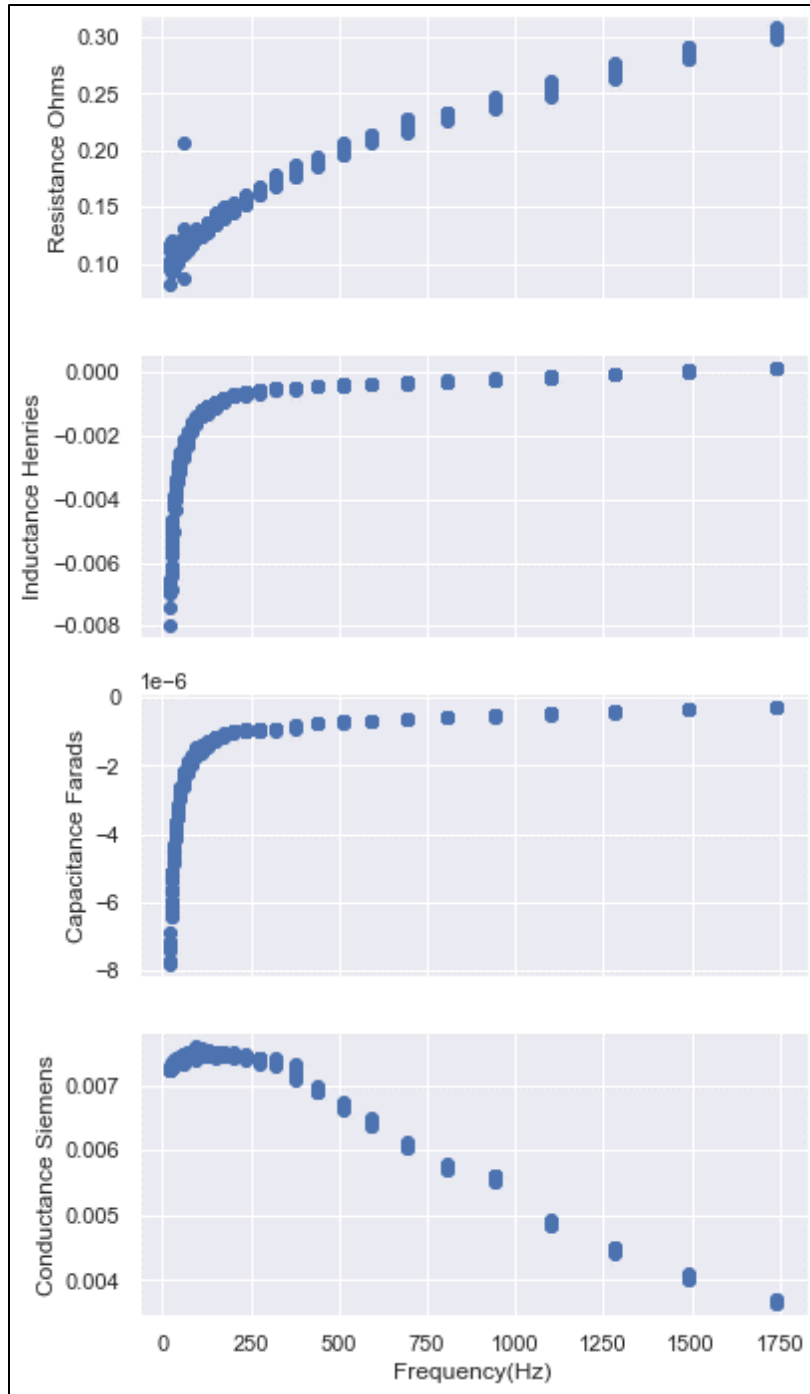


Figure 21. Track Impedance Variables (RLCG) vs. Frequency for 1 Day

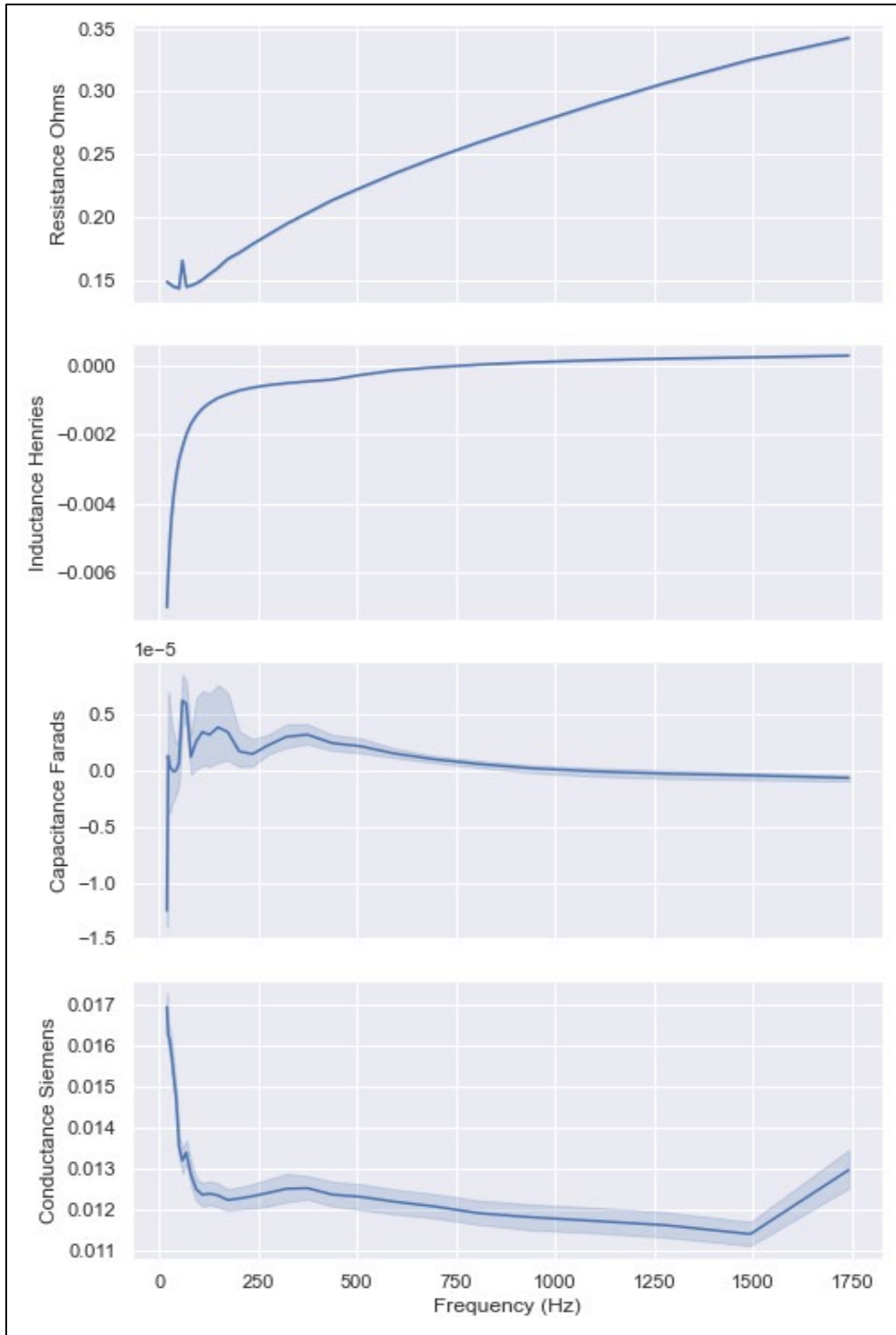


Figure 22. Track Impedance Variables (RLCG) vs. Frequency for 9 Months

High resistance readings correspond to high temperatures on some days, but the readings are out of the reasonable range for how much the resistance over 650 feet of track. According to [Figure 22](#), the fitted line and 95 percent confidence interval for the resistance values for all data show resistances of up to 0.35 ohms while the data having higher resistance values are minimal

compared to the rest of the data acquired. However, over the days in different months, the resistance seemed to increase at lower rail temperatures as seen in [Figure 23](#).

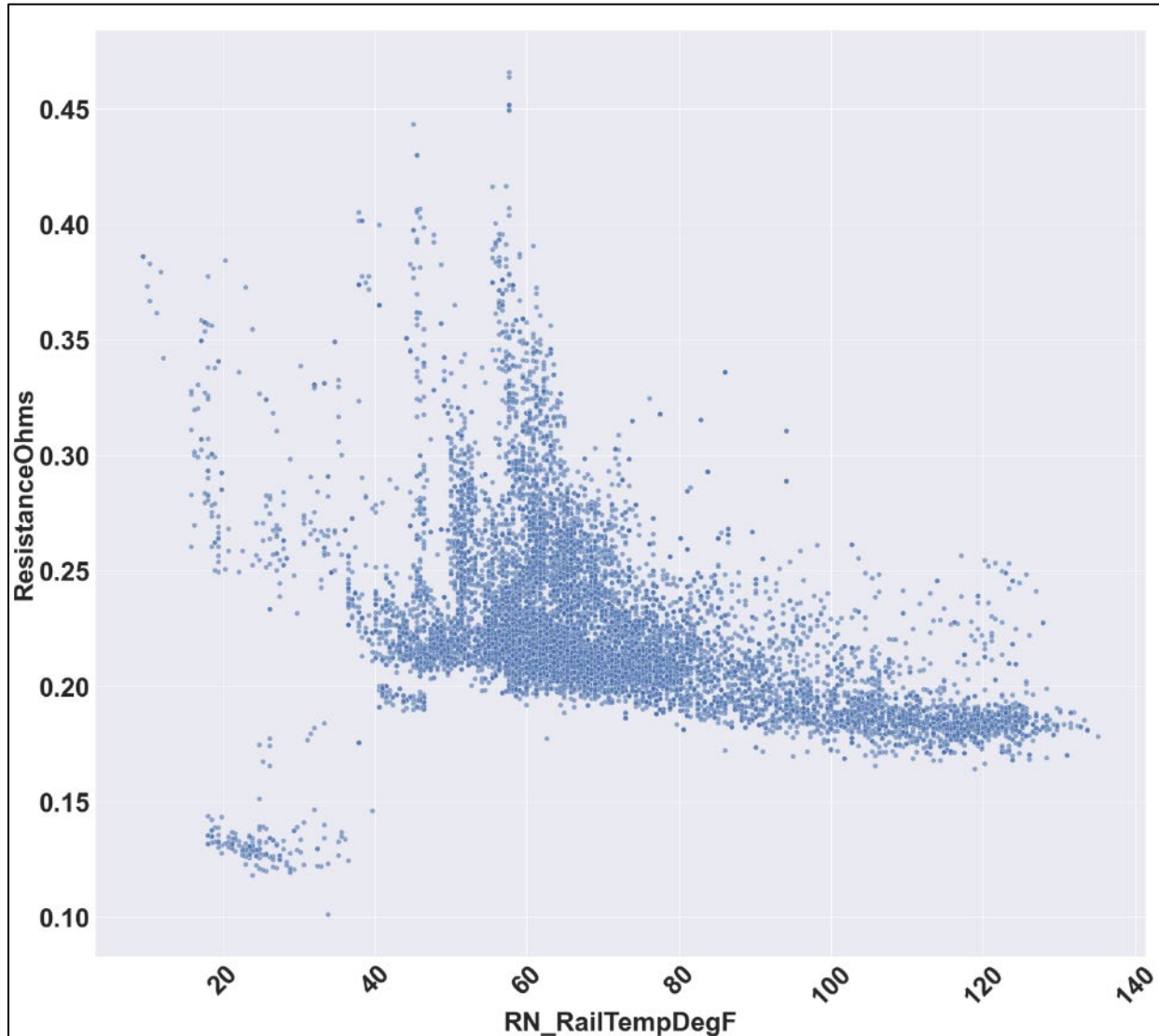


Figure 23. Track Resistance vs. Rail Temperature

Due to the test track receiving limited ballast moisture readings with little precipitation, a tank car was used to dump approximately 11,000 gallons of water on the track to simulate higher precipitation conditions and a wetter ballast. As expected, the conductance in the ballast increased after wetting the track, with a corresponding decrease in the open loop impedance. This decrease can be seen in [Figure 24](#) that shows where the track wetting simulation took place on January 12. It should be noted that a lower reading on the moisture sensor in the second plot in [Figure 24](#) corresponds to more moisture in the ballast. The moisture sensor reading did not go very low (indicating high moisture content in the ballast) because the moisture sensor was placed outside the gauge right next to the rail, as seen in [Figure 9](#) and as opposed to [Figure 10](#) where the moisture sensor is buried next to the orange case enclosure while the water was dumped in the middle of the gauge.

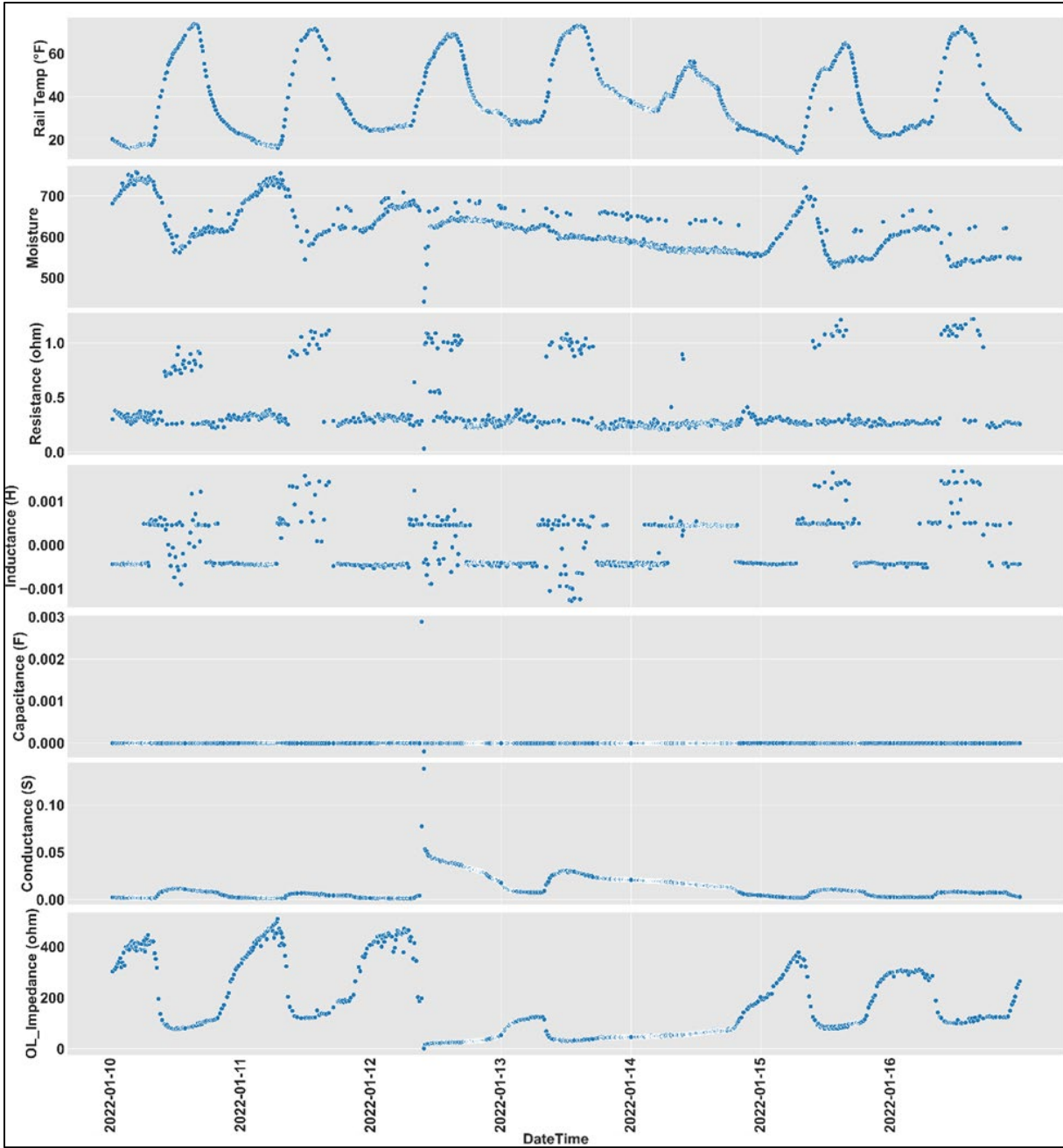


Figure 24. Time Series for Rail Temperature, Ballast Moisture, RLCG and Open Circuit Impedance

3.5.2 Data Analysis of Characteristic and Input Impedance of the Track

The characteristic impedance was calculated based on the transmission line theory and the RLCG data collected. The characteristic impedance magnitude, phase angle, and real and imaginary components were calculated for the same range of frequencies as the input signal and are shown in [Figure 25](#). Refer to [Appendix H](#) for examples of the calculations of the characteristic and input impedance with observations of the results obtained.

The characteristic impedance magnitude increases as the frequency increases to a frequency of 942 Hz then it starts decreasing to 1.5 kHz before increasing again. A similar behavior can be observed for the real component of the characteristic impedance. The imaginary component has a positive correlation with the frequency where this component increases as the frequency of the input signal increases, suggesting that using relatively lower frequencies for the input signal will decrease the impedance seen by the signal and would allow the signal to propagate for longer track distances.

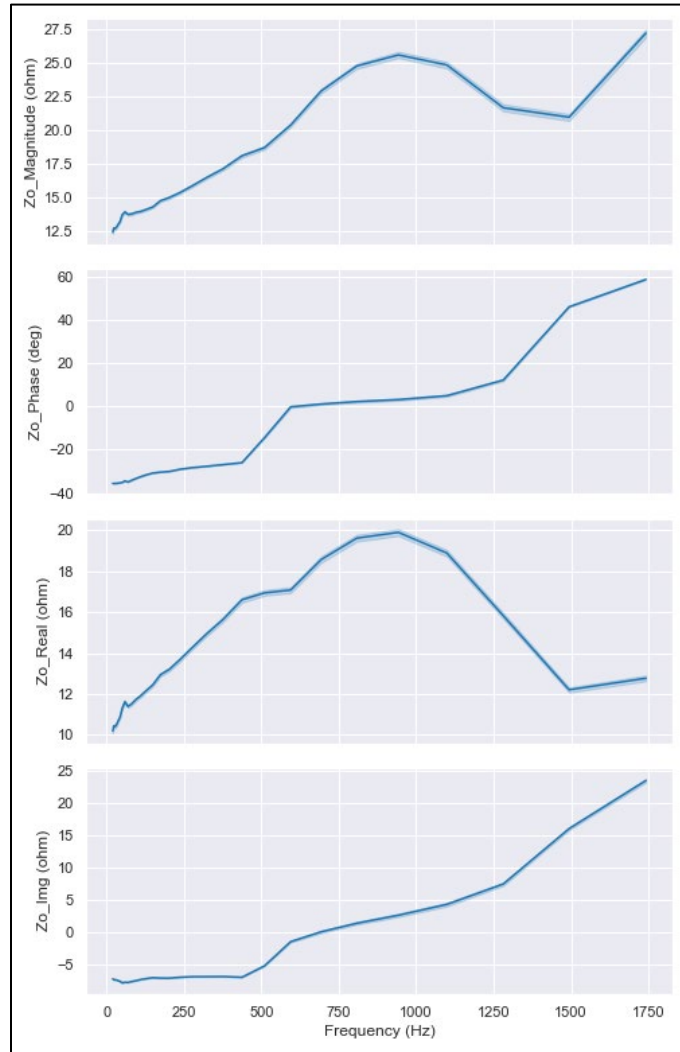


Figure 25. Characteristic Impedance vs. Frequency

After using a tank car to dump water on the track to simulate higher precipitation conditions and a wetter ballast, on January 12, the characteristic impedance magnitude and real component decreased as shown in [Figure 26](#). The moisture sensor readings decreased on January 12 (indicating higher moisture in the ballast), and lower magnitude and real component values of the characteristic impedance can be seen following the wetting of the ballast. The impedance values after wetting the ballast were approximately half the previous measurement values. The moisture sensor reading did not go very low (indicating high moisture content in the ballast) because the moisture sensor was placed outside the gauge right next to the rail.

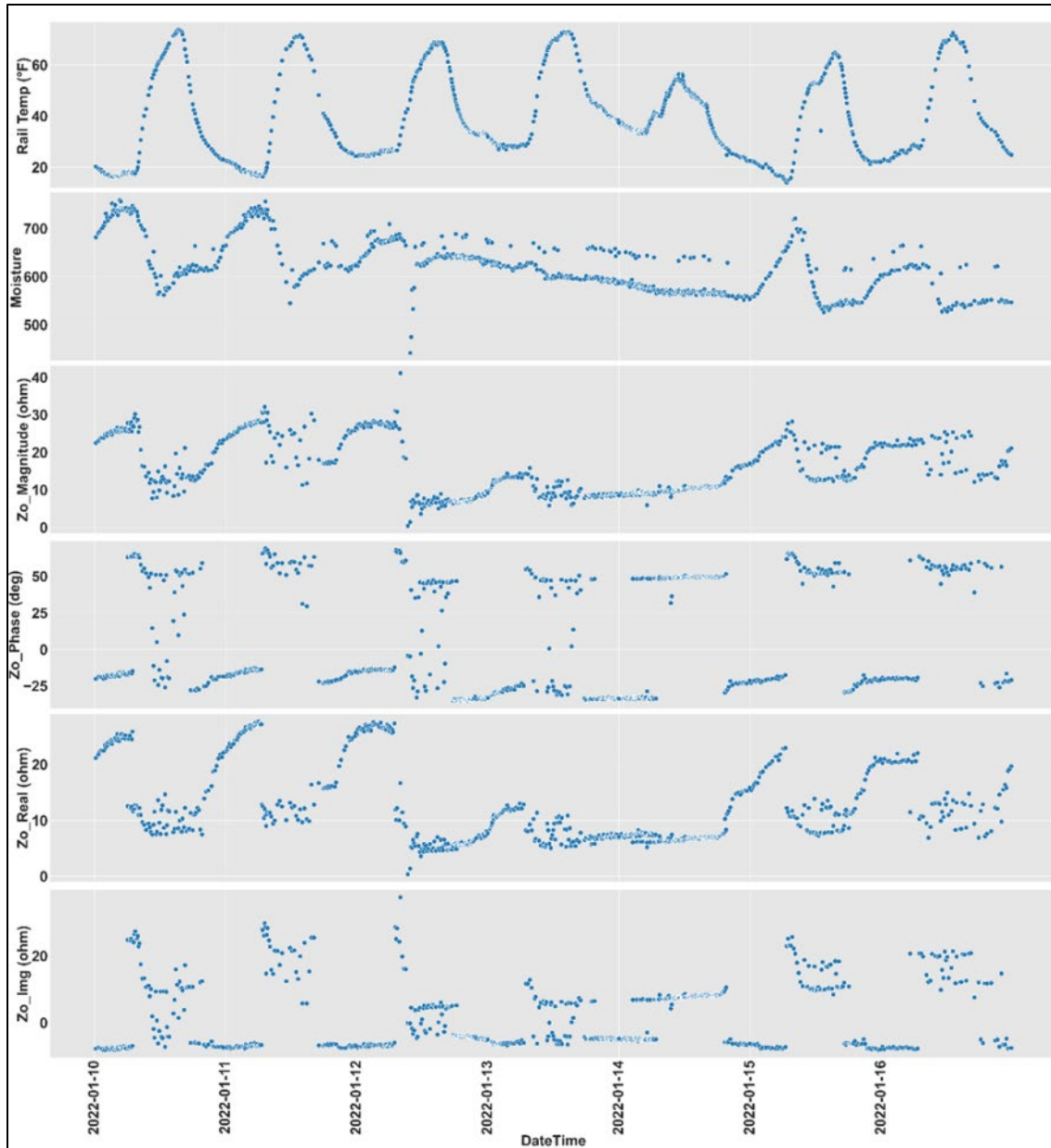


Figure 26. Time Series for Rail Temperature, Ballast Moisture, and Characteristic Impedance Magnitude, Phase Angle, Real and Imaginary Components

Table 1 summarizes the relationship between the input signal frequency and the track measured impedance variables as well as the characteristic impedance. Table 2 summarizes the relationship between track condition variables and the track measured impedance variables as well as the characteristic impedance. Per Table 1, the characteristic impedance showed an increase with the frequency with some ranges showing some decrease. Therefore, the relation is denoted with (in general) to indicate that large increase in frequency will cause increase in the characteristic impedance.

Table 1. Relationships Between Input Signal Frequency and Track Impedance Variables

Track Condition/Frequency	Impedance Variables	Relationship
Frequency	Resistance	Proportional
Frequency	Conductance	Inversely Proportional (In general)
Frequency	Characteristic Impedance Magnitude	Proportional (In general)
Frequency	Characteristic Impedance Imaginary Component	Proportional

Table 2. Relationships Between Track Condition and Track Impedance Variables

Track Condition/Frequency	Impedance Variables	Relationship
Rail Temperature	Resistance	Inversely Proportional
Rail Temperature	Characteristic Impedance Magnitude	Inversely Proportional
Rail Temperature	Characteristic Impedance Real Component	Inversely Proportional
Rail Temperature	Characteristic Impedance Imaginary Component	Inversely Proportional
Wet Ballast	Conductance	Directly Proportional
Wet Ballast	Open Loop Impedance	Inversely Proportional
Wet Ballast	Characteristic Impedance Magnitude	Inversely Proportional
Wet Ballast	Characteristic Impedance Real Component	Inversely Proportional

The input impedance was calculated at different track lengths based on the transmission line theory. Since the frequency of the input signal affects the impedance, three different frequencies were selected to show the input impedance change with distance as the frequency changes. [Figure 27](#) shows the input impedance versus track distance for frequencies of 20.3, 594, and 1,494 Hz. The graphs show that as the distance increases, the input impedance increases as well. On the other hand, as the frequency of the input signal increases (i.e., 1,494 Hz), the input impedance imaginary component (Z_{in_Img}) increases with distance, causing a decrease in the corresponding phase angle (Z_{in_Phase}). For the cases of the lower frequencies (20.3 and 594 Hz), the input impedance imaginary components decrease with distance, causing an increase in the corresponding phase angle.

The input impedance phase angle 95 percent confidence interval range for each frequency may be used to define a tolerable range for how much the phase of the received signal changes from the phase angle of the input signal (i.e., induced signal in the track from the Tx coil), based on the

distance from the load (i.e., shunt). Based on the data in Figure 27, using an input signal frequency of 20.3 Hz, if the signal at the receiving coil has a phase angle change between 52–57 degrees from the input induced signal phase, could indicate that there is a shunt at a distance range of 8,000–10,000 feet. These ranges can also be set based on the magnitude of the input impedance and how much the factor of the input signal magnitude the receiver is seeing. This approach needs further analysis to define those ranges both clearly and reliably.

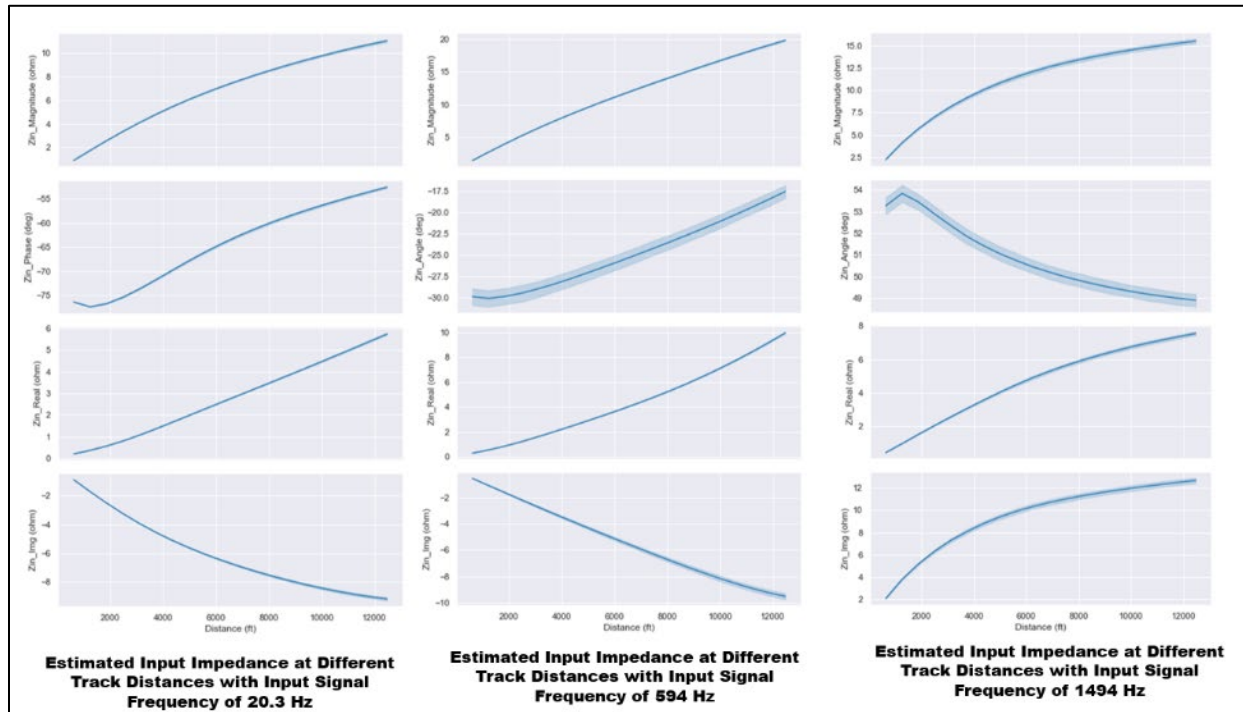


Figure 27. Estimated Input Impedance vs. Distances and for Different Frequencies

3.6 Conclusion

A track impedance measurement system was installed on the PTT to collect the following over a period of 9 months:

- Track impedance variables
- Track temperature variables
- Moisture variables
- Weather variables

The system measured the impedance variables (i.e., resistance, inductance, conductance, capacitance, open circuit impedance and phase angle, and the short circuit impedance and phase angle) for 30 frequencies ranging from 20 Hz to 1.7 kHz. As the frequency increases, the resistance increases while the conductance decreases. There was a correlation between the temperature of the rail with the weather temperature, but the rail temperature was lagging with higher peaks compared to the weather temperatures. After using a tank car to dump water on the track to simulate higher precipitation conditions, the conductance of the ballast showed an increase.

Applying the transmission line theory using the impedance variables measured calculates the characteristic impedance and the propagation constant. The characteristic impedance showed an increase with the frequency of the input signal except within the range of approximately 1–1.5 kHz where it decreased slightly before increasing again, suggesting an input signal with low frequencies would allow better propagation of the signal through the tracks. An optimization of usable frequencies that allows sufficient input voltage at the Tx coil to induce higher currents in the rail while also decreasing the input impedance of the rail is needed. With acquiring an accurate estimation of the input impedance of the track at a specific frequency, a tolerable range of the change in the phase angle of the received signal compared to the phase angle of the input signal (i.e., induced signal in the track from the Tx coil) may be defined to infer the distance from the load (i.e., shunt).

The results of this data analysis provide good insight about characterizing rail track impedance and highlight opportunities for further analysis that can benefit OBRD technologies. Further analyses and test experiments need to be conducted to achieve those goals. It is recommended that similar data collection and data analysis be performed over a section of track that corresponds to braking distance of trains in revenue service (e.g., at least 12,000 feet) to verify the track impedance data for such track lengths and the estimations done using the transmission line theory model.

4. Evaluation of Tx and Rx Coils

Several test cases were carried out in both environments to characterize the Tx and Rx coils. The testing culminated in testing the Tx and Rx coil on a moving locomotive. The selected locomotive did not have a running engine and was pushed by an active locomotive to keep the electromagnetic noise generated by the motor at a minimum to avoid corrupting the measurements of desired signal data being collected (Liu, C., Yang, S., Cui, Y., et al., 2020). The effects of engine noise (if any) will need to be determined and accounted for in the final OBRD system design.

4.1 Lab Testing

The research team performed lab testing in the Component Test Lab at the TTC. The laboratory test cases, designed to test how the Tx coil, including the RNB, were used to develop a baseline approach to the subsequent field testing. The laboratory test cases included:

- RNB
- Tx coil
- Rx coil
- Power supply amplifiers
- Signal generator
- Various loads

The testing moved to the field environment after determining the baseline testing, functionality, and parameters.

4.1.1 Lab Testing – RNB

The coil relies on a RNB to 1) increase the signal voltage going to the coil and 2) set the resonant frequency of the coil. The RNB is tuned to four specific frequencies that can be adjusted to a limited extent. The actual resonance point of each frequency varies based upon the objects located within the magnetic field produced by the coil. The RNB box testing provided a baseline of RNB functionality prior to the in-lab Tx coil testing.

4.1.1.1 Signal Generation: Theory of Operation

The core principle behind the OBRD concept is the induction of an emf in the rail that propagates the current through the rail and is detected by a Rx coil. A sufficiently large magnetic field needs to be generated by the Tx coil to generate a useful signal. The creation of such a field is accomplished by using a RNB that comprises a capacitor network and two symmetrical outputs that use the principle of resonance to increase the voltage applied to the Tx coil, generating a magnetic field proportional to the driving current. The magnetic coil is designed to work at four resonant frequencies, as shown in [Table 3](#), whose resonance points are determined by the configuration of jumpers in the RNB. The RNB consists of two equivalent circuits, each with an input and output to provide power to the two physical coils that reside inside the red Tx coil housing box. A standard signal generator provides the input signal to two amplifiers. The signal generation setup consists of ([Figure 28](#)):

- One signal generator: This component generates the driving signal, typically set at about 2–5 peak volts (V) as this puts the amplifiers into saturation.
- Two Kepco bipolar 400 W power supply amplifiers: This component amplifies the output of the signal generator to serve as the input to the RNB.
- A resonant network box: This component further increases the twin resonant signals to drive the Tx coil.
- A Tx coil: This custom component generates a magnetic field and induces an emf in a conductor (e.g., rail) within its magnetic field.

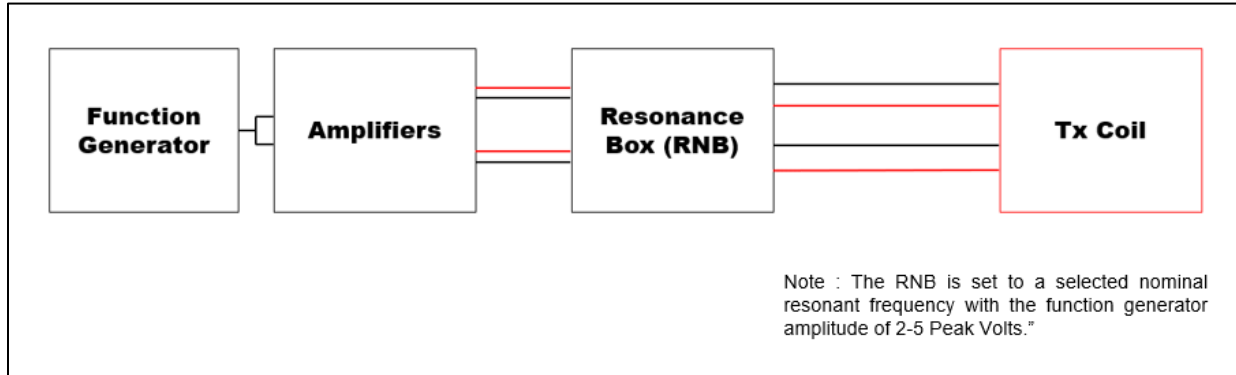


Figure 28. Diagram of Tx Coil and its Drivers

Table 3 shows the nominal resonance frequencies, jumper settings, and RNB output terminal currents.

Table 3. RNB Vendor Defined Jumper Settings

Resonance Frequency (Hz)	Jumper Settings	Current at A and B Terminals (rms)
1,420	All Jumpers Open	18 A
707	J2A J2B J4A J4B Jumped	30 A
419	J3A J3B J4A J4B Jumped	42 A
373	All Jumpers Jumped (Default)	48 A

The Tx coil generates a detectable magnetic field at a given resonance frequency setting.

4.1.1.2 Setup

The equipment was set up as depicted in Figure 29 following the setup instructions for the Power Supply, Resonant Network, and Tx coil.

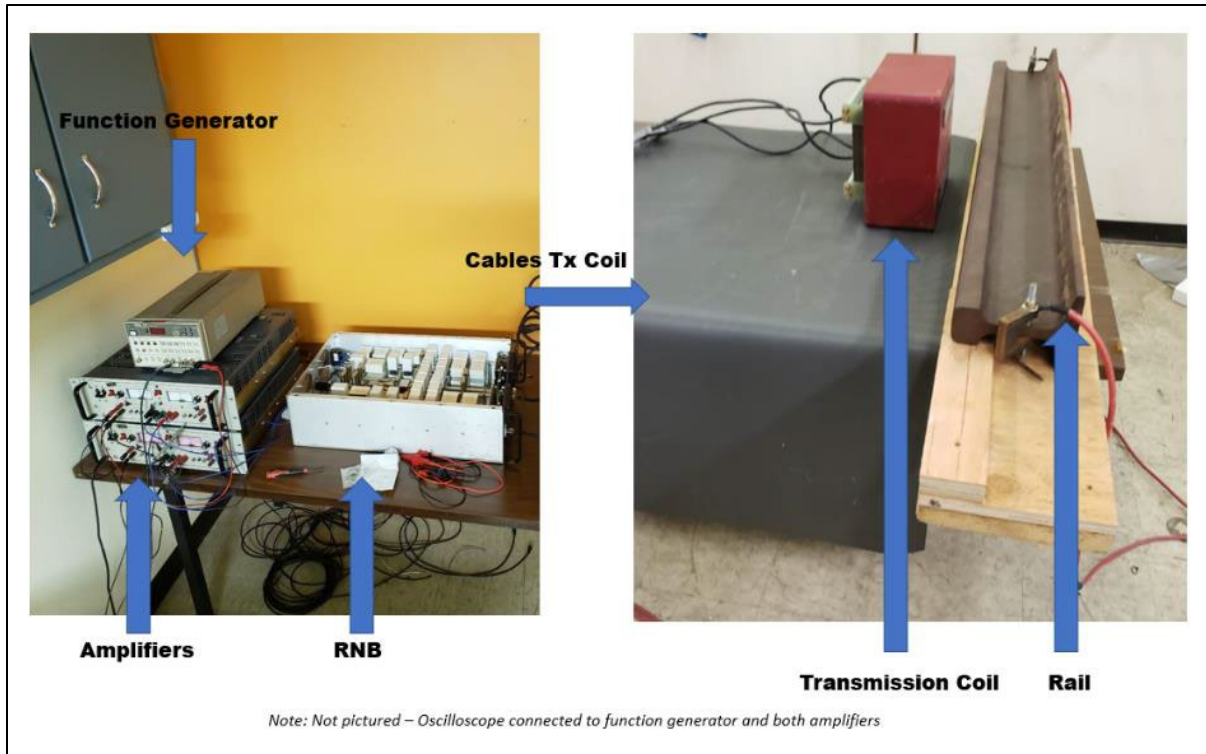


Figure 29. RNB Testing Setup

Power Supply Setup

- Connect both power supplies to 120 VAC sources.
- Each power amplifier must receive the same 3 V peak signal from the signal generator to ensure that each coil current is in phase with the other. Connect the signal generator across both “Voltage Programming Inputs.”
- Connect “Common” to “Ground” to ensure everything is grounded at this point.
- Connect voltage or current diagnostics tool (e.g., multimeter, oscilloscope, etc.) to monitor the power supply output.

Resonant Network Setup

- Connect the RNB to 120 VAC source. This only serves to power the fans to cool the capacitors that are switched on at the connector. The RNB electronics are passive. The fans should always be on during operation.
- On the back of the RNB, connect the “A” terminal to the “Output” of one of the power supplies. Connect the “B” terminal to the “Output” of the other power supply.
- On the back of the RNB, connect the “Common” from both power supplies to the “GND” terminal.
- Ensure that the wires used to connect the power supplies to the RNB are rated for at least 20 A/20 V.

The signal generator's output is split into the input of both power amplifiers to ensure the phase of the output of both amplifiers is in sync. One of the power amplifiers drives the "A" side of the RNB, and the other drives the "B" side of the RNB, as shown in [Figure 30](#).

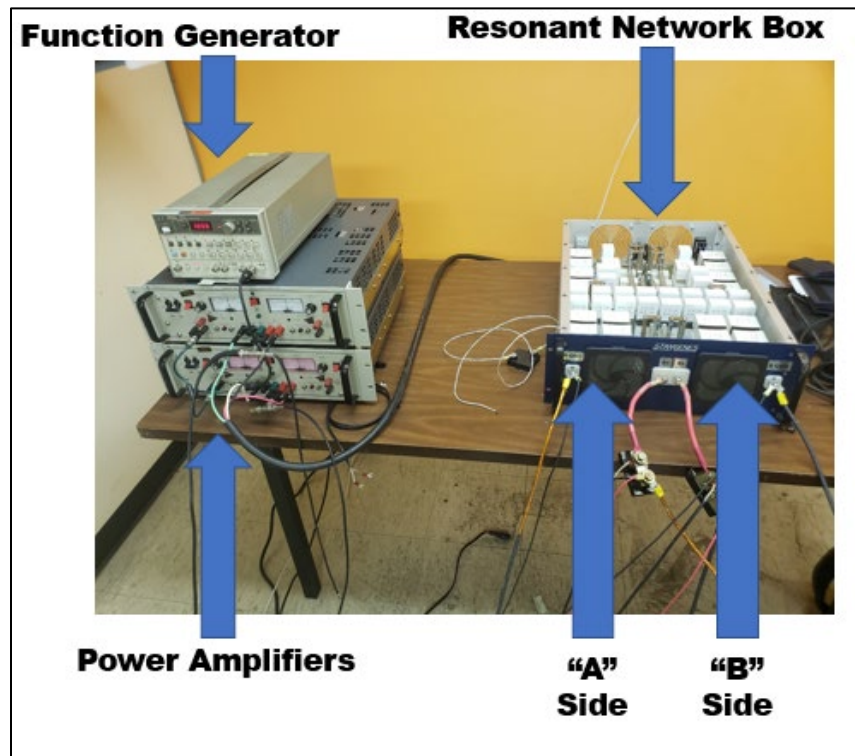


Figure 30. Resonance Signal Generation Equipment

The "A-" and "B-" side outputs are connected to the four inputs of the Tx coil.

Tx Coil Setup

- The polarity of the connections is important. If the polarity is incorrect, the magnetic fields will buck, the circuit will not work, and no field will be generated.
- From the front of the RNB, the "A+" terminal should be wired to the "A+" terminal on the magnet. Likewise, the "AGND" terminal should be wired to the "A-" terminal.
- From the front of the RNB, the "B+" terminal should be wired to the "B+" terminal on the magnet. Likewise, the "BGND" terminal should be wired to the "B-" terminal.
- If a wire extension needs to be made, ensure that the extension used is rated 100 A/2,000 V at the utilized frequency. Note that, electrically, these terminals are the most electrically dangerous of the circuit.

[Appendix B](#) contains the specifications and images of the Tx coil showing the terminals. According to the Tx coil simulation, the magnetic field generated with an at 80 A input per coil, at a point in the center of the magnet plane located 3 inches from the magnet is 300 Gauss.

4.1.1.3 Approach

The equipment setup instructions described above were followed to carry out the testing. The frequencies varied around the resonant point, and the data was recorded for all Jumper settings. The same signal generator was used as the input for each amplifier to ensure the signals had the same phase. The rail was used to measure the current induced by the coil.

4.1.1.4 Results and Analysis

The tests were first completed with one amplifier to verify that a current was induced. These tests were then followed up by a test with both amplifiers. [Table 4](#) and [Table 5](#) recorded and tabulated the results.

Table 4. Induced Signal Measurement with One Amplifier

Resonance Frequency (Hz)	Signal Generator Peak Voltage (V)	Amplifier 1 RMS Voltage (V)	Induced Rail Current (mA)
1,420	2	23.8	19
"	4	29.1	36
"	8	29	70
"	10	28	85
707	2	27.4	21
"	4	28	38
"	8	27.4	68
"	10	29.3	83
419	2	25	2
"	4	25	2
"	8	25	3
"	10	25	4
373	2	23.8	15
"	4	23.6	27
"	8	23	48
"	10	21	56

Table 5. Induced Signal Measurements with Two Amplifiers

Resonance Frequency (Hz)	Signal Generator Peak Voltage (V)	Amplifier 1 RMS Voltage (V)	Amplifier 2 RMS Voltage (V)	Induced Rail Current (mA)
1,420	2	27.1	32	142
"	3	26.8	32.3	211
"	5	25.6	31	341
"	7	24.7	29.4	458
707	2	31.4	37.3	168
"	3	31.4	36.7	265
"	5	30.4	37.9	440
"	7	29.1	35.6	590
373	2	25.6	3.02	198
"	3	25.3	4.35	293
"	5	25	7	464
"	7	24.8	9.8	613

Initially, the configuration for 419 Hz produced negligible voltage, as it was nowhere near its resonance point (as seen in [Table 4](#)). However, after stepping through frequencies and measuring the voltage at the output of the RNB, it was determined that the resonance point for the 419 Hz configuration was around 574 Hz. As evidenced by observing the measured output of the RNB at 419 Hz was at 1.7 V while at 574 Hz, the voltage was 180 V, indicating that the resonance frequency for that setting was closer to 574 Hz. Both measurements used the same 2 V Peak input signal from the signal generator.

4.1.1.5 Conclusions

The measurements yielded frequencies that closely match the original designed resonance points. The frequency table was updated, as shown in [Table 6](#).

Table 6. Updated RNB Resonant Frequency Jumper Settings

Resonance Frequency (Hz)	Jumper Settings
1,420	All Jumpers Open
707	J2A J2B J4A J4B Jumped
560–580	J3A J3B J4A J4B Jumped
373	All Jumpers Jumped (Default)

The resonance frequency ranges in [Table 6](#) were used for all subsequent testing.

4.1.2 Laboratory Testing – Tx Coil

The in-laboratory coil testing was performed to provide a baseline for the coil field testing. The in-lab test used a circuit consisting of inductors and resistors to simulate 2 miles of track. The coil relies on the RNB to amplify the voltage going to the coil and the set resonant frequency of the coil. The RNB can be adjusted around four specific frequencies. The actual point of resonance varies based upon the objects in the magnetic field produced by the coil, and from prior testing, which were found to be around 373, 560, 707, and 1,420 Hz.

4.1.2.1 Setup

The lab equipment and tools consisted of:

- One signal generator
- Two Kepco bipolar 400W power supply amplifiers
- RNB
- Tx coil
- Oscilloscope
- Multimeters
- National Instrument A/D, a data acquisition (DAQ) bucket with voltage measuring cards
- Resistors, capacitors, and inductors of various ratings
- Breadboard

Resonance Signal Generation Equipment Setup:

The amplified signal provided by the RNB powers the coil that operates as described in [Appendix A](#).

Tx Coil Setup:

The Tx coil was set up in two orientations as described below and shown in [Figure 31](#) and [Figure 32](#):

- Tx coil setup 1: Coil and rail on a table at distances of 1, 3, and 8 inches from the base of the coil to the top of the rail head.
- Tx coil setup 2: Coil in an aluminum stand at distances of 1, 3, and 8 inches from the base of the coil to the top of the rail head.

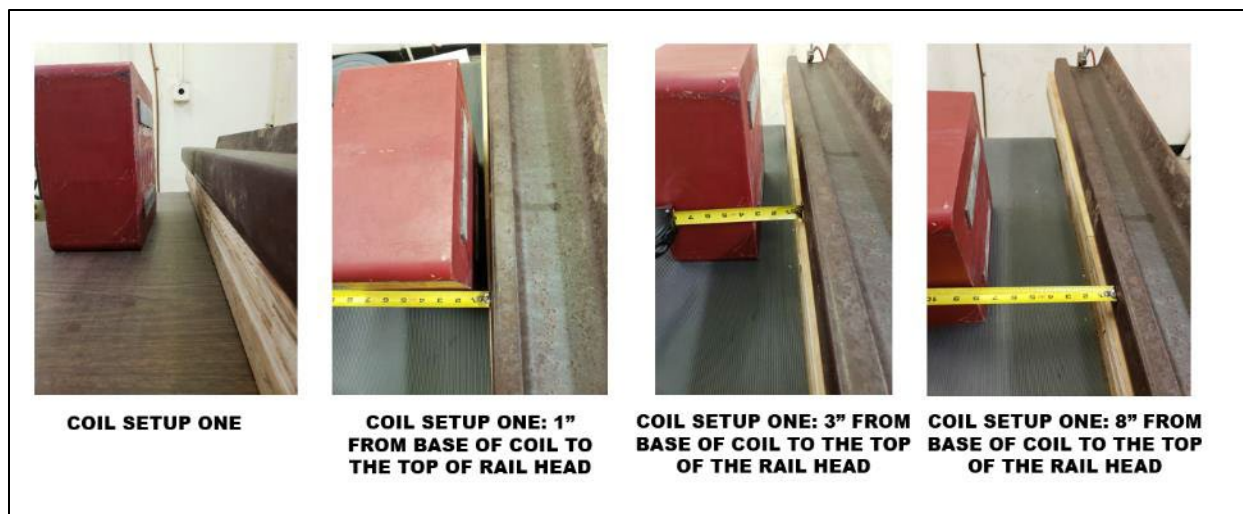


Figure 31. Tx Coil Setup One



Figure 32. Tx Coil Setup Two

Simulated Track Setup:

A circuit consisting of inductors and resistors was constructed on a breadboard to simulate the electrical properties of 2 miles of track. All resistors used were 1 percent tolerance, and inductors were un-shielded. The circuit layout and component values are shown in [Figure 33](#) through [Figure 35](#) shows the simulated track circuit built on a breadboard. The inherent series resistance of the inductors was comparable to the value of the resistance of the rail, so the series resistors were not used.

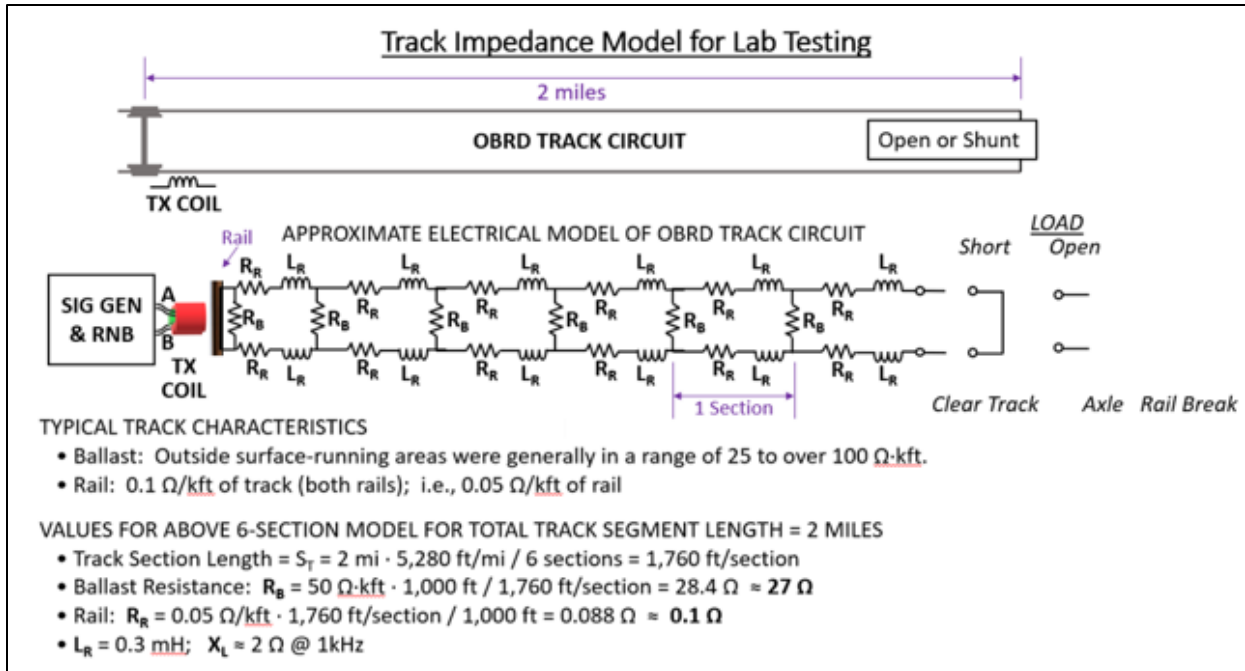


Figure 33. Track Impedance Model Used for Lab Testing

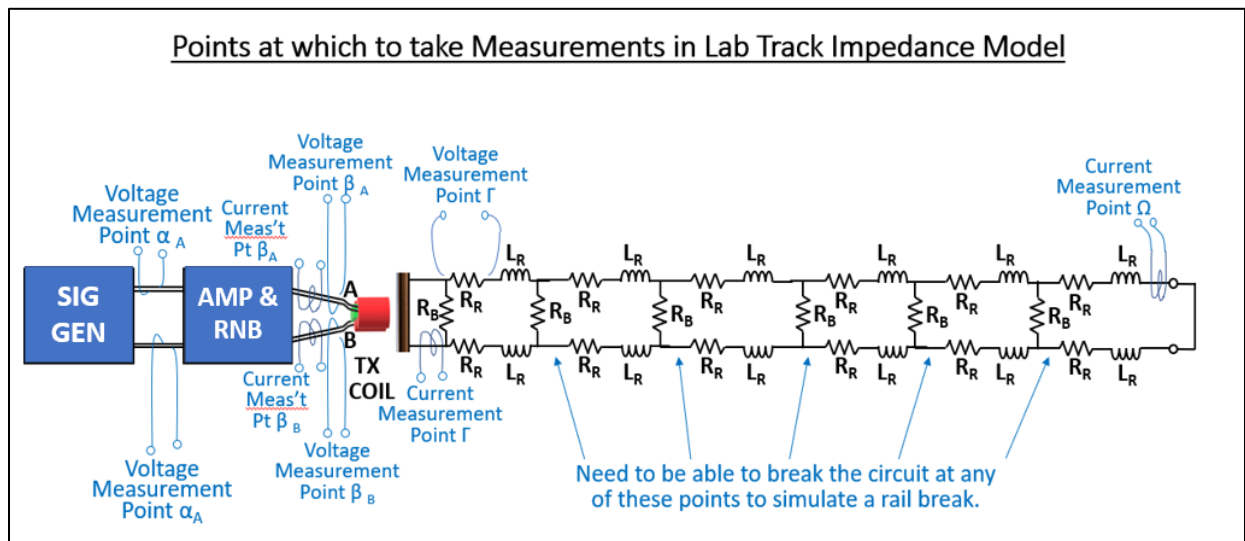


Figure 34. Lab Track Impedance Model Measurement Setup

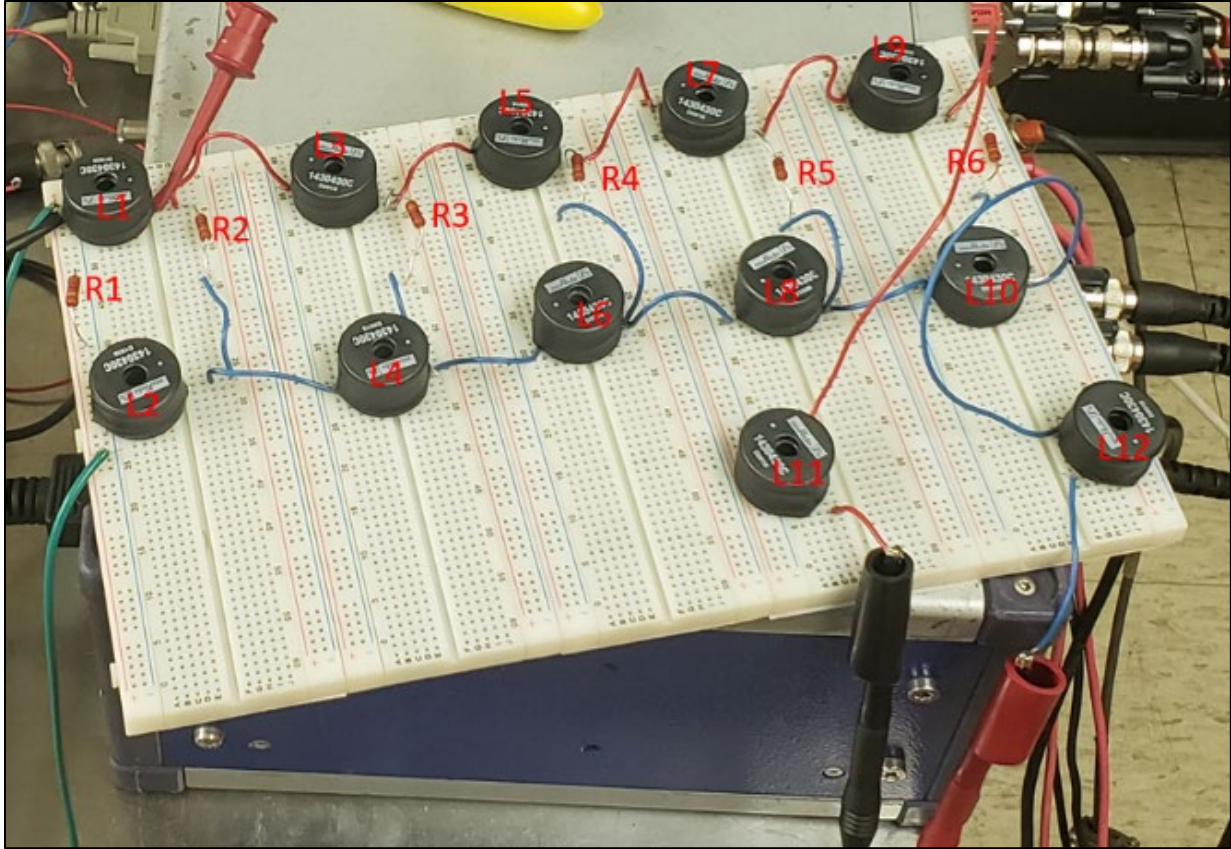


Figure 35. Image Simulated Track Circuit

4.1.2.2 Approach

The equipment setup instructions were followed in accordance with [Appendix A](#). The frequencies were varied around resonant points, and the data was recorded for all coil setups.

A DAQ bucket with voltage measuring cards and DAQ software were used to acquire data. Voltage measurements were taken at the output of each power amplifier and at the A- and B-side outputs of the RNB. Current measurements were made at the output of the A and B sides of the RNB. Measurements on the simulated track circuit breadboard were taken using a multimeter.

As referenced in the [Figure 34](#), the following measurements were taken:

- Alpha measurements: Voltage readings between the signal generator and signal amplifiers
- Beta measurements: Voltage and current readings between the amplifiers and Tx coil
- Gamma measurements: Voltage and current readings of the first simulated track section
- Omega measurements: Voltage and current readings of the last simulated track section

4.1.2.3 Results and Analysis

Measurements were taken at the resonance point for each frequency setup and two frequencies above and below resonance for a total of five measurements at each frequency setup. These measurements provide insight into the loss of power as the input signal frequency strays from the

resonance point of the system. Each frequency was tested with a short and an open circuit at the load. A sample graph of gamma and omega measurements around a nominal resonant frequency of 345–400 Hz are shown for various heights above the rail at the table and the stand (Figure 36).

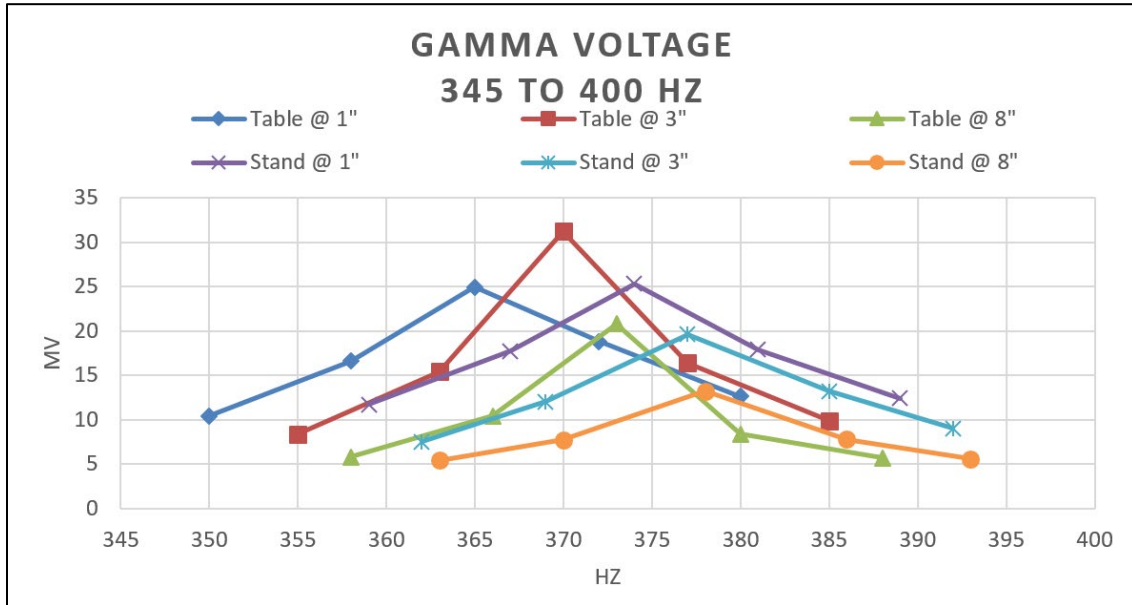


Figure 36. Gamma Voltage Measurements from 345–400 Hz

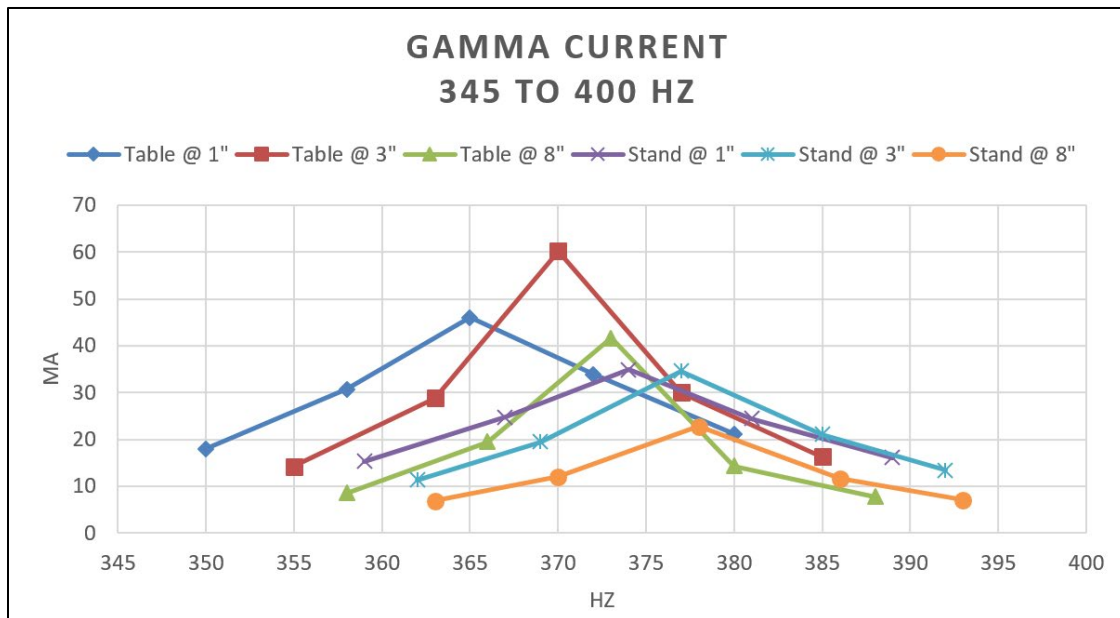


Figure 37. Gamma Current Measurements from 345–400 Hz

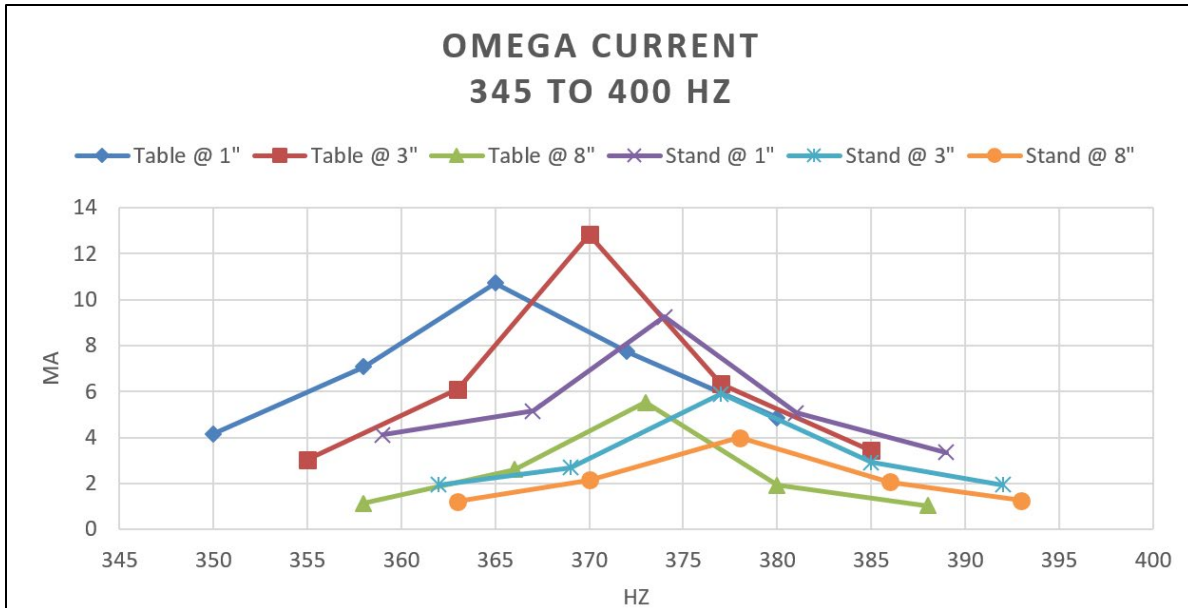


Figure 38. Omega Current Measurements from 345 Hz–400 Hz

Supplemental numerical values for test results and graphs with additional data can be found in [Appendix D](#).

The collected data was analyzed and these observations were made:

Resonance Shifts: As expected, the system’s resonant frequency varies based upon what the magnetic field encompasses. During the “Table” testing, the resonant point for each system configuration was about 3 percent lower than the resonance points for the “Stand” testing.

RNB Configuration: In all four frequency configurations, the current was detected on the level of tens of millivolts at the end of 2 miles of simulated track built on a breadboard. The 560 Hz configuration seemed to outperform the other configurations for each test.

4.1.2.4 Conclusion

The success of the in-lab testing was quantified by detecting a reasonable amount of current at the end of 2 miles of simulated track in all frequency and test setup configurations.

It was noted that the current induced into the circuit drops off quickly as one strays off the resonance set point. In general, the induced current varied as follows:

- ~60 percent of current induced when 2 percent off-resonant frequency
- ~40 percent of current induced when 4 percent off-resonant frequency

The in-lab testing provided insight into how the system works and promising results to carry into field testing. This insight was used in designing the scenarios for static and dynamic testing.

4.1.3 Lab Testing – Rx Coil

In-lab tests were conducted to test a locomotive cab signal Rx coil and a handmade Rx coil. A portable cab signal (PCS) tester was used to test common cab signal frequencies, and the signal generator setup was used to test the frequencies that aligned with the resonant frequencies of the

transmit coil. This test was carried out to characterize and compare the performance of the Rx coils. Tests were conducted at varying frequencies and heights to determine the amount of signal induced from the test circuits into the coil.

4.1.3.1 Setup

A signal generator and amplifier were used to supply the test signal with an ammeter in series to measure the detected current. The PCS tester includes a display showing input current (see [Appendix H](#)). The Cab Signal Tester and signal generator setups are shown in [Figure 39](#) and [Figure 40](#), respectively.

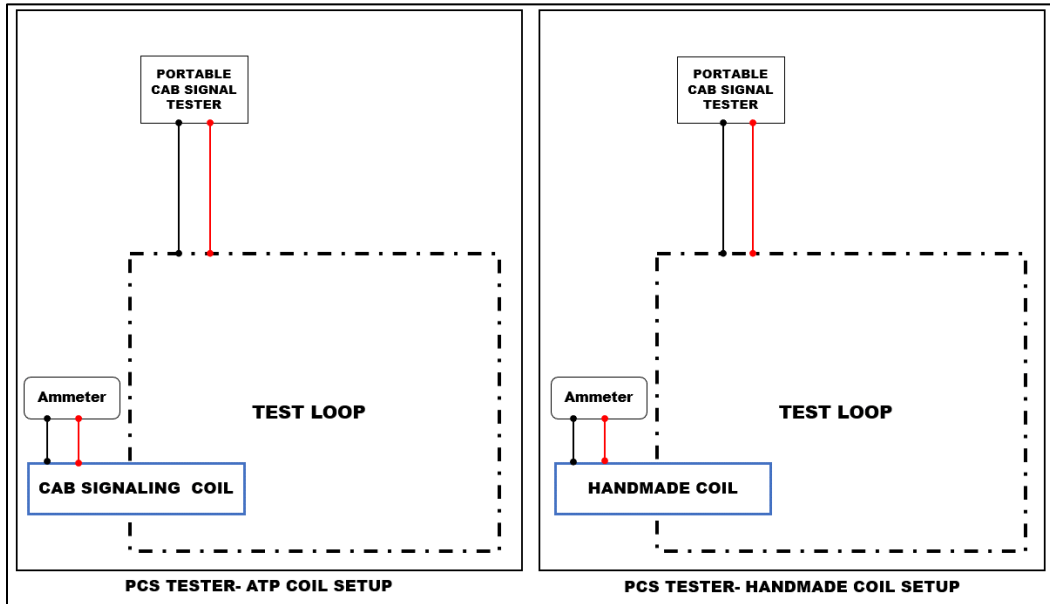


Figure 39. Portable Cab Signal Tester-Rx Coils Setup

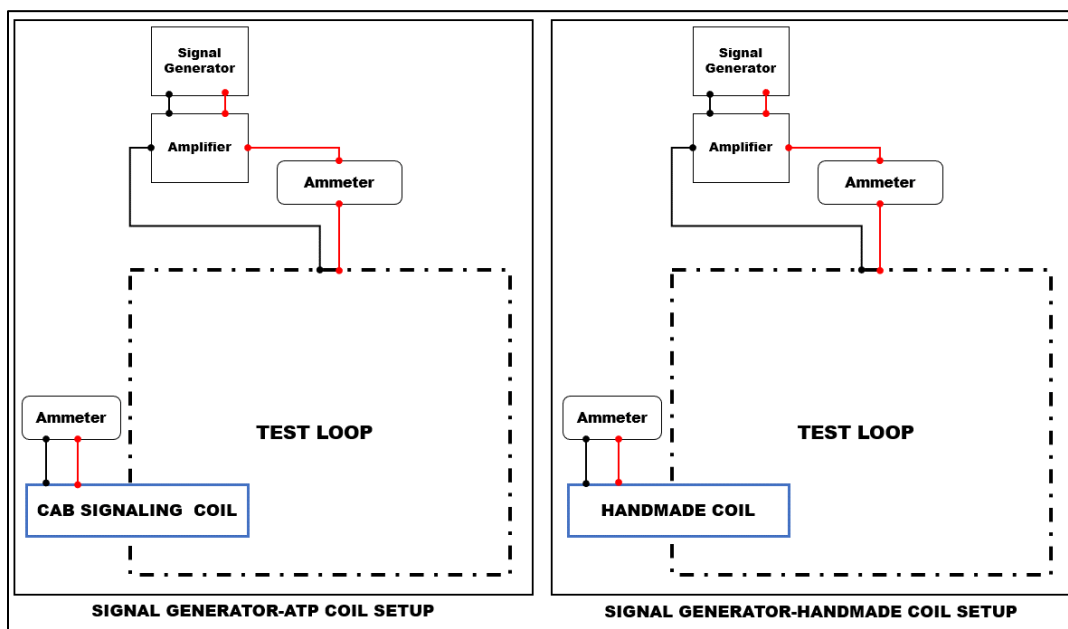


Figure 40. Signal Generator-Rx Coils Setup

4.1.3.2 Approach

Tests were conducted using two different setups. First, the 60 and 100 Hz tests were conducted using a PCS receiver tester. The signal generator setup was used for 373, 560, 707, and 1,420 Hz. The wires used to connect both input configurations (PCS tester and signal generator/RNB setup) and the PVC test loop had a resistance of 0.8 Ω .

Two types of coils were tested:

- The cab signaling coil used is an Alstom Automatic Train Protection (ATP) Rx coil.
- The handmade coil was constructed using braided aluminum wire wrapped about 65 turns around a 3 inch diameter iron metal pipe.

4.1.3.3 Results and Analysis

A baseline of the induced magnetic field was measured using a gaussmeter at 1 inch above the test loop. Testing with the gaussmeter directly measures the background magnetic field and background magnetic fields in the X, Y, and Z directions. The orientations of the gaussmeter are shown in [Figure 41](#).

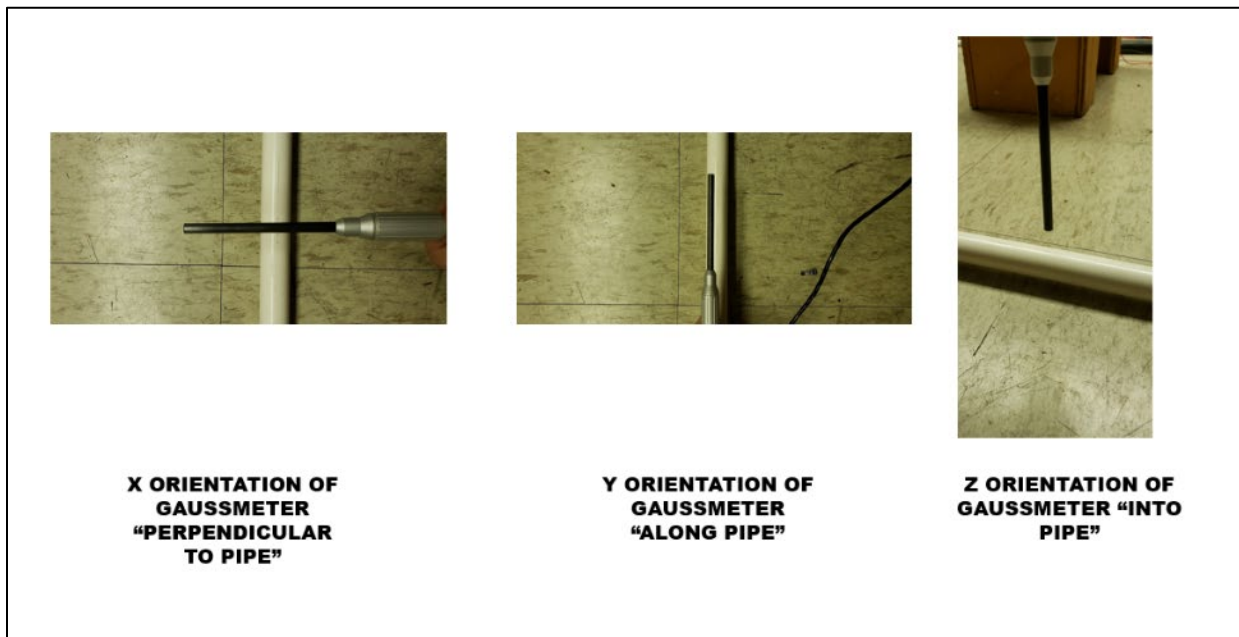


Figure 41. Gaussmeter Testing Orientation

The gaussmeter measurement results are tabulated in [Table 7](#).

Table 7. Gaussmeter Measurements

Frequency (Hz)	Loop Current Input (mA)	Perpendicular to Pipe “X” (G)	Along the Pipe “Y” (G)	Into Pipe “Z” (G)	Background (G)
60	1,400	0.071	0.004	0.061	0.003
100	1,400	0.075	0.004	0.062	0.003
373	516	0.023	0.004	0.021	0.003
560	510	0.026	0.004	0.02	0.003
707	504	0.028	0.004	0.022	0.003
1,420	465	0.014	0.004	0.013	0.003

Testing was conducted at 0 inch (coils in contact with the test loop) and 8 inches above the loop. The 0-inch test provides the best-case scenario as the magnetic field generated by the test loop is the strongest at the core of the test loop. The 8-inch test shows the worst-case scenario as the magnetic field generated by the test loop is at the furthest coil placement height defined for this project. The results were tabulated in [Table 8](#) and [Table 9](#).

Table 8. Rx Coil Readings at 0 Inch from Test Loop

0 Inches Above Loop	Cab Signaling Coil		Handmade Coil	
Frequency (Hz)	Input Current (mA)	Induced Current through Coil (mA)	Input Current (mA)	Induced Current through Coil (mA)
60	1,400	1.04	1,400	0.98
100	1,400	1.71	1,400	1.41
373	527	2.22	530	0.86
560	522	3.17	524	0.99
707	517	3.84	518	1.07
1,420	477	6.28	478	1.25

Table 9. Rx Coil Current Measurements at 8 Inches from the Test Loop

8 Inches Above Loop	Cab Signaling Coil		Handmade Coil	
	Input Current (mA)	Induced Current through Coil (mA)	Input Current (mA)	Induced Current through Coil (mA)
60	1400	0.51	1,400	0.28
100	1400	0.81	1,400	0.45
373	502	1.01	506	0.37
560	496	1.46	501	0.42
707	493	1.78	496	0.46
1,420	458	3.12	460	0.55

4.1.3.4 Conclusion

The handmade coil was able to detect current at 0 and 8 inches, but it did not perform as well as the cab signaling coil. A significant amount of improvement can be made to the handmade coil, including designing a pickup coil optimized for use with the Tx coil. However, further coil optimization was halted due to time constraints, and the ATP/cab signaling coil was selected for subsequent static and dynamic tests.

4.2 Field Testing – Static and Dynamic

Static and dynamic tests were both carried out on the TTT. The TTT consists of 119 pound/yard jointed rail up to T33 that transitions to welded rail with a mix of wood and concrete ties spaced approximately 19 inches apart interspaced by clean ballast. The test area varied from T21–T39 for different tests, an area that is divided by IJs into three blocks that segment the track every 6,000 feet (~1.1 miles). [Figure 42](#) illustrates the TTT test areas (in red) with key test locations highlighted (in green).

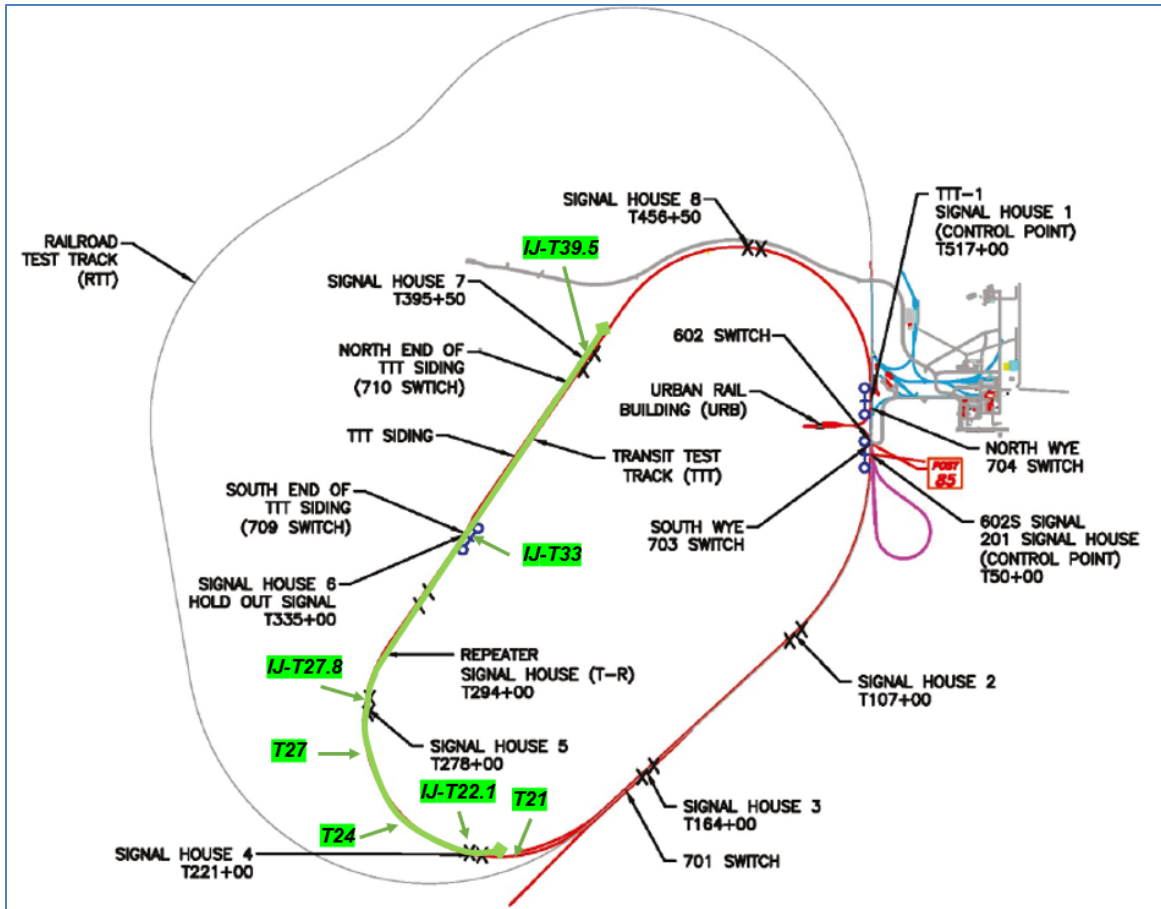


Figure 42. TTT Testing Zone

Test cases were carried out both clockwise (increasing milepost direction) and counterclockwise (decreasing milepost direction). The IJs were located across from the signal houses and were shunted or open depending on the testing being carried out. Prior to the OBRD tests, the IJs were tested using both a Rogowski loop and multimeters to ensure their functionality. IJ readings were then recorded and rechecked prior to every cycle of testing ([Appendix E](#)).

The TTT test area with key points highlighted are listed below:

- Signal house 4 – T210+00 (T21.0)
- Insulated joint 21 – T210+00 (T21.0)
- Signal house 5 – T278+00 (T27.8)
- Insulated joint 27 – T278+00 (T27.8)
- Signal house 6 – T335+00 (T33.5)
- Insulated joint 33 – T335+00 (T33.5)
- Switch 709 – T335+06 (T33.6)
- Switch 710 – T38 +70 (T38.7)
- Signal house 7 – T395+50 (T39.5)

- Insulated joint 39 – T395+50 (T39.5)

Depending on the dynamic test case being carried out, the switches were either lined for normal movement or reverse movement on the main track. In addition, some grounding and shield tests were carried out in the siding between Switch 709 (T33.6) and Switch 710 (T38.7). The connections from the bungalows to the track are made via insulated underground 50-foot 6-gauge cables.

4.2.1 Static Testing – Tx Coil

This section provides the setup, results, and analysis of the OBRD static testing, including testing the Tx coil over three (6,000 feet) block lengths on the TTT. The analysis covers an assessment of the electrical signals induced, propagated, and detected in the rail tracks and the field testbed variables that affected the results obtained.

The static test with both the Tx and Rx coils was carried out to determine the induced signal propagation range and detectability. The field coil test was performed on the TTT track from T39 to T21 ([Figure 42](#)). Three scenarios were performed for each set of test distances:

- No signal
- Occupancy with signal
- No occupancy/Broken Rail (BR) with signal

The Tx coil was placed on a stand across the rail.

4.2.1.1 Setup

The static tests included testing the Tx coil over three block lengths on the TTT using the following equipment.

- One Signal generator
- Two Kepco bipolar 400W power supply amplifiers
- The resonant network box (see [Section 4.1.1](#) for explanation of the RNB)
- The Tx coil
- Ohmmeter/Ammeter
- Test shunts – 6 gage cables²

The field and equipment setup included the following:

- Location: TTT
 - Track location: TTT MP T21–T39

² Since the focus of this research was to determine if a sufficiently useful signal can be induced/detected and how far it can propagate under baseline conditions, broadband (wire) shunts were used in the testing rather than tuned shunts. This was done to avoid creating undesired variable effects upon rail impedance that could be caused by reactive shunts.

- Type of ties: Concrete, wood
- Ballast condition: Dry
- Ballast resistance: Various (see tests)
- Rail type: Welded
- Coil heights from rail:
 - Tx coil: 3–8 inches
 - Tx coil: Mounted on a fixed metal frame mount (not on a locomotive)
- Tx coil electrical settings:
 - Signal generator: 3 V peak
 - RNB output: Various
 - Frequency: Various

Pretest Setup

The pretest setup consisted of the track circuit shunted on one end with a multimeter set to measure resistance (ohms). The test track for measuring the track resistance was setup as shown in Figure 43. The shunt was progressively moved from T33 to T21 with the IJs in the middle of the test block were shunted to increase the measured block length.

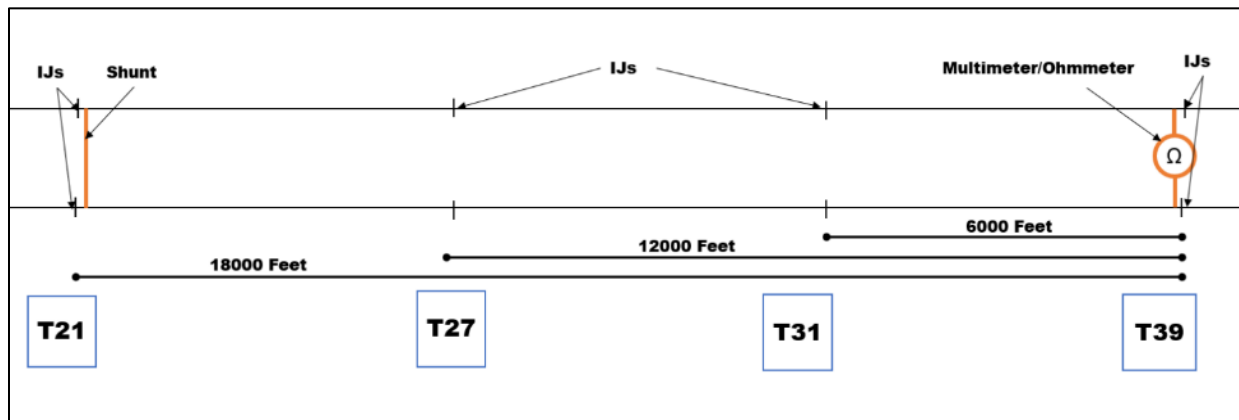


Figure 43. Track Resistance Measurement Setup

Tx Coil Setup

The Tx coil was mounted on a metal frame mount at varying heights of 3–8 inches above the rail (not attached to a locomotive). A stationary locomotive that housed the signal generation equipment was placed just before the insulated joint of the test block to avoid shunting the track and to allow for enough clearance for the Tx coil to be inside the test block. Figure 44 and Figure 45 illustrate the respective setups.

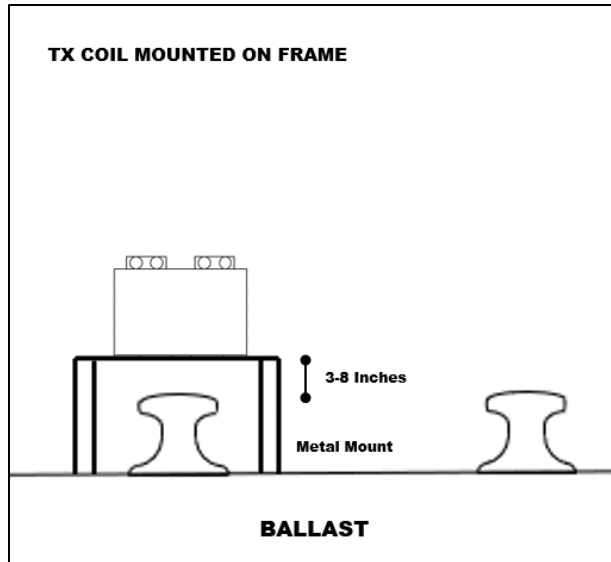


Figure 44. Tx Coil Setup for Static Testing

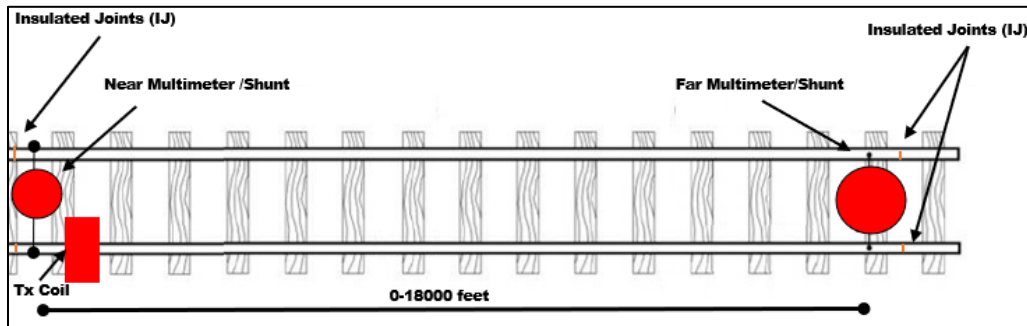


Figure 45. Test Setup for Static Testing

Three block lengths were selected for testing. The connections were made through the Association of American Railroads (AAR) terminals at the respective bungalows. The test block lengths were 6,000, 8,000, and 12,000 feet. The AAR terminals are connected to the track via insulated 50-foot, 6-gauge cables. The field setup for each block length is shown in [Figure 46](#) through [Figure 48](#), respectively.

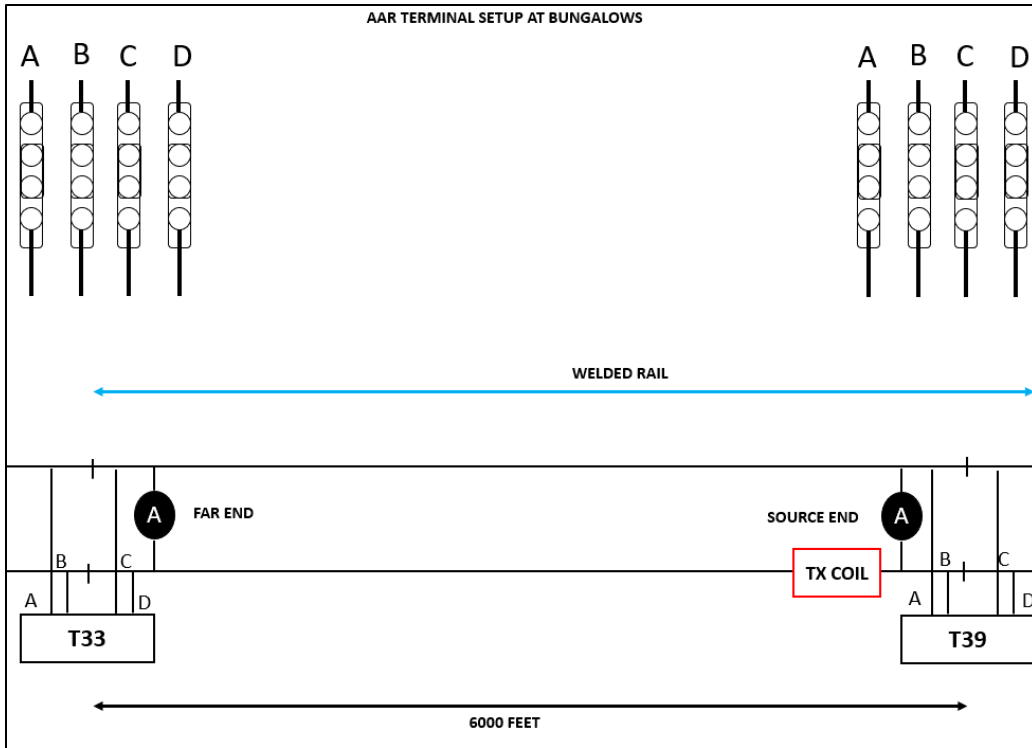


Figure 46. 6,000-foot Block Configuration for Static Testing

The total resistance of the 6,000-foot track block as measured at T39 with a shunt at T33 was 0.4 ohms.

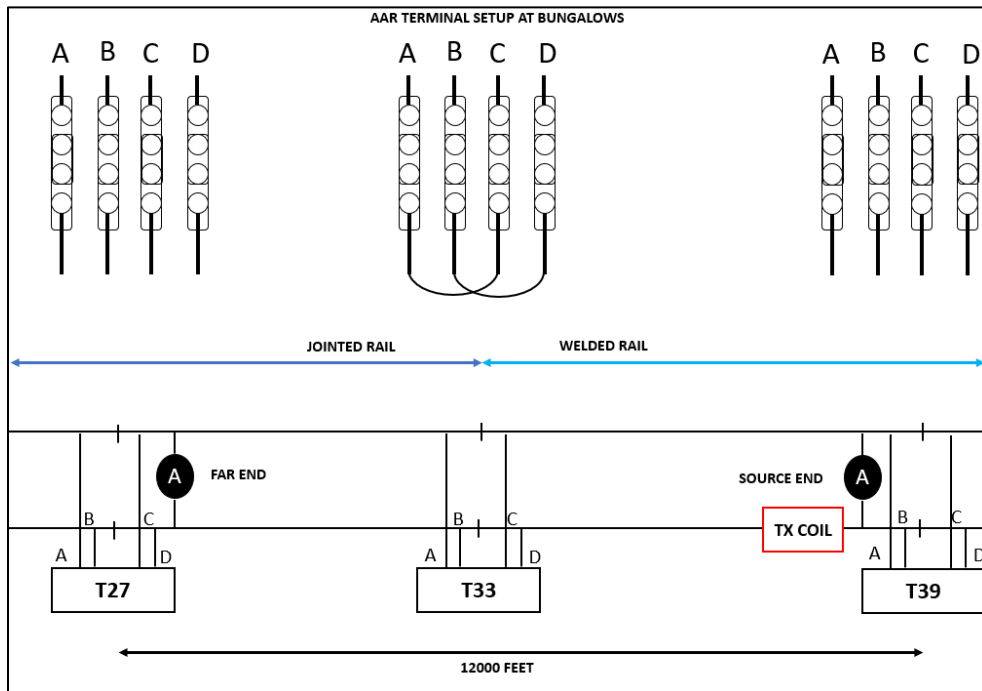


Figure 47. 12,000-foot Block Configuration for Static Testing

Based on the ohmmeter reading, the total resistance of the 12,000-foot circuit loop was 3.3 ohms. Two sets of tests were performed, each with a different height and each height with four different frequencies.

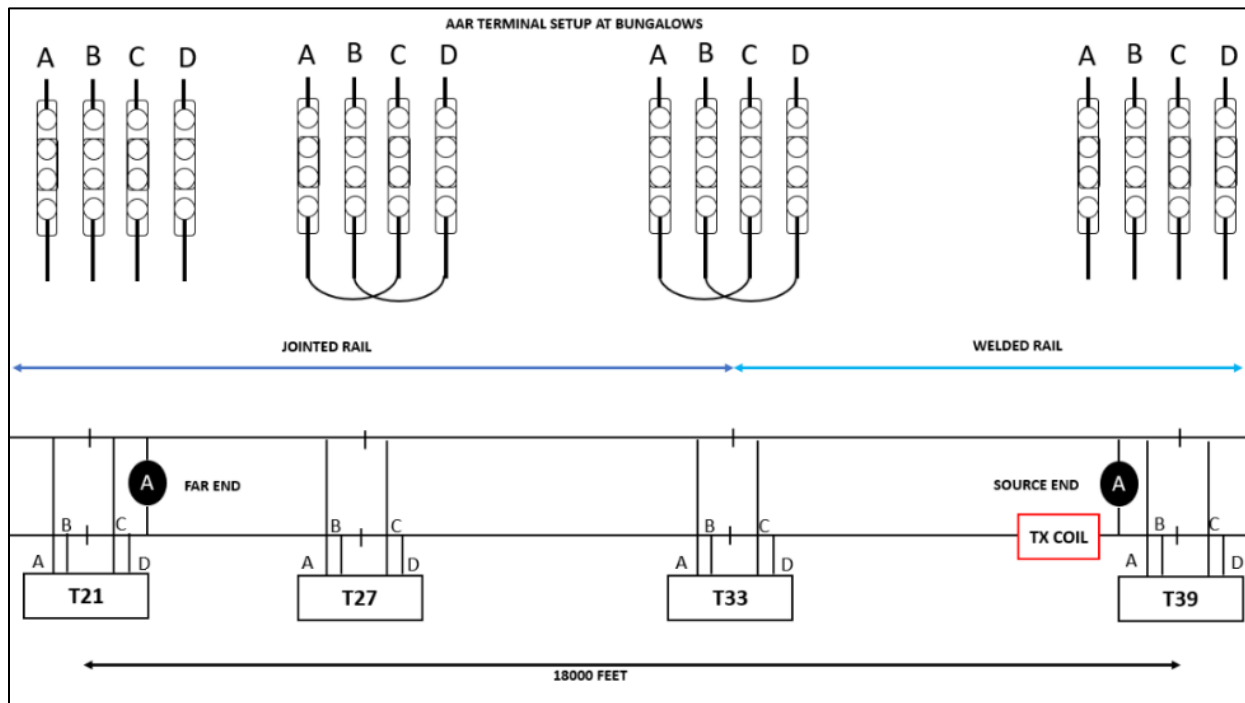


Figure 48. 18,000-foot Block Configuration for Static Testing

The 18,000-foot test was carried out to prove that an induced signal may be able to propagate beyond 2 miles. Due to a higher-than-expected impedance observed at T27, the total resistance of the 18,000-foot track was 19.5 ohms.

4.2.1.2 Approach

Prior to the testing, the track resistances were measured for various block lengths. The resistances of the various blocks were measured using an ohmmeter across the track at one end and a shunt across the track on the far end to complete the circuit. The shunt was set at T33 (6,000-foot block), T27 (12,000-foot block) and T21 (18,000-foot block), and ohmmeter readings were measured and recorded at each location. To get the longer block lengths of 12,000 feet and 18,000 feet, the IJs at T33 and T27 were shorted, respectively. An “X”-foot-long block of measured track implies a track circuit of “2X” feet.

The track resistance measurements were followed by the Tx coil testing. The first phase of static tests included testing the Tx coil over three block lengths on the TTT. The Tx coil equipment setup instructions as described in [Appendix A](#) were followed. The frequencies were varied around the nominal resonant frequency. Distances of the Tx coil from the shunt and Tx coil heights above the rail were varied, and the data was recorded. Testing at one coil height (1–8 inches) with one frequency setting (nominal frequencies of 373, 560, 707, and 1,402 Hz) was performed, and the measured signal data recorded. Frequencies were varied from the nominal frequency because the coupling with the rail slightly shifted the peak resonant frequency.

4.2.1.3 Pretest Track Resistance Measurement Results and Analysis

The block lengths and the resistance measured for each block for the setup in [Figure 43](#) are shown in [Table 10](#).

Table 10. Resistances of Three Test Track Blocks

Block	Block Length (ft)	Resistance (ohms)
T39–T33	6,000	0.4
T39–T27	12,000	3.3
T39–T21	18,000	19.5

Observations on the resistance of the test blocks include:

- The 6,000-foot block has values in the expected range since typical track resistance is approximately 0.02 ohm/1,000 feet and track cables are 0.1–0.2 ohms.
- The 12,000-foot block shows higher resistance than expected track resistance values for a nominal 12,000-foot section of railroad track, which could cause the detected induced current signal to be lower than nominal values.
- The 18,000-foot block shows much higher resistance than the expected values, which would significantly affect an induced current signal.
- The high resistances may have been a result of the 50-foot cables between the track and the bungalows or the bad conditions of the jointed track sections between T33 and T21. The results of the detected signal clearly show the effect of the high resistance blocks on the detected induced current signal as shown in [Figure 51](#). Typically, the resistance of these blocks should be much lower, resulting in a higher detected signal.

4.2.1.4 Tx Coil Tests Results and Analysis

[Table 11](#) summarizes the test data from the executed tests, where the red check marks indicate combinations of tests performed. [Table 12](#) summarizes the data collected for the 6,000-foot, 12,000-foot, and 18,000-foot track lengths.

Table 11. Summary of Executed Tests

Block length	12,000 feet		18,000 feet		6,000 feet	
Height	3 inches	8 inches	3 inches	8 inches	3 inches	8 inches
Frequency (Hz)						
377	✓	✓				
560	✓	✓		✓		✓
707	✓	✓				
1420	✓	✓				

The data for each length of the test track and coil height combination is shown in [Table 12](#) followed by an analysis of the tabulated data. [Table 12](#) also shows the output voltage of the RNB and the open-circuit voltage at the shunt at different frequencies. The Resonant Frequency column shows the actual setting the signal generator was set to so as to achieve optimal Tx coil resonance. The table is followed by various graphic illustrations of the data. [Figure 47](#) shows a plot of results for each Frequency/Height Set defined in [Table 12](#).

Table 12. Static Test Measurements with Tx Coil at Various Heights from Rail and Distances from Far End Shunt

Frequency/Height Set	Block Length (ft.)	Coil Height Above Rail (in.)	Resonant Frequency (Hz)	RNB Output Peak Voltage (V)	RNB RMS Voltage Across Resistor (mV)	Closed Loop Far End Shunt Current (mA)	Closed Loop Far End Noise Floor (mA).	Closed Loop Source End Shunt Current (mA)	Closed Loop Source End Noise Floor (mA)	Open Loop Far End Voltage (mV)	Open Loop Ballast Current (mA)
1	6,000	8	586	445	132	54	4	52.8	1.41	533	6.3
2			378	185.9	58.1	26	4	28.5	2.1m	307m	-
3		3	586	349.8	145.3	35	4	35.2	2.1	566	13
4			716	234.3	97.2	18	4	20.3	2.1	374.5	-
5			1,448	278.6	215.5	11	4	12.33	2.1	490	13.78
6			378	223.2	40	19	4	20.95	2.1	234	-
7		8	586	440	103.1	26.6	4	27.99	2.1	444	15.96
8			719	296.6	70.2	14	4	15.86	2.1	298	10.16
9			1,448	376.1	181.9	9	4	10.6	2.1	404	11.68
10			586	440	102.1	17	5	21.1	3.2	444	16.89

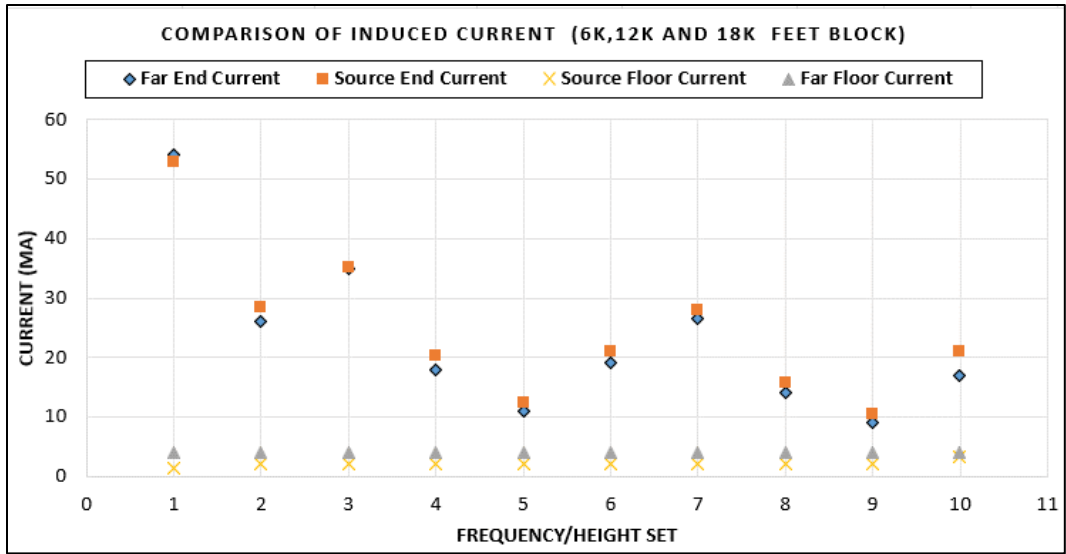


Figure 49. Comparison of Induced Currents at Far and Source Ends at Various Tx Coil Heights Above Rail and Distances from Far-End Shunt for Static Tests

From Figure 49, note that the induced signal measured at the far end of the rail can be discerned from the noise floor for all signal frequency heights.

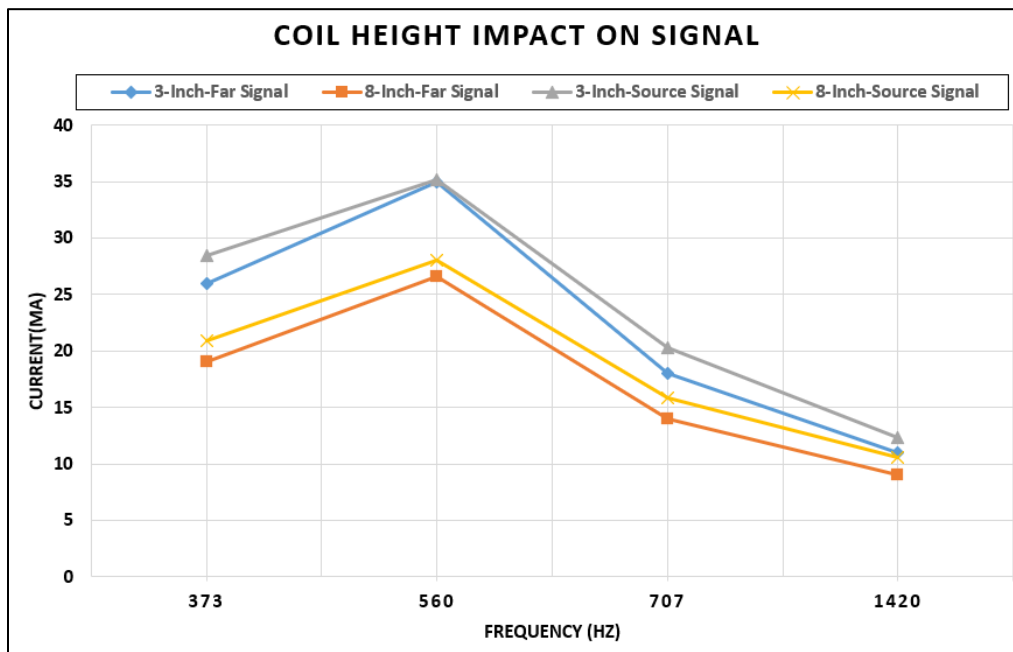


Figure 50. Comparison of Induced Current at Far and Source Ends at 12,000 feet vs. Tx Coil Height at Different Frequencies

From Figure 50, see that the height of the coil above the rail has an impact on the induced signal. This is expected as the magnitude of the induced current due to the magnetic field crossing the rail is inversely proportional to the distance between coil and rail.

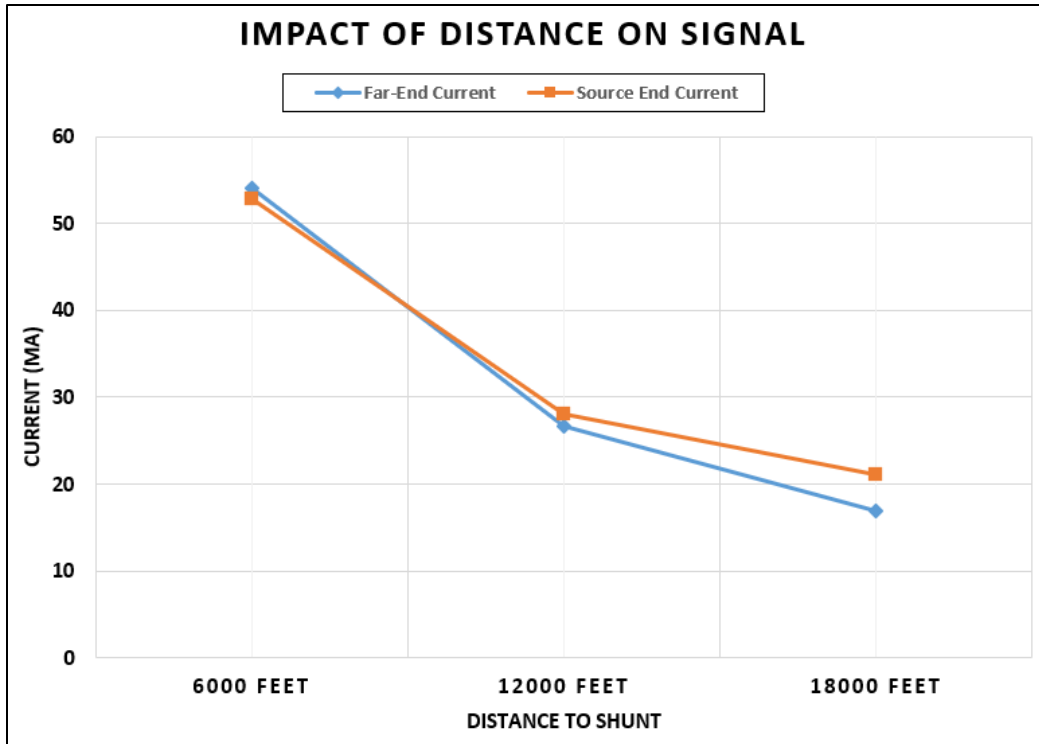


Figure 51. Comparison of Induced Current at 568 Hz to Distance from Source

Based on [Figure 51](#), observe that distance (or track resistance, as the resistance increases with the length of the track) affects the signal. It should be noted that, due to a higher-than-expected resistance between the 12,000-foot and 18,000-foot section, the measurement at 18,000 feet may contain some error. However, it displays the relationship between the track block length and signal, showing the signal strength is inversely proportional to the distance from the source. Additionally, it shows the possibility of propagating the induced signal beyond 12,000 feet.

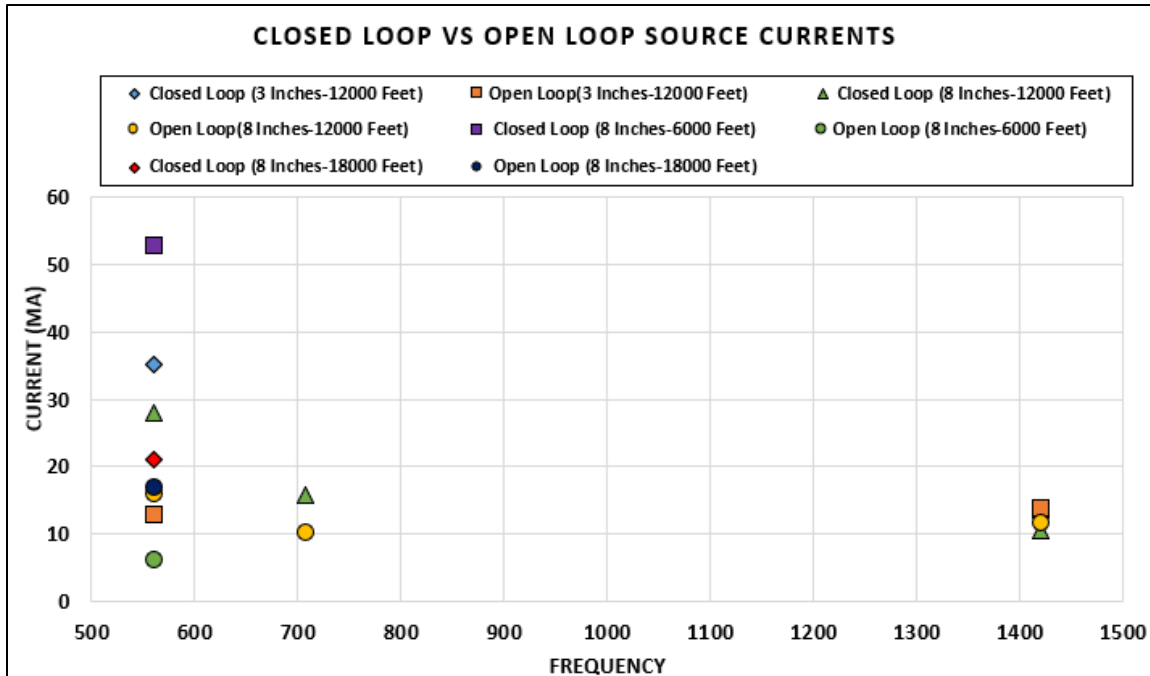


Figure 52. Comparison of Induced Current at Far and Source Ends for Closed (Shunt) and Open (No Shunt) Track Circuit at Different Tx Coil Heights and Different Frequencies

The following can be inferred from the data above:

- The test results in [Table 12](#) show the Tx coil can induce a distinguishable signal from the noise floor or open shunt in which the signals are measured. The frequencies affect the magnitudes of the voltages and therefore, the current induced in the rails.
- As shown in [Figure 49](#), the cases that use a nominal signal frequency of 560 Hz where the Tx coil is mounted at heights of 3 and 8 inches perform best.
- In all cases, the induced closed loop current in the track is significantly higher than the noise floor, while the open-circuit current is larger than the closed shunt signal in a few cases, as shown in [Figure 52](#), where the test signal frequency is set at 1,420 Hz.
- From [Figure 52](#), it can also be observed that the ballast will complete the circuit when there is no shunt. For some frequencies, the difference in rail impedance may not be large enough to distinguish between a shunted (occupancy) state versus the open (broken rail) state of the track circuit (due to current flowing through the ballast). However, if the clear track state (no rail break and no occupancy) is distinguishable from the non-clear state (rail break and/or occupancy), the system will be able to determine the state of the track.
- The 12,000-foot block and the 18,000-foot block have a much higher rail resistance than the expected values at normal rail conditions with 3.3Ω and 19.5Ω , respectively. This resistance is a major reason for low induced-current values in the tests done on those blocks. The Tx coil should perform better if tested with track sections that have more typical resistance values.
- The detected current with an open loop track circuit could be higher if tested under wet ballast conditions. Therefore, the induced signal in shunted scenarios may not be

distinguishable from non-shunt scenarios for some cases that showed positive results in this test.

4.2.1.5 Conclusions

Occupancy detection:

By comparing the track circuit loop measurements with the ballast loop measurements, a significant difference between closed-circuit loop current versus ballast loop current can be confirmed for certain frequencies, so it is possible to design a function to detect a shunt (for detecting train occupancy).

Broken rail/roll-out detection:

By comparing the track circuit loop measurements with the ballast loop measurements, the difference between a good track circuit loop and a broken rail/no occupancy loop, which can detect a rail break between two trains, can be identified. Rail break detection is an initial design prerequisite for an alternative broken rail and rollout detection (ABRRD) system that will meet the needs of FMB.

For real-world operations, the system would require tuned shunts to act as band-pass filters to enable the detection of a rail break at different intermediate distances in advance of a train, up to at least the train's braking distance. Use of tuned shunts will also allow the system to distinguish an occupancy ahead versus clear track or a rail break.

Closest shunt detection:

This field test proved that this system could induce a sufficient track signal that could be detected at distances up to at least 18,000 feet from the Tx coil. This test result provides the basis to support conducting further analysis that focuses on performance and functionality possibilities.

All the above insights were used in designing further static testing scenarios.

4.2.2 Static Testing – Tx Coil and Rx Coil – Locomotive

A locomotive with the Tx coil attached with an aluminum frame (Figure 54, left-hand side) was introduced into the field testing, and this configuration is referred to as the “original setup.” Subsequently, an alternative configuration using non-conductive straps to suspend the Tx coil from the locomotive and referred to as the “strap setup” was used and is shown in the right-hand side of Figure 54.

Testing was conducted to determine the impact of the aluminum frame being used in the original setup to brace the bottom of the Tx coil and the extent of the “crosstalk” between the Tx and Rx coils with both attached to the front of the same locomotive. All tests in this configuration were conducted at a signal frequency of 578 Hz and the Tx and Rx coils mounted 8 inches on a locomotive above the rail. To avoid interference from the electrical equipment while the test measurements were taken, the locomotive was never self-powered.

4.2.2.1 Setup

The signal generation setup consisted of:

- One signal generator
- Two Kepco bipolar 400 W power supply amplifiers
- One RNB
- One Tx coil

Tx Coil Setup

The Tx coil was set up in two orientations as described below and shown in [Figure 53](#):

- Tx coil setup 1: Coil mounted on aluminum frame
- Tx coil setup 2: Coil mounted using non-conductive straps

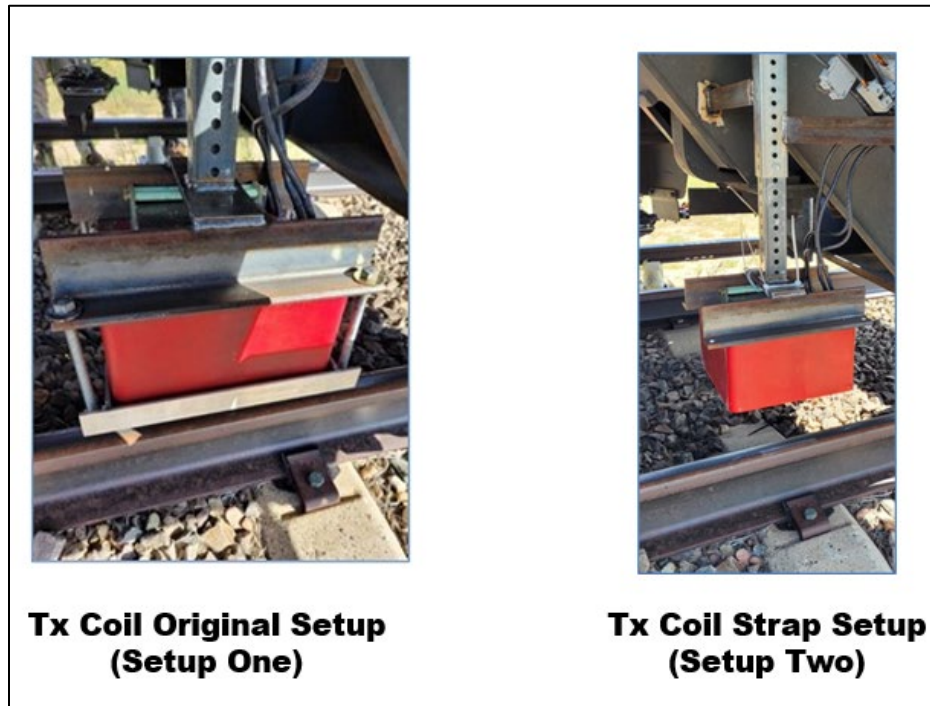


Figure 53. Tx Coil Setups

Rx Coil Setup

The Rx coil is composed of two coil sections separated by a nonconductive composite material. The larger coil (Rx Coil A) and the smaller coil (Rx Coil B) each have a positive and negative lead and can detect an electromagnetic field incident on the coils. The Rx coil was connected for measurement as shown in [Figure 54](#).

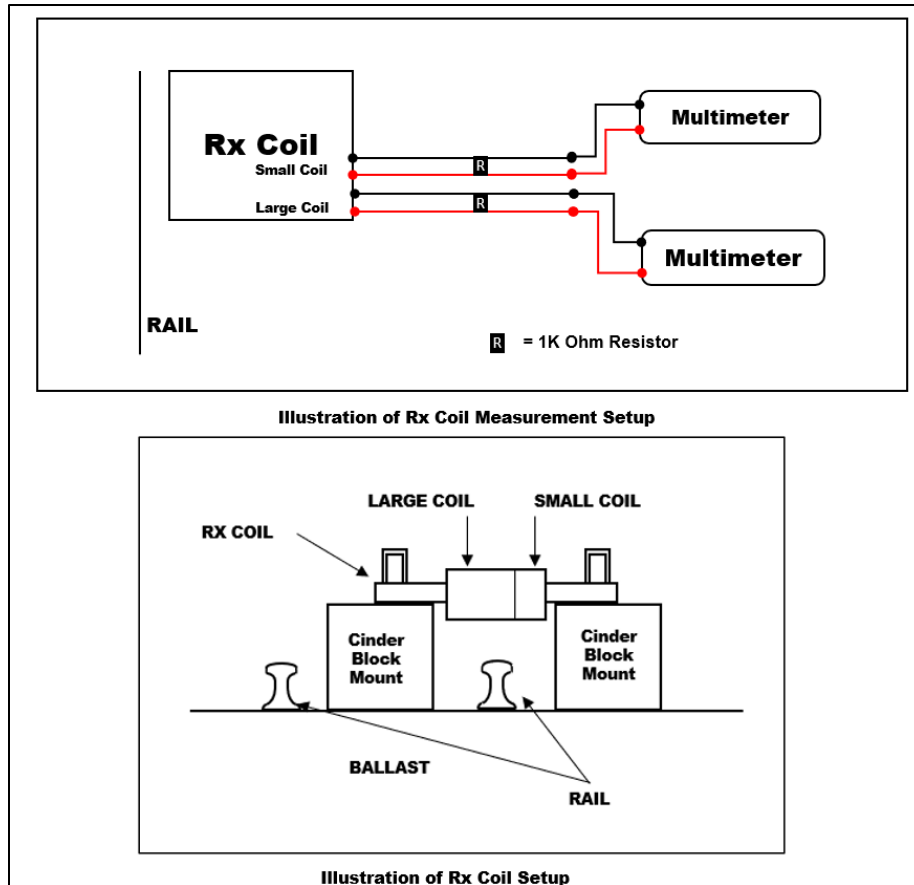


Figure 54. Rx Coil Setup

4.2.2.2 Approach

The equipment setup instructions described in [Appendix A](#) were followed. The frequency was set at 578 Hz, and the data was recorded. The following two test cases were carried out:

Test Case 1: The tests under this case were conducted with the Tx and Rx coils mounted to the locomotive just ahead of the leading axle with the distance to the shunt varied as shown in [Figure 55](#).

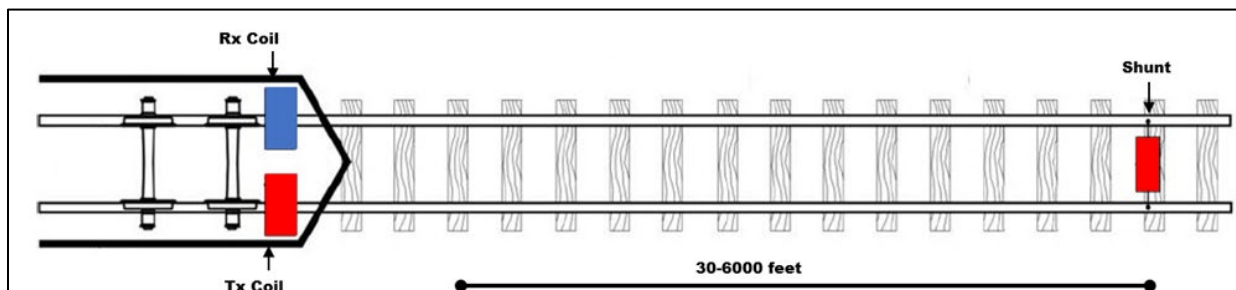


Figure 55. Test Case 1 Setup with Rx Coil on Locomotive

Test Case 2: The test carried out under this case was conducted with the Tx coil mounted to the locomotive and the Rx coil placed 8 inches above the rail and at varying distances in front of the locomotive (30 feet, 1,000 feet, 6,000 feet). This process was carried out to ensure there is no

possibility of the Rx coil being in the range of the magnetic field created by the Tx coil as shown in Figure 56.

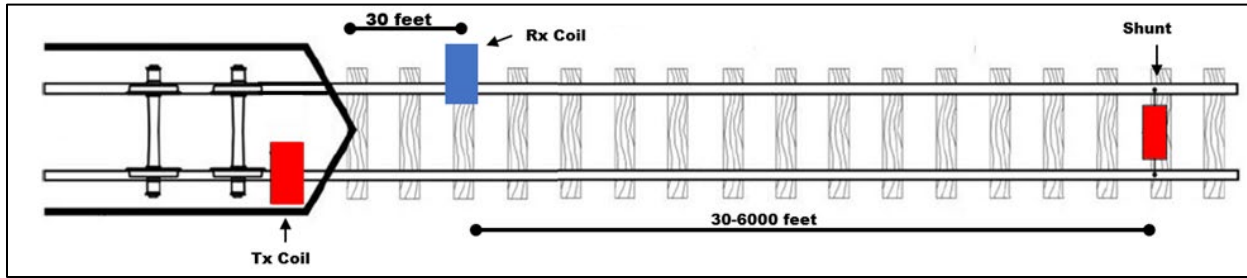


Figure 56. Test Case 2 Setup with Rx Coil Located 30 feet from Locomotive

An additional test of the difference in the results between the two cases was used to quantify crosstalk.

4.2.2.3 Results and Analysis

Test Setup 1: Tabulated test results of the tests carried out under Test Setup 1 are shown in Table 13 and Table 14.

Table 13. Shunt at 30 feet from Tx Coil Under Test Setup 1

Tx Coil Mount	RNB Output Peak Voltage (V)	Small Rx Coil RMS Voltage (mV)	Large Rx Coil RMS Voltage (mV)	Small Rx Coil RMS Voltage (mV) (Tx Coil Off)	Large Rx Coil RMS Voltage (mV) (Tx Coil Off)	Small Rx Coil RMS Voltage (mV) (No Shunt)	Large Rx Coil RMS Voltage (V) (No Shunt)	Current Through Shunt (mA)
Aluminum "original"	350.1	144.4	37.89	4.2	5.8	147.4	38.6	219
Plastic Strap	351.3	160.4	42.4	4.2	5.8	165	42.8	240.8

Table 14. Shunt at 6,000 feet from Tx Coil Under Test Setup 1

Tx Coil Mount	RNB Output Peak Voltage (V)	Smaller Rx Coil RMS Voltage (mV)	Large Rx Coil RMS Voltage (mV)	Smaller Rx Coil RMS Voltage (mV) (Tx Coil Off)	Large Rx Coil RMS Voltage (mV) (Tx Coil Off)	Small Rx RMS Voltage (mV) (No Shunt)	Large Rx RMS Voltage (V) (No Shunt)	Current Through Shunt (mA)
Aluminum "original"	350	144.2	37.96	4.2	5.8	147.4	38.6	3
Plastic Strap	351.3	159	41.4	4.2	5.8	157	40.95	61

Table 15. Tx Coil Strap Mounted with Rx Coil at Various Distances from Tx Coil

Tx Coil Mount	Distance of Rx Coil from Locomotive (ft.)	RNB Output Peak Voltage (V)	Small Rx Coil RMS Voltage (mV)	Large Rx Coil RMS Voltage (mV)	Small Rx Coil RMS Voltage (mV) (Tx Coil Off)	Large Rx Coil RMS Voltage (mV) (Tx Coil Off)	Small Rx Coil RMS Voltage (mV) (No Shunt)	Large Rx Coil RMS Voltage (V) (No Shunt)	Current Through Shunt (mA)
Plastic Strap	30	351.3	4	341 V	4	20	61	4	257
Plastic Strap	1,000	351.3	4	175	4	20	61	4	140
Plastic Strap	6,000	351.3	4	31	4	20	61	4	45

Test Setup 2: Tabulated test results for the tests carried out under Test Setup 2 are shown in [Table 15](#).

The test results show that the aluminum frame under the coil’s base does affect the strength of the signal induced into the rail. [Table 14](#) and [Table 15](#) show the 6,000-foot tests for the original setup and the strap setup. In the original configuration with the aluminum frame under the coil, the measurable current at the shunt was 3 mA. The strap configuration measured a current of 61 mA at the shunt at 6,000 feet. The strapped configuration closely matched the values measured from the non-locomotive static tests ([Section 4.2.1](#)).

[Table 16](#) shows the Rx coil voltages with the RNB output at 580 V under the strap configuration. The maximum RNB output voltage achievable in the original configuration was around 350 V. The measurements in the table were taken to show the maximum voltage output variation between the two setups. However, all other tests were done with similar RNB output voltages to accurately compare the test configurations.

Table 16. Maximum RNB Voltage with Tx Strap Mount Configuration

Tx Coil Mount	RNB Output Peak Voltage (V)	Smaller Rx RMS Coil Voltage (mV)	Large Rx Coil RMS Voltage (V)	Large Rx Coil RMS Voltage (V) (No Shunt)	Smaller Rx Coil RMS Voltage (mV) (No Shunt)
Plastic Strap	580	263.8	70	70	263.8

4.2.2.4 Conclusion

These results show that the current induced into the rail is lower when the aluminum frame is under the coil than when using the zip tie configuration. Therefore, the coil is thought to induce the current into the aluminum frame and ground out through the locomotive. Additionally, the crosstalk was noted to be more significant with the coil at the locomotive than when 30 feet from the locomotive.

These insights led to the replacement of the aluminum frame with the plastic strap for all subsequent tests. Additionally, the testing provided insight regarding the effects of crosstalk and noise that led to testing and researching to mitigate crosstalk.

4.2.3 Shielding Testing – Locomotive

Prior to the dynamic testing of the coils, several tests were conducted to establish the effects of electromagnetic noise and coupling on the system. The results of the previous test indicated enough “crosstalk” from the Tx coil to mask the Rx coil’s ability to detect the induced signal in rail. Therefore, several methods were proposed to mitigate the effects of noise and coupling between the coils. The mitigations included shielding the coils using a material with low magnetic permeability, increased air gap, and grounding. The investigative testing regarding the efficacy of the proposed solutions proceeded as follows:

4.2.3.1 Setup

The field test setup and equipment setup included:

- Locations: TTT
 - Track location: TTT MP 39
 - Type of ties: Concrete, wood
 - Ballast condition: Dry
 - Ballast resistance, measured over “X” ft: 7 K Ohms at 135 feet
 - Rail Type: Welded
- Coil Heights from Rail
 - Tx Coil: 3–8 Inches
 - Rx Coil: 3–8 Inches
 - Tx Coil: On Locomotive
 - Rx Coil: Various Locations
- Tx Coil Electrical Settings:
 - Signal generator: 3 V peak
 - RNB Output: 364 V and 22.4 Amps
 - Frequency: 568 Hz
- Oscilloscope:
 - Channel 1: Rx Coil
 - Channel 4: Tx Coil (at RNB Terminal)

The Tx coil equipment setup followed instructions described in [Appendix A](#).

The Rx coil was connected for measurements as shown in [Figure 57](#).

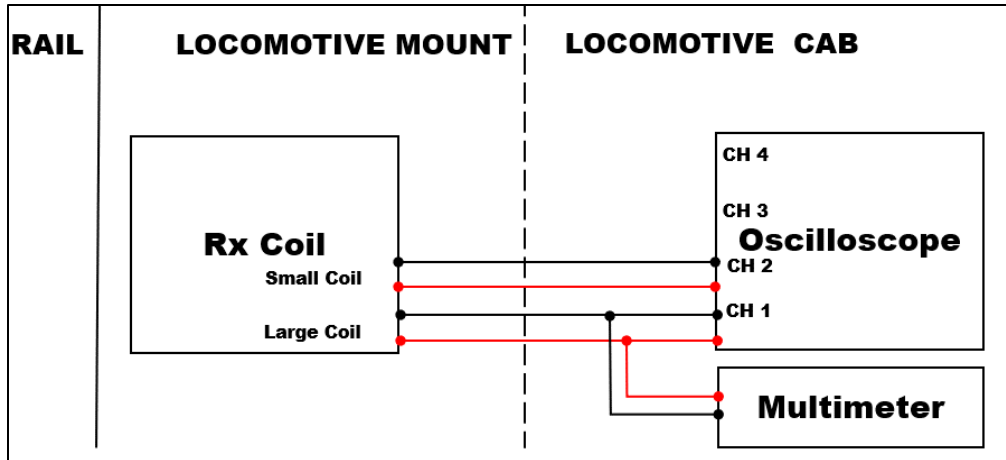


Figure 57. Rx Coil Setup

4.2.3.2 Approach

The Tx coil system was powered up, and different materials were placed in various orientations around the respective coils or between the coils. The test cases included the following:

- Case I: Rx coil at mount (Figure 58)
 1. No Shielding
 2. Aluminum foil over cardboard partition between the Tx and Rx coils
 3. Aluminum metal enclosure around Rx coil
 4. Aluminum foil over cardboard partition behind Tx coil and aluminum metal enclosure at Rx coil
 5. Aluminum foil over cardboard partition between the Tx and Rx coils and aluminum metal enclosure at Rx coil
 6. Aluminum foil over cardboard partition at the Tx coil and aluminum metal enclosure at Rx coil
- Case II: Rx coil at Cow Catcher - Air Gap
- Case III: Rx coil at 20 feet from Cow Catcher ahead of locomotive - Air Gap
- Case IV: Rx coil at 135 feet from Cow Catcher ahead of locomotive - Air Gap

Figure 58 illustrates the various shielding orientations for Case 1.

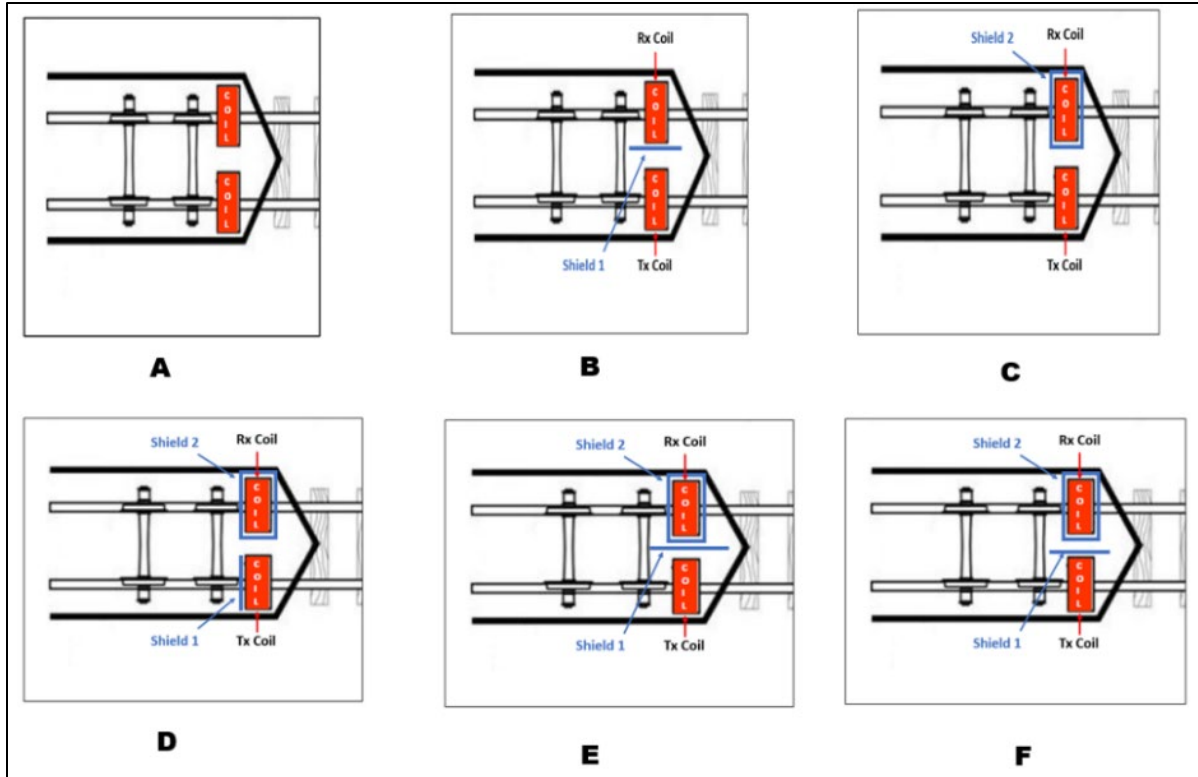


Figure 58. Case 1 Shielding Orientations

The aluminum foil over cardboard partition had four layers of 25-micron heavy duty foil, and the aluminum metal was 1/8-inch gauge. The Rx coil voltages across the larger Rx coil due to crosstalk from the Tx coil were recorded. No shunt was placed across the track for the 6,000-foot block that was terminated by IJs on both rails. The measured data was recorded and compared.

4.2.3.3 Results and Analysis

Table 17 recorded and tabulated the measurement results for each test case of different shields.

Table 17. Detected Crosstalk Voltage at Rx Coil for Various Shields

Test Case	Frequency (Hz)	Large Rx Coil RMS Voltage(mV) (Tx signal off)	Large Rx Coil RMS Voltage(V) (No Shunt)
Case I – Rx coil at mount (A)	568	1.4	60
Case I – Rx coil at mount (B)	568	1.4	58
Case I – Rx coil at mount (C)	568	1.4	45
Case I – Rx coil at mount (D)	568	0.0014	40
Case I – Rx coil at mount (E)	568	0.0014	39
Case I – Rx coil at mount (F)	568	0.0014	36.5
Case II – Rx coil at cow catcher	568	0.0014	0.5

Test Case	Frequency (Hz)	Large Rx Coil RMS Voltage(mV) (Tx signal off)	Large Rx Coil RMS Voltage(V) (No Shunt)
Case III – Rx coil at 20 ft. from cow catcher	568	0.0014	0.2
Case IV – Rx coil at 135 ft. from cow catcher	568	0.0014	0.003

Figure 59 shows the tabulated data as a graph.

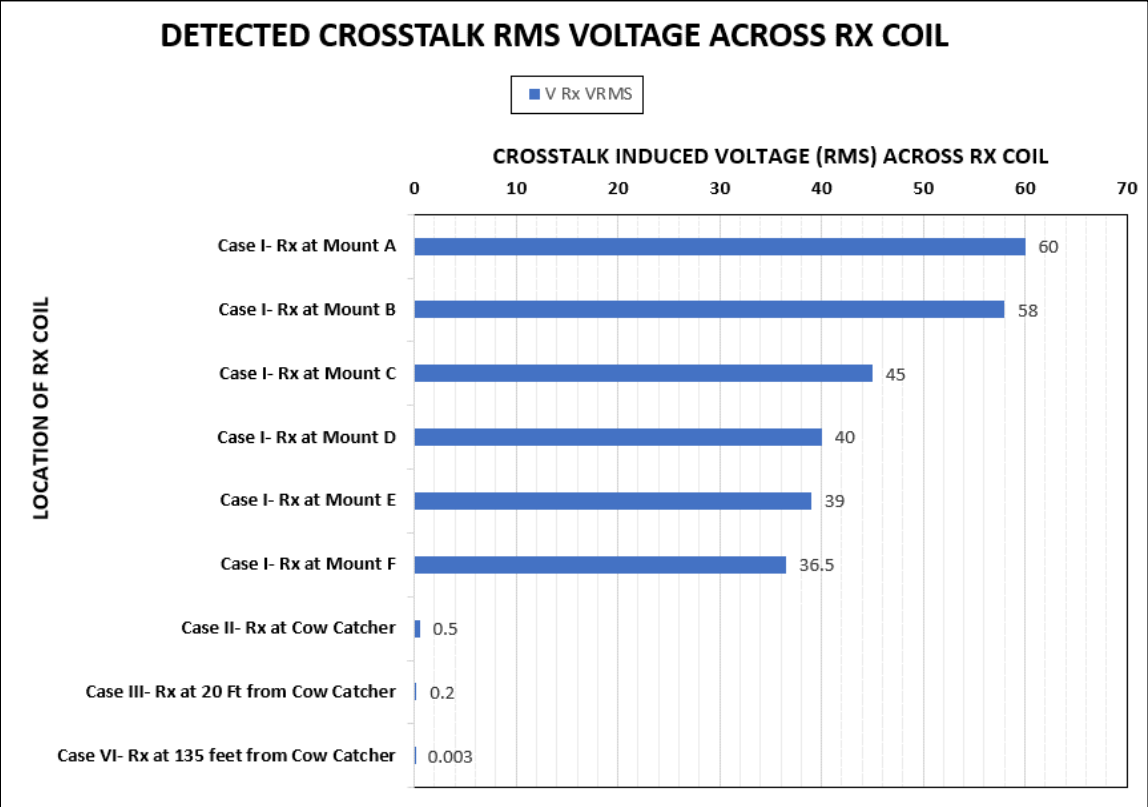


Figure 59. Detected Cross Talk RMS Voltage Across Rx Coil for Various Shields

4.2.3.4 Conclusion

As expected, the distance between the Tx and Rx coils had the most significant effect in reducing crosstalk due to coupling. However, the shielding with the enclosure did show some promise, and further analysis was carried out to identify a more suitable material to enclose the coils. Potential materials and thicknesses were analyzed for future testing using the collected data and the skin depth equation (δ), which defines the depth at which the current density induced on the surface of material falls to about 37 percent (Dorf, R. C., 2000). A graph of the skin depth for several materials was developed and used to determine the most appropriate material and material thickness needed to provide adequate shielding for follow-on testing (Figure 60 shows the skin depth equation as given by:

$$\delta = \sqrt{\frac{2\rho}{\omega\mu}} \quad (10)$$

Where:

ρ = resistivity of the conductor

ω = angular frequency of current

μ = permeability of the conductor

The skin effect versus frequency variance graph shown in Figure 60 for different materials was developed using the skin depth equation.

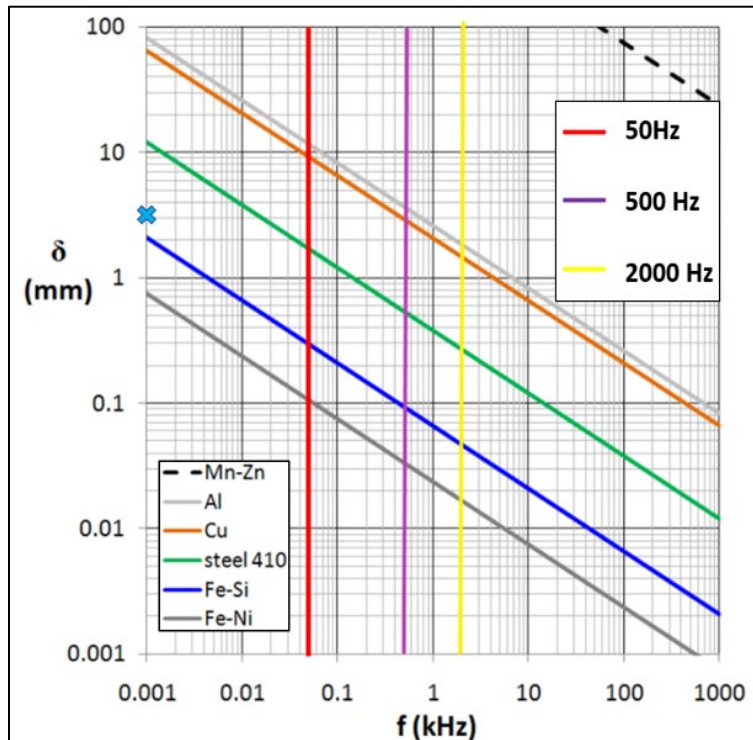


Figure 60. Skin Effect Depth Variance with Frequency for Various Materials

Using both the equation and graph, 1/8-inch steel gauge (3.175 mm) was identified as an adequate shielding material for the range of frequencies (20–1500 Hz) used, i.e., using this shielding material could reduce the effect of the electromagnetic coupling between the Tx and Rx coil by approximately 66 percent. Shield enclosures for the Tx and Rx coils were fashioned and used for subsequent testing.

The Tx coil shield was open on both the top and bottom, with the bottom section of the shield sitting parallel to the bottom section of the Tx coil. Each side of the coil was 2.5 inches equidistant from each side of the Tx coil. The Tx coil and shield are shown in Figure 61.

The Rx coil shield was open at the bottom and fully enclosed on all other sides. The Rx coil was placed inside the enclosure with the bottom of the coil sitting parallel to the bottom of the Rx coil shield enclosure. The Rx coil and shield are shown in Figure 61.



Figure 61. Images of Shielded Tx and Rx Coils

4.2.4 Shielding Phase II Testing – Locomotive

Prior to the dynamic testing of the coils, several tests were performed to establish the effects of electromagnetic noise and coupling on the system. Several methods for mitigating the effects of noise and coupling between the coils were investigated. Signal generation, propagation, and detection data were collected and analyzed with the goal of finding the most optimal orientation of the Tx and Rx coils to mitigate the issues of magnetic coupling and electrical background noise. The Tx and Rx coil shielding methods evolved over several iterations, with final shields being fashioned out of 1/8-inch gauge steel. The images in [Figure 62](#) show the evolution of the Tx coil shielding, and [Figure 63](#) shows the evolution of the Rx coil shielding.

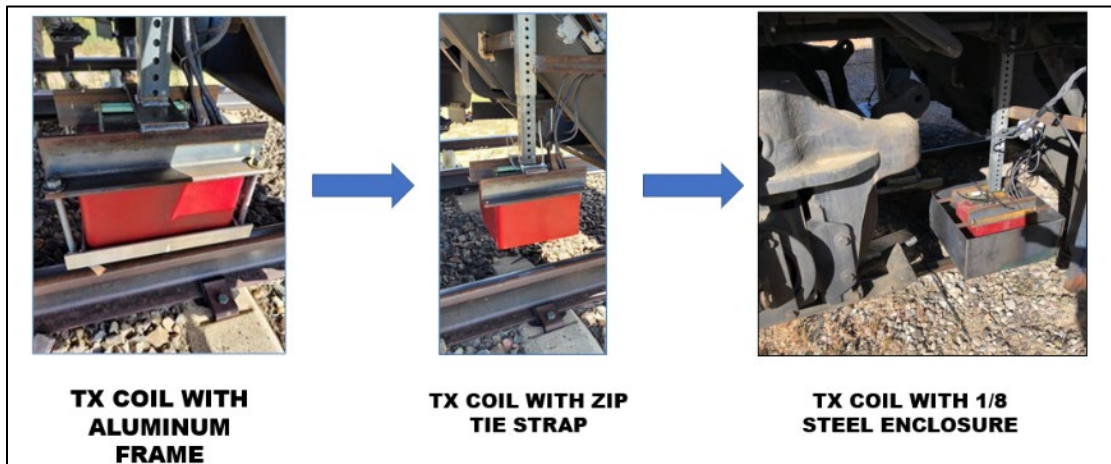


Figure 62. Evolution of Tx Coil Shielding



Figure 63. Evolution of Rx Coil Shielding

With the updated shielding and understanding of the system behavior determined prior testing, the following pre-dynamic static testing was carried out and the results were used to select the configuration used in dynamic testing, i.e., the coils are on the same locomotive, or the Rx coil is set at the far end of the test block.

4.2.4.1 Setup

The field test setup and equipment setup included:

- Locations: PTT Track
- Coil Heights from Rail:
 - Tx Coil: 3–8 Inches
 - Rx Coil: 3–8 Inches
- Tx Coil Electrical Settings:
 - Signal generator: 3 V peak
 - RNB Output: 248 V and 10 Amps
- Oscilloscope:
 - Channel 1: Rx Coil
 - Channel 4: Tx Coil (at RNB Terminals)

The Tx coil equipment setup followed the instructions described in [Appendix A](#).

4.2.4.2 Approach

As with the static testing, data was collected with shunts placed at various locations ahead of the locomotive, the shunt current and detected signal at the coils were recorded, and the recorded data included the screenshot of the oscilloscope readings.

4.2.4.3 Results and Analysis

The measured data was collected and tabulated as shown in [Table 18](#).

Table 18. Summary of Pre-Dynamic Test Results

Measured data	Open track/No Shunt	Signal with shunt at 10 ft. ahead of the locomotive	Signal with shunt at 300 ft. ahead of the locomotive	Signal with Shunt at 650 ft. ahead of the locomotive
Frequency (Channel 1; Rx coil)	568 Hz	568 Hz	568 Hz	568 Hz
Phase difference (CH1-CH4; Rx Coil - Tx coil)	91.35°	109.96°	92.78°	92.11°
Amplitude (CH1; Rx coil)	700 mV	1,440 mV	800 mV	720 mV
RMS (CH1; Rx coil)	254 mV	514.43 mV	286.96 mV	266 mV
Current through shunt	0 A	-	0.9 A	0.4 A

The signal detected by the Rx coil with a shunt at 650 feet was 5 percentage points above the crosstalk baseline of 254 mA. This indicates that the detected signal would not be discernible from the crosstalk signal when trying to detect the difference between a shunted and an open track section at large distances from the locomotive.

4.2.4.4 Conclusion

Although the signal detected was largely masked by the crosstalk and did not meet the benchmark objective of reducing the coupling signal from a root means square (RMS) value of 254 mA to less than 50 mA, it was decided that both configurations of the Rx coil, i.e., on the locomotive and at the far end of the test block, would be tested under dynamic conditions 1) to prove the concept of OBRD and 2) to collect empirical data that could be used to develop a model that could be used to further development an optimal OBRD system. A crosstalk mitigation is necessary and recommended for the development of a future project.

4.2.5 Dynamic Testing – Locomotive

The field testing culminated in the dynamic testing of the system with the primary purposes of 1) proving the proposed OBRD concept under different system configurations and 2) generating empirical field data under various track conditions for use in developing a system model and for future refinement of the concept. The dynamic field testing focused on two system configurations (“A” and “B”) that were based on previous static tests of Tx and Rx coils, grounding, and shielding tests.

4.2.5.1 Test Equipment and Setup

The Tx and Rx coil test configurations included:

- System configuration A: The Tx and Rx coils are located on the same locomotive.
- System configuration B: The Tx coil is located on the locomotive, and the Rx coil is located at the far end of the track test block.

Occupancy by another train was simulated by a shunt connected in series with an ammeter to record the current through the shunt at the far end of the test block (e.g., at T39). The configurations for dynamic testing are illustrated in [Figure 64](#).

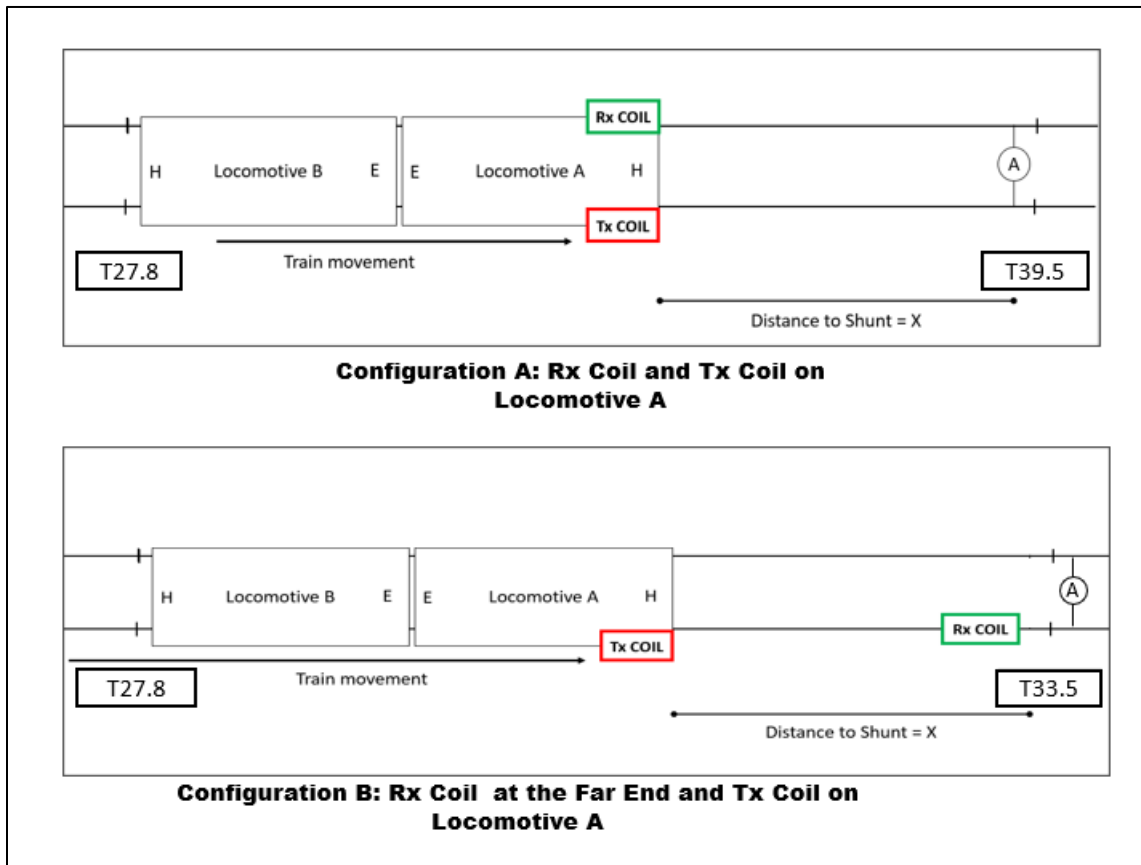


Figure 64. Locomotive, Tx and Rx Coil Configurations for Dynamic Test Cases 4, 5, 6, 7, 8, and 9

Distance “X” in [Figure 64](#) is the starting point for each dynamic test and is equal to 6,000 feet (T27.8 (IJ) to T33.5 (IJ)) or 12,000 feet (T27.8 (IJ) to T39.5 (IJ)). [Table 20](#) shows the test case matrix. Test cases 7, 8, 9, and 12 used system configuration A while test cases 4, 5, 6, and 11 used system configuration B.

Locomotives and Rail Cars

Two locomotives were used in the series of dynamic tests. Locomotive A (ID: AAR 2000) was the platform where most of the test equipment was mounted. This locomotive has no engine power and was pushed by a powered locomotive, referred to as Locomotive B, for the duration of the dynamic testing. Care was taken not to use dynamic braking during the test, keeping the

potential engine electromagnetic noise from the locomotives to a minimum. The locomotive speeds were maintained at an average speed of 20 mph (± 4) during each test. To simulate wet track conditions prior to the wet ballast dynamic testing, a tank car filled with 11,000 gallons of water was towed by Locomotive B and was used to wet the track.

Tx and Rx Coils

The Tx coil for this test and all tests is a custom-designed coil described and shown in [Appendix B](#). The Rx coil used for testing was an Alstom cab signal coil (ATP Rx coil assembly). An illustration of the Rx coil is shown in [Appendix C](#). This Rx coil was used for all on-track tests. The Rx coil has two separate windings, one large, the other small. Each Rx coil winding had a 1 K resistor connected across its terminals during all tests, to simulate the loading it was designed to experience.

Power Supplies

Multiple power sources were used based on different test scenarios. Two power generators were mounted in the front nose of Locomotive A to provide the necessary power supply for test equipment. Bungalows at T27, T33, and T39 also had mainline power.

Measurement Equipment

- **Clamp meter:** A clamp meter provided the non-contact measurement of current and voltage for some scenarios. The clamp meter used in this test is branded as Bluetooth (BT) Meter BT-570C, allowing a wireless connection for data monitoring via BT.
- **Multimeter:** Based on test scenarios, several fluke multimeters were used in this test as ohmmeter, voltmeter, and ammeter.
- **Oscilloscope:** The Rx coil voltage and other related data were measured by oscilloscope and verified by the multimeter. The oscilloscope allows data to be saved to a Universal Serial Bus (USB) in real-time. The oscilloscope was used for the following reasons:
 - To measure the signals of the connected device (i.e., Tx and Rx coils, and signal generator)
 - To compare the relative amplitude and relative phase between the Tx and Rx signals, primarily to assess how relative amplitude and phase vary with differing test conditions, e.g., shunt present, shunt absent, rail break present, changes in the distance among transmitter, receiver, shunts, and rail breaks
 - To verify that the signals being measured were the desired signals without additional extraneous signals
- **Global Positioning System (GPS) receiver:** A mountable GPS receiver was placed at the top front of Locomotive A to provide speed and location data that was logged for post-test analysis.

Other Devices, Equipment, and Tools

[Table 19](#) lists the other tools and equipment that were used during testing.

Table 19. Other Devices, Equipment, and Tools

Equipment/Tool	Amount	Brand/Model
Portable cab signal tester	1	GE
1-ohm resistor	1	N/A
Jumper wires	6	N/A
Clip wire	4	N/A
Knife switch	1	N/A

Field Setup

The field equipment setup for dynamic testing was as follows:

- Location: TTT
- Coil heights from rail for both configurations:
 - Tx coil: 3 inches
 - Rx coil: 3 inches
- Tx coil electrical settings:
 - Signal generator: 3 V–3.19 V peak
 - RNB output per channel: 180 V–248 V and 9–10 amps
- Oscilloscope:
 - Channel 1: Rx coil (large coil)
 - Channel 2: Rx coil (small coil)
 - Channel 3: Tx coil (at RNB Terminal B)
 - Channel 4: Tx coil (at RNB Terminal A)

The Tx coil equipment setup followed the instructions described in [Appendix A](#).

Test Track

The test block used for dynamic testing was 12,000 feet long to simulate a typical field track circuit block. As with the previous testing, the blocks between T27 to T39 of the TTT provided the desired length of at least 12,000 feet and were used for the dynamic field test. The IJs are located on both rails at T27.8, T33.5, and T39. Switch sections (turnouts) are located at T33.6 and T38.7. Both switches were locked to normal during the test for 12,000 feet. During the 6,000-foot tests (T27–T33.5), the switches were locked in reverse to break the track continuity for the section of track between T33.5 and T39. [Figure 65](#) and [Figure 66](#) illustrate the 12,000-foot and 6,000-foot test track sections, respectively, as well as the high-level wiring and the bungalow locations with each bungalow having the track wires connected to the bungalow AAR terminal.

For most test cases, wires A and C were connected to each other, and wires B and D were connected to each other through the AAR terminal to short each IJ. To simulate a changing broken rail scenario in the test block, Terminals B and D at the T33.5 IJ were periodically connected to jumper a shunt across the IJ and disconnected approximately every 30 seconds to simulate a rail break when disconnected. A recorded change in the voltage of the terminals was used to indicate when the terminals were connected or disconnected to indicate whether there was a broken rail condition between T27.8 and T39.5 at T33.5.

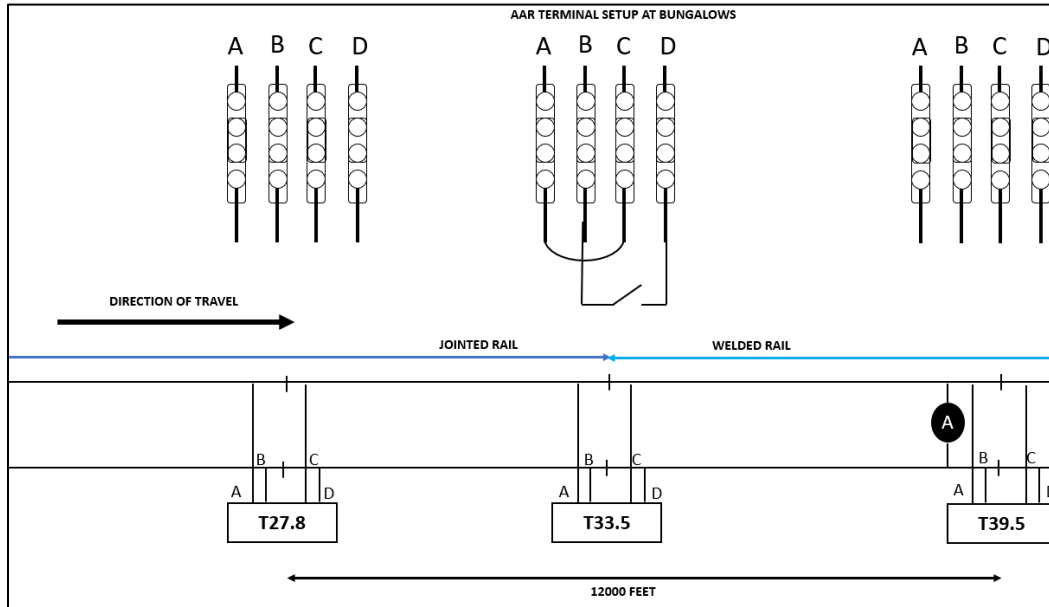


Figure 65. TTT Section and Track Connection Diagram for 12,000-foot Block Tests

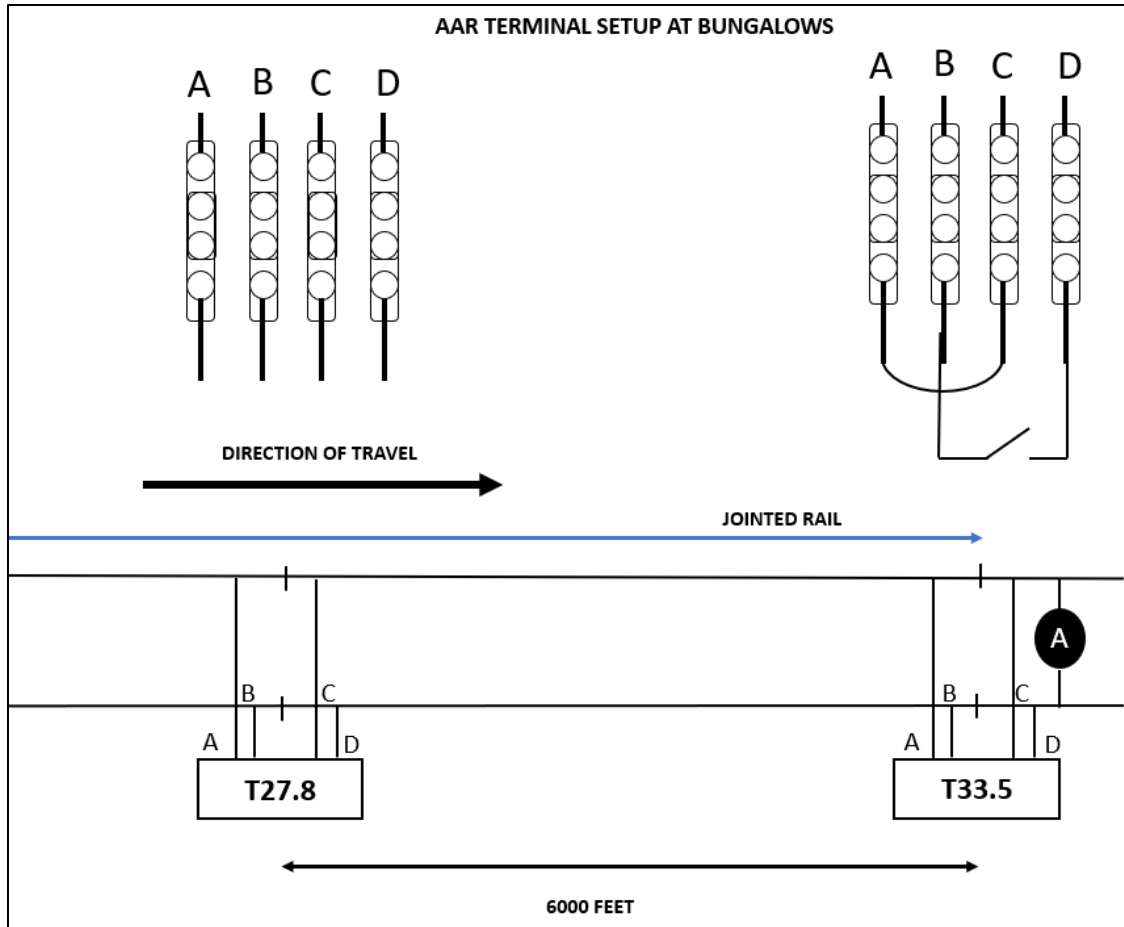


Figure 66. Test Track Section and Track Connection Diagram for 6,000-foot Block Tests
4.2.5.2 Transmit and Receive Coils Set Up

Tx Coil Set Up

The Tx coil was mounted and located under the front of Locomotive A. The bottom of the Tx coil was 3 inches above the rail (not including the shield). A steel shield was used to attenuate the crosstalk between the Tx coil and the Rx coil. The metal connection with Locomotive A grounded the shield to the locomotive chassis.

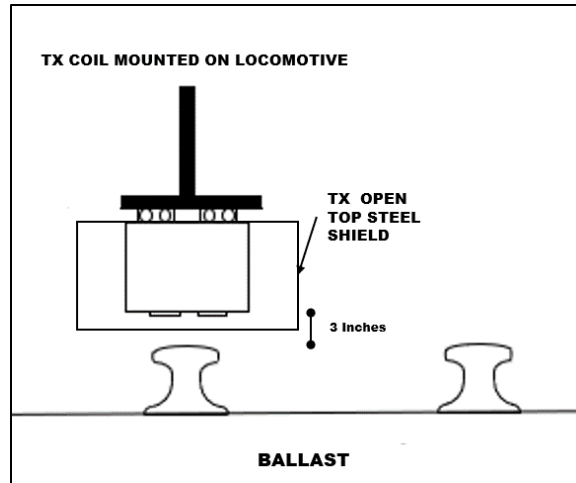


Figure 67. Illustration of Tx Coil Setup When Attached to Locomotive

Figure 68 shows the electrical configuration associated with the Tx coil for Configuration A. For the duration of testing, the signal generator was set at a frequency of 568 Hz and an amplitude setting of 3 ± 0.2 volts. The cables between the locomotive cab and coil mounts had an American Wire Gauge (AWG) rating of 12 gauge or lower.

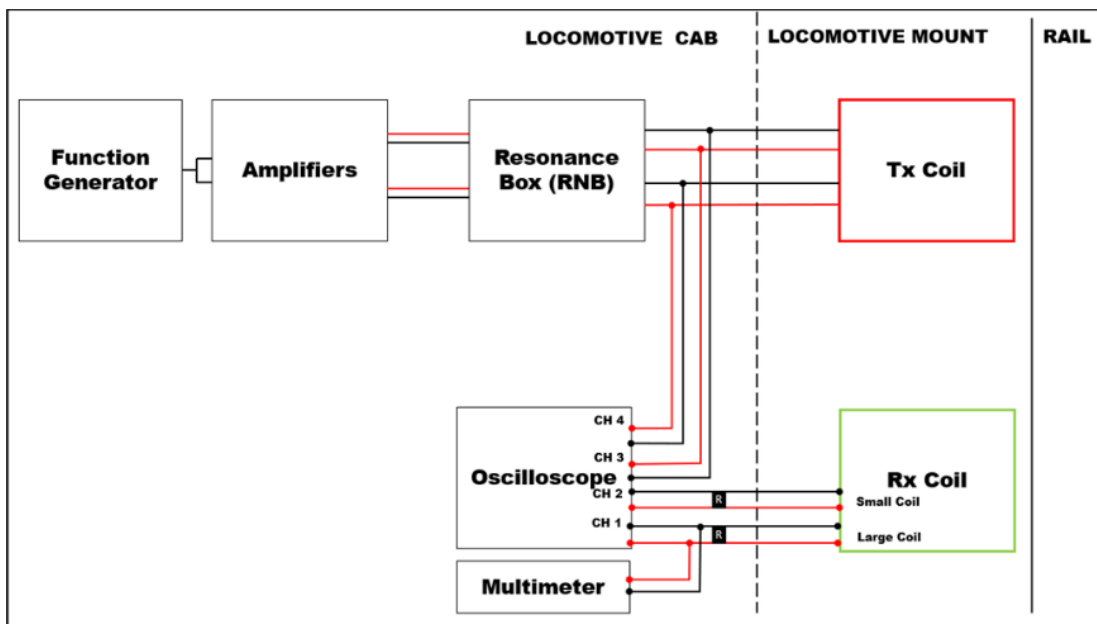


Figure 68. Electrical and Measurement Configuration of Tx and Rx Coil for Configuration A

A second oscilloscope monitored the Rx coil when the system was set up in Configuration B.

Rx Coil Set Up

Two Rx coil system configurations were tested as shown in Figure 69. They were:

- Rx coil Configuration A: The steel cage shielding the Rx coil was mounted on Locomotive A, parallel to the Tx coil. The bottom of the Rx coil was 3 inches above the rail. The metal connection with Locomotive A grounded the shield.

- Rx coil Configuration B: The steel cage shielding the Rx coil was positioned at the far end of the test block and was mounted on cinder block bases (not on a locomotive), 3 inches above the rail. Shielding was grounded via a cable and a ground rod.

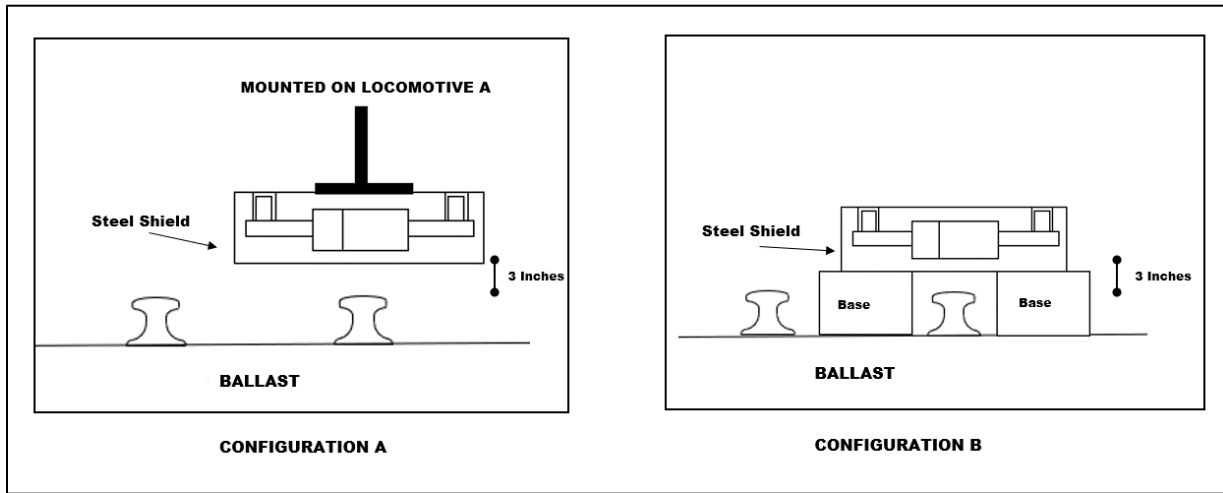


Figure 69. Rx Coil Configurations and Setup

4.2.5.3 Approach

Several test cases were carried out over 2 days with the goal of determining the signal behavior under dynamic conditions for both Configuration A and Configuration B. [Table 20](#) lists all the test cases that were run.

Table 20. List of Test Dynamic Testing Test Cases

Case No.	Name	Rx coil configuration
1	Track integrity verification	Pretest
2	Test box verification	Pretest
3	Static test box test, Rx coil at the far end	Pretest
4	Static system test, Rx coil at the far end	B
5	Dynamic system test, Rx coil at the far end	B
6	Dynamic system test, Rx coil at the far end, with rail break	B
7	Static system test, Rx coil on the same locomotive	A
8	Dynamic system test, Rx coil on the same locomotive	A
9	Dynamic system test, Rx coil on the same locomotive, with rail break	A
10	Wet track preparation	Pretest
11	Dynamic system test, Rx coil at the far end, Wet	B
12	Tx coil phase changes with track conditions	A

4.2.5.4 Results and Analysis

All testing was performed using test cases that were covered by one run combined as shown in [Table 20](#). Test cases 7, 8, and 9 were combined into one locomotive test run from T27–T39.5 as this run provided the coverage for test cases 7 (Static system test, Rx coil on the same locomotive), 8 (Dynamic system test, Rx coil on the same locomotive), and 9 (Dynamic system test, Rx coil on the same location, with rail break). Similarly, test cases 4 (Static system test, Rx coil at the far end) and 5 (Dynamic system test, Rx coil at the far end) were combined into one locomotive test run from T27–T33.5 since the run provided coverage for test case 4.

In addition, the track was wetted in the last few test cases to simulate the rainy weather conditions. Test cases performed on day 1 used a 12,000-foot block, from post 27 to post 39, that focused mainly on Configuration A (Tx and Rx coils on the same locomotive). Test cases performed on day 2 used a 6,000-foot block, from post 27 to post 33, that focused mainly on Configuration B (Rx coil on the far end of the test block). The test section was shortened because some track sections were out of service and not usable as test track during this testing period. The data was monitored by the devices described in the test plan. All dynamic tests began with the locomotive at post 27 and moved in the direction of increasing posts at a constant speed 20 mph (± 4 mph). Measurement and video records for each test case were saved and organized for further analysis and research.

Table 21. List of Conducted Dynamic Test Cases

Day	Case No.	Rx Coil Configuration	Block Length	Comments
1	7, 8, 9	A	12,000 ft. (T27.8 (IJ)–T39.5 (IJ))	Combined Tests
1	12	A	12,000 ft. (T27.8 (IJ)–T39.5 (IJ))	
2	4, 5	B	6,000 ft. (T27.8 (IJ)–T33.5 (IJ))	Combined Tests
2	6	B	6,000 ft. (T27.8 (IJ)–T33.5 (IJ))	
2	11	B	6,000 ft. (T27.8 (IJ)–T33.5 (IJ))	

The track integrity checks at the time of the tests indicated the resistance of the track blocks for 6,000-foot and 12,000-foot test sections to be 1.5 and 3.3 ohms, respectively ([Figure 43](#)). The track resistance measurements were carried out with a shunt on one end of the track block and the ohm meter reading taken on the other end of the track block.

Prior to the start of testing with the Rx coil in Configuration B at the T33.5 (IJ), the PCS tester was used to test the Rx coil. The PCS was connected to the track at the bungalow at T27.8 (C and D terminals) and set to a frequency of 60 Hz. The output current was set at 1 amp and 1.5 amps. The Rx amplitude was captured as 200 mV (RMS) and 320 mV (RMS). Testing resumed after receiving confirmation that the Rx coil worked in this configuration.

In Rx coil Configuration A, the locomotive went past T39.5 (IJ), while in Rx coil Configuration B, the locomotive stopped approximately 100 feet from the Rx coil placed about 10 feet from T33.5 (IJ).

4.2.5.5 Combined Test Cases 4 and 5 with Rx Coil Configuration B

The purpose of test cases 4 and 5 was to analyze the system performance when the Rx coil uses Configuration B (i.e., Tx coil and Rx coil at different locations). The test was performed on day 2 over a 6,000-foot block. The data for the shunt current and the Rx coil amplitude were measured by the oscilloscope and are shown in Figure 70 and Figure 71, respectively. A two-data-points moving average trendline was added to the Rx coil amplitude data in Figure 71 to show the Rx amplitude trend.

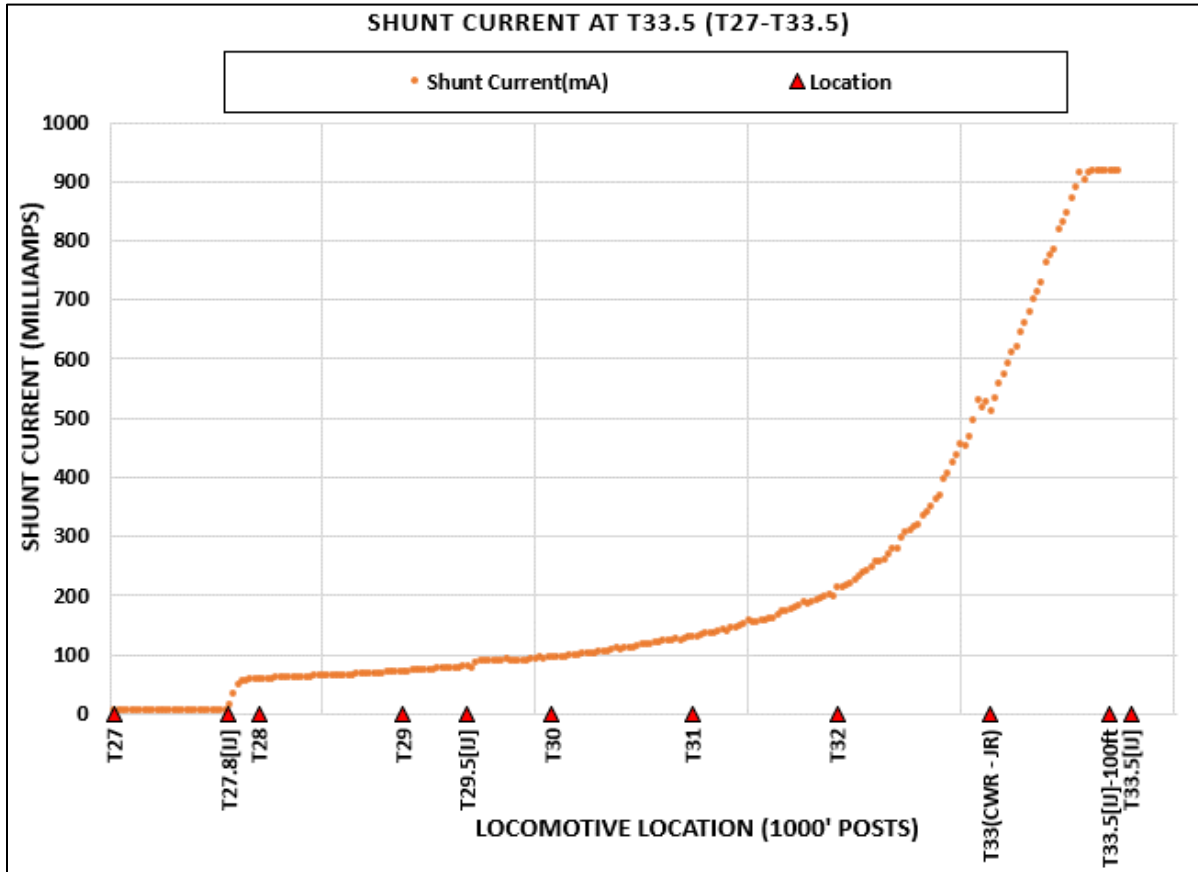


Figure 70. Shunt Current at T33.5 for Dynamic Test Cases 4 and 5 vs. Locomotive Location

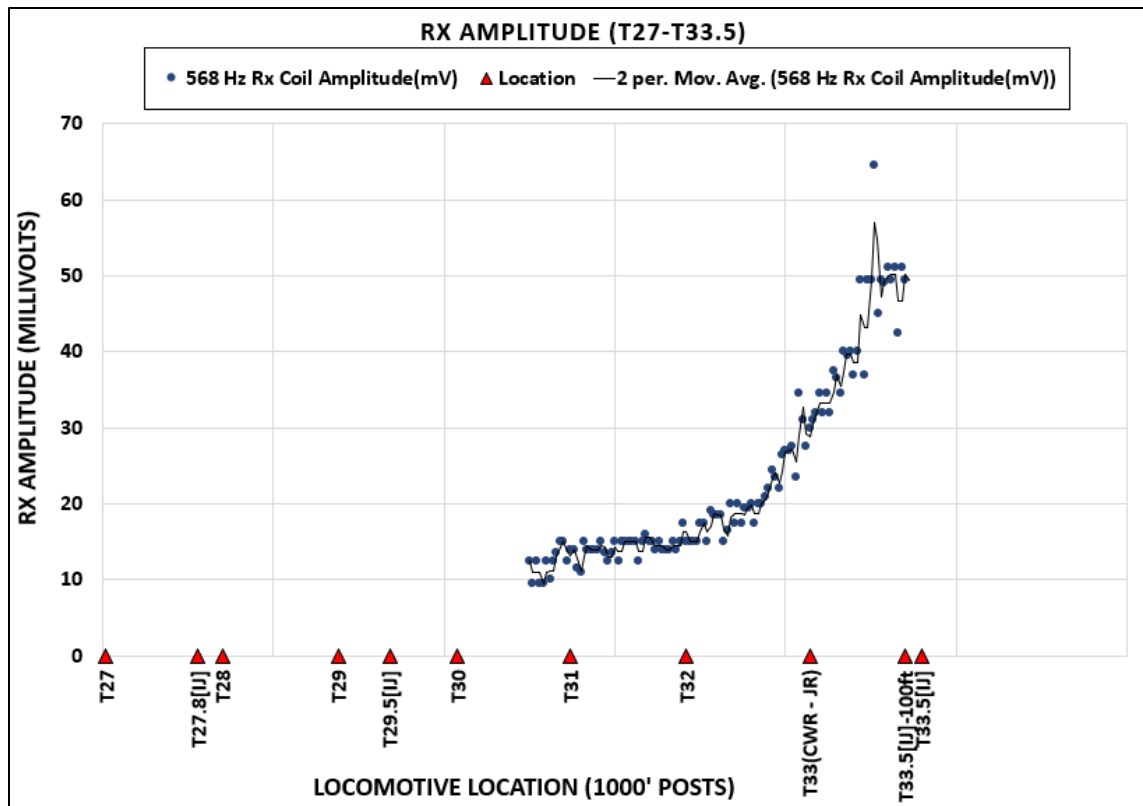


Figure 71. Rx Coil Signal Amplitude for Dynamic Test Cases 4 and 5 vs. Locomotive Location

Test Case 6 with Rx Coil Configuration B

The purpose of test case 6 was to analyze the system performance when the Rx coil uses Configuration B (i.e., Tx and Rx coils at different locations) with and without a broken rail condition. The broken rail was located at the T33.5 IJ, with a shunt at about 2 feet from the IJ at T33.5 (Figure 66). The rail break was simulated by removing a shunt across the T33.5 IJ. To easily compare the results with a rail break versus without a rail break, the shunt was applied for 30 seconds and then removed for the next 30 seconds. This cycle was repeated as the train moved from T27 to the other end of the block at a constant speed.

The test was performed on day 2 over the 6,000-foot block section. The shunt current at T33.5 and Rx coil amplitude are shown in Figure 72 and Figure 73, respectively. A two-data-point moving average trendline was added to the Rx coil amplitude to show the Rx amplitude trend (Figure 73).

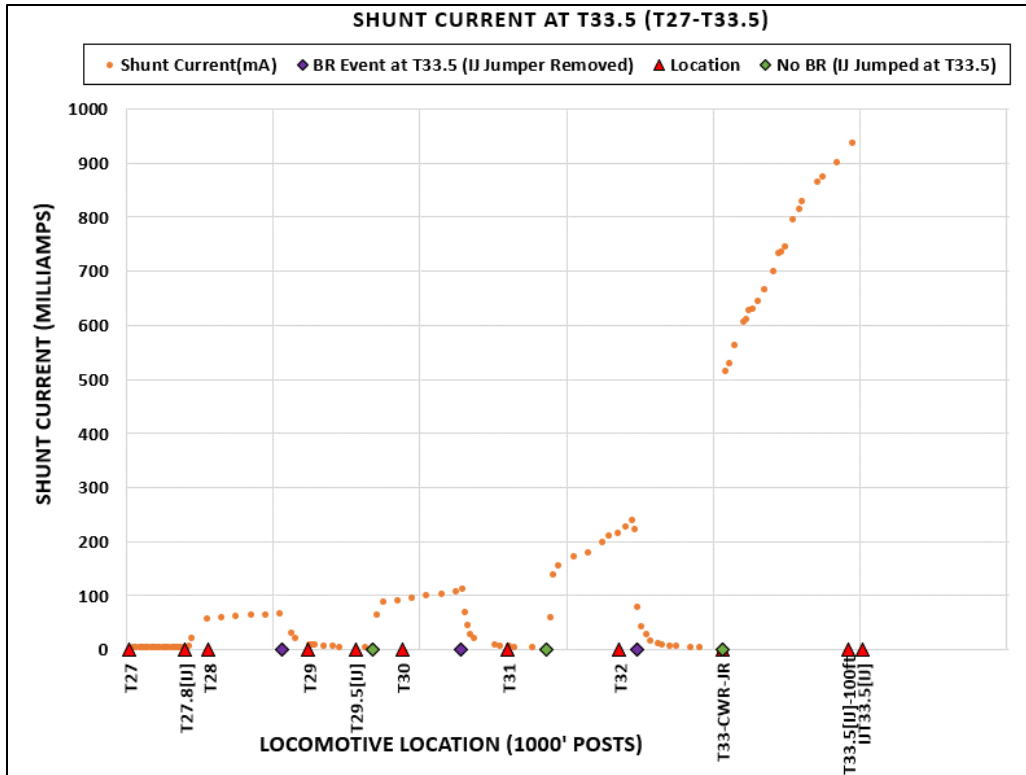


Figure 72. Shunt Current at T33.5 for Dynamic Test Case 6 vs. Locomotive Location

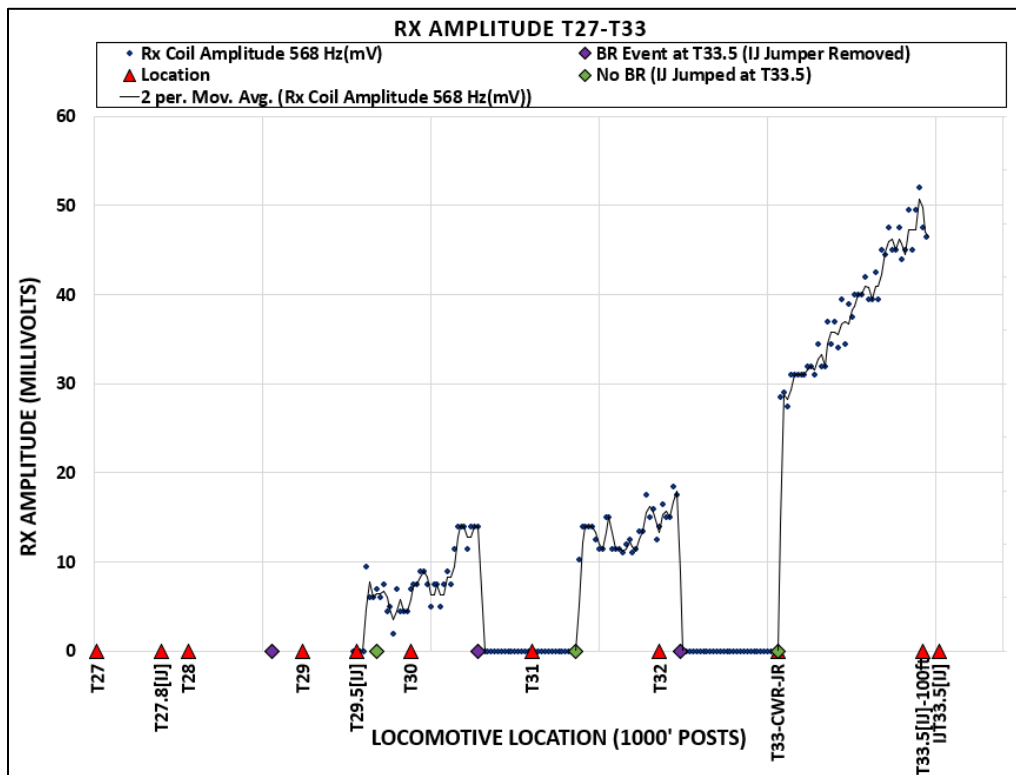


Figure 73. Rx Coil Amplitude for Dynamic Test Case 6 vs. Locomotive Location

4.2.5.6 Combined Test Cases 7, 8 and 9 with Rx Coil Configuration A

The purpose of test cases 7, 8, and 9 was to analyze the system performance when the Rx coil uses Configuration A (i.e., the Tx and Rx coils at same location, mounted to Locomotive A) with a broken rail condition at T33.5 and clear track from T33.5 to T39.5. The test was performed on day 1 over a 12,000-foot block. The shunt current at T39.5, the broken rail condition at T33.5, and the amplitude of the signal received at the Rx coil were monitored and recorded. The measurements of the shunt current, Rx coil amplitude, and phase difference between the Tx and Rx coils are shown in Figure 74 through Figure 76, respectively.

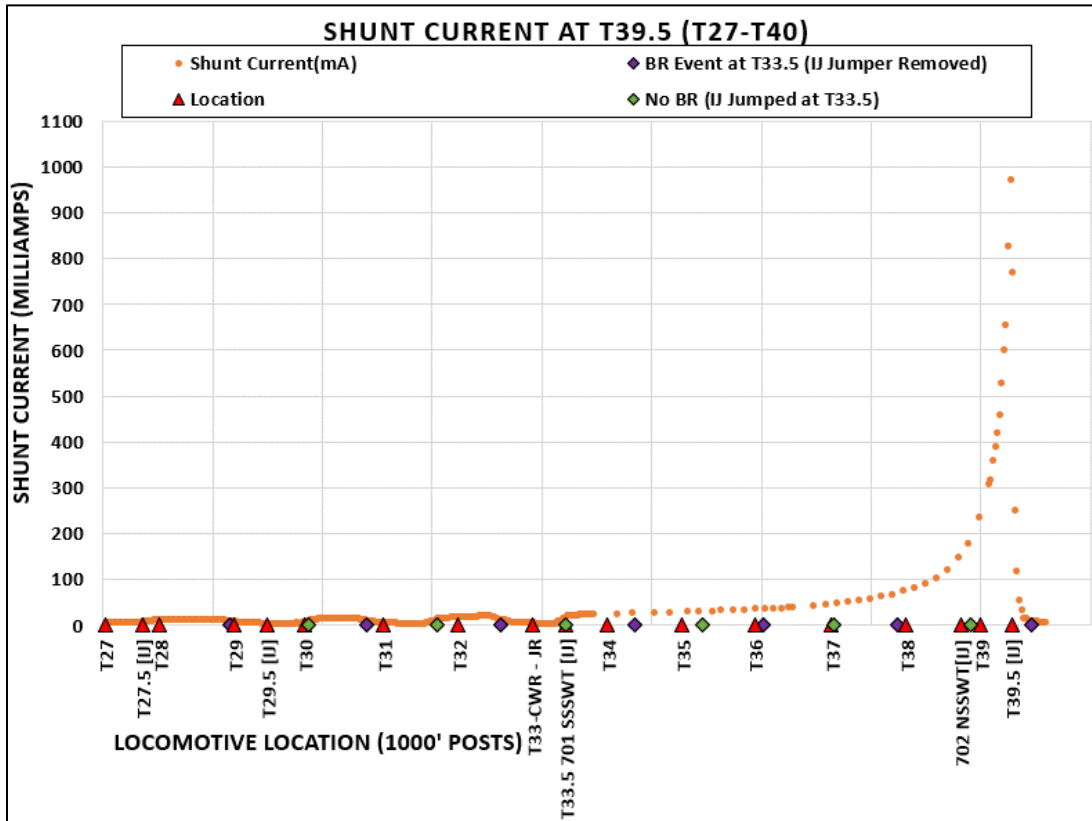


Figure 74. Shunt Current at T39.5 for Combined Dynamic Test Cases 7, 8, and 9 vs. Locomotive Location

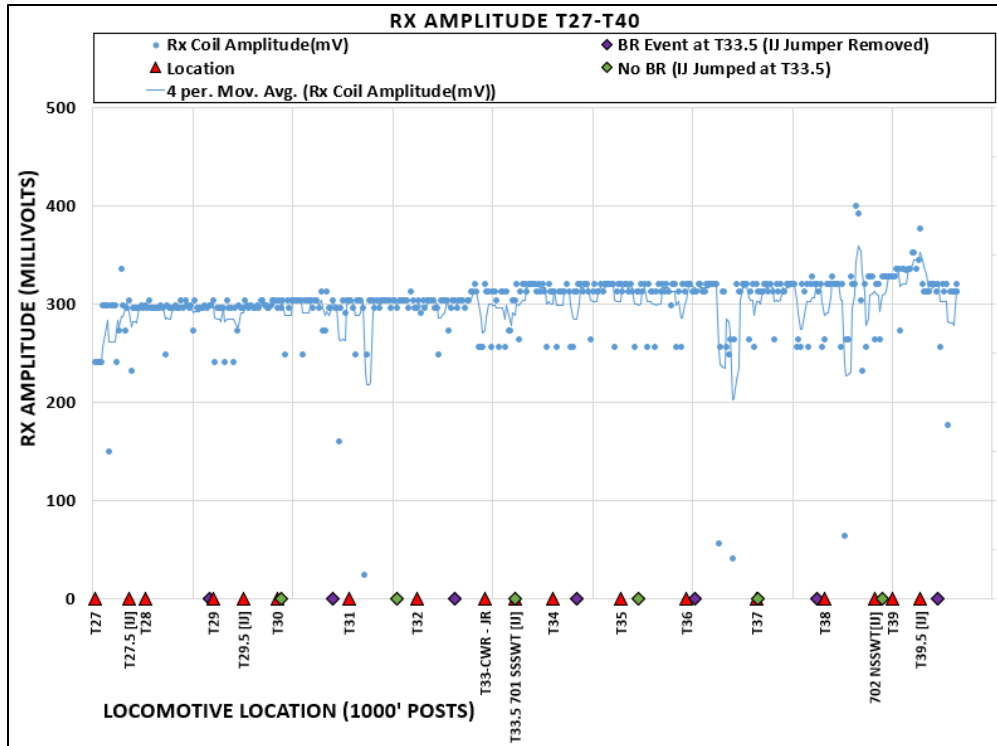


Figure 75. Rx Coil Amplitude for Combined Dynamic Test Cases 7, 8, and 9 vs. Locomotive Location

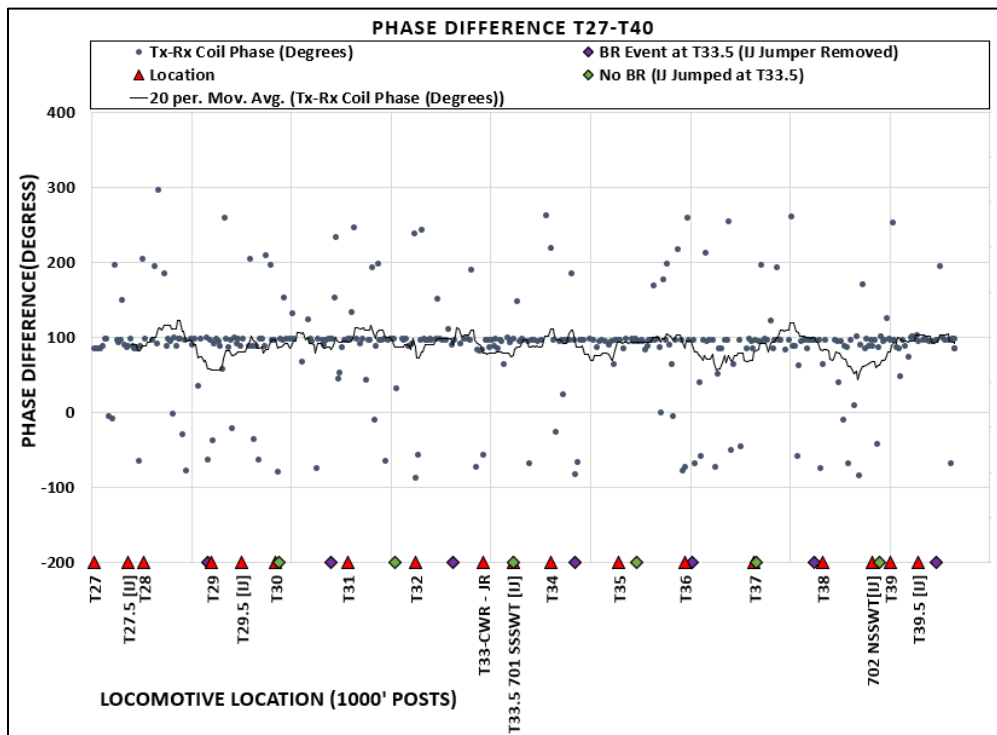


Figure 76. Phase Difference Between Tx and Rx Coils for Combined Dynamic Test Cases 7, 8, and 9 vs. Locomotive Location

4.2.5.7 Test Case 11 with Rx Coil Configuration B

The purpose of test case 11 was to analyze the system performance under altered track impedance conditions due to wet ballast. The test track section was wetted with approximately 11,000 gallons of water while the Rx coil used Configuration B, and the test was performed over the 6,000-foot block. The measured shunt current for test case 11 is shown in Figure 77. The shunt current was normalized and compared to the normalized shunt current from test case 5. The results are shown in Figure 78.

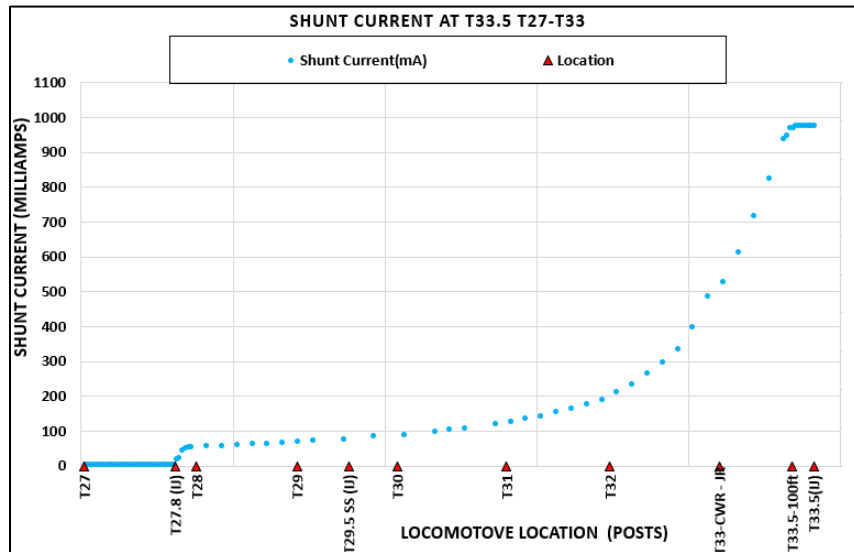


Figure 77. Dynamic Test Cases 11 Showing Effects of Wet Ballast on Induced Signal vs. Locomotive Location

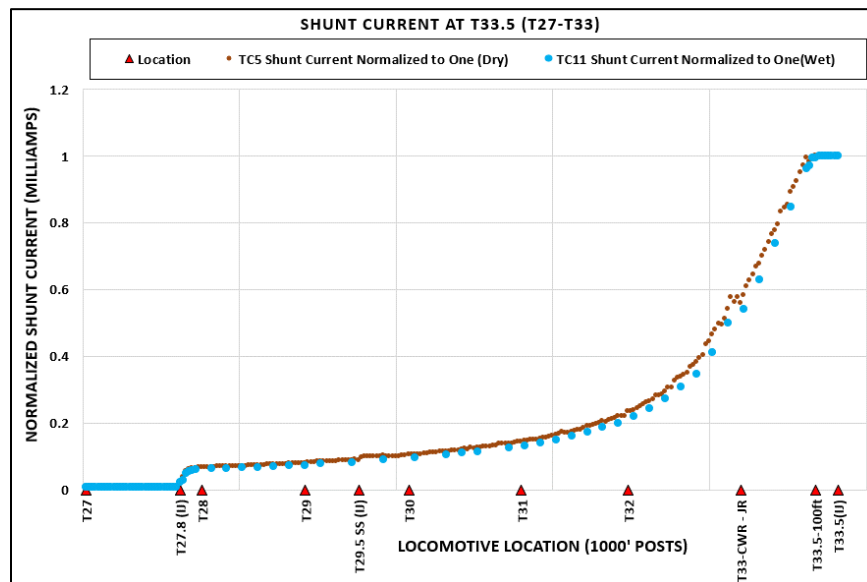


Figure 78. Dynamic Test Cases 11 and 5 Comparison Showing Effects of Wet Ballast on Induced Signal vs. Locomotive Location

4.2.5.8 Test Case 12 Configuration A

The purpose of test case 12 was to provide an indication of the extent to which Tx coil impedance is affected by track conditions by monitoring the phase change between the signal generator output that drives the amplifiers and the amplifier outputs into the Tx coil. The test was performed on day 1 over a 12,000-foot block and Tx and Rx coils on the same locomotive. The phase difference between Tx and the function generator was consistent at 60 degrees (± 1 degrees). The results are shown in Figure 79.

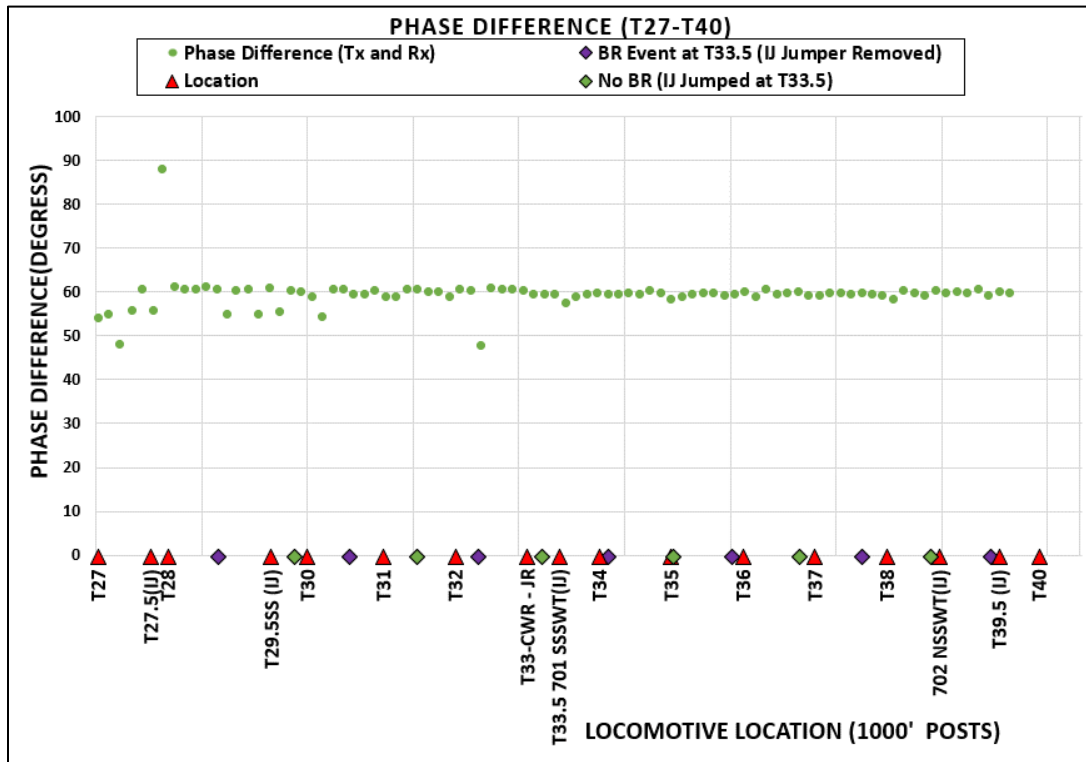


Figure 79. Dynamic Test Case 12: Phase Difference Between Signal Generator and Tx Coil vs. Locomotive Location

4.2.5.9 Analysis

The overall purpose of the field dynamic test was to simulate a scenario similar to actual operations by using the Tx and Rx coils tested during this phase to determine feasibility of the concept and to help determine the direction for the future development of the OBRD system. According to the test results, the system can identify the different track conditions presented, and the signals received for both Configuration A and Configuration B can be distinguished from the noise or clear track conditions. The difference in system configuration affects some characteristics of Rx coil measurements, such as amplitude. This difference is due to the Tx coil affecting the Rx coil signal (crosstalk) when both coils are co-located on the same locomotive.

The analysis is broken down into the following topics:

- Operational scenarios
- Transmit range
- Signal reception
- System performance with wet ballast

Operational Scenarios

The data from test cases 7, 8, and 9 (Rx coil Configuration A), test cases 4, 5, and 6 (Rx coil Configuration B), and other test cases indicate that this system can induce a clearly detectable current in a shunt far in advance of the train and that signal increases as the locomotive approaches the shunt. This is a very important finding because it proves an induced signal can propagate over an appreciable length of track without being mostly dissipated through ballast leakage.

Figure 80 shows an overlay of the induced shunt current and the peak Rx coil voltage amplitude for the combined test cases 7, 8, and 9. Figure 81 shows the same data up to T33.5.

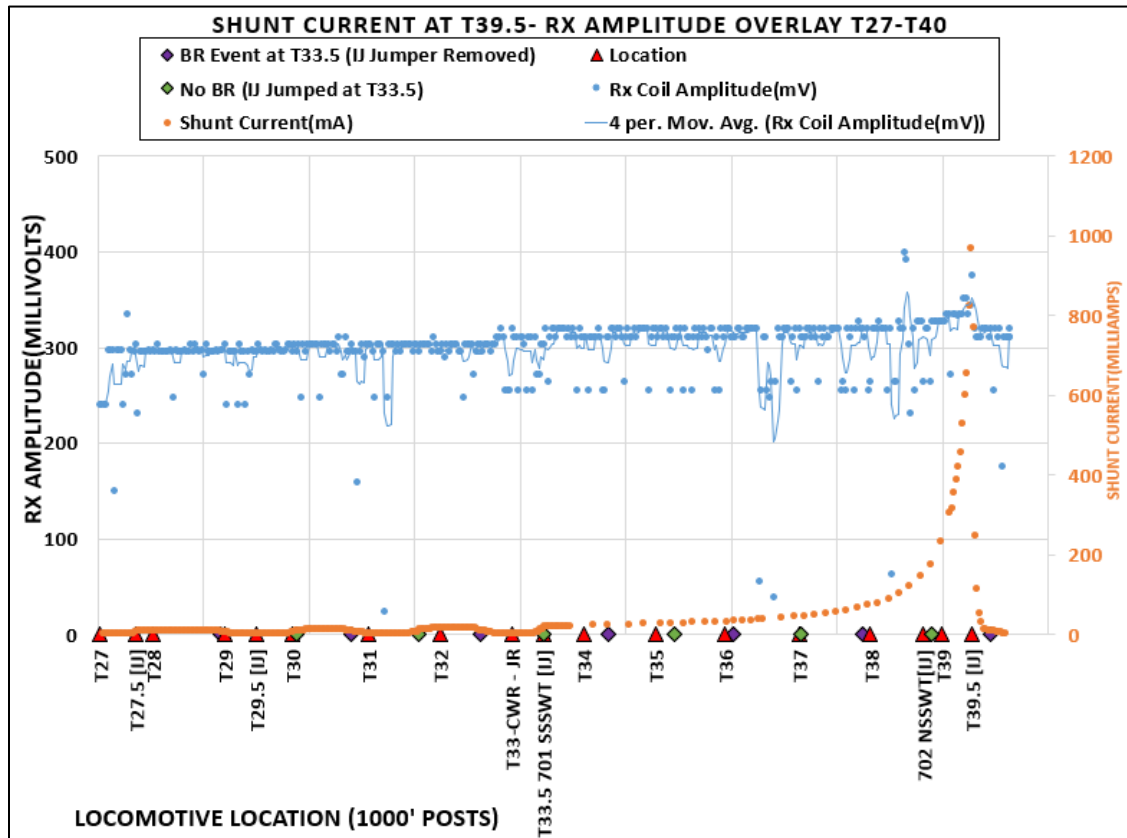


Figure 80. Dynamic Test Cases 7, 8, and 9 Tx and Rx Overlay vs. Locomotive Location from T27–T40

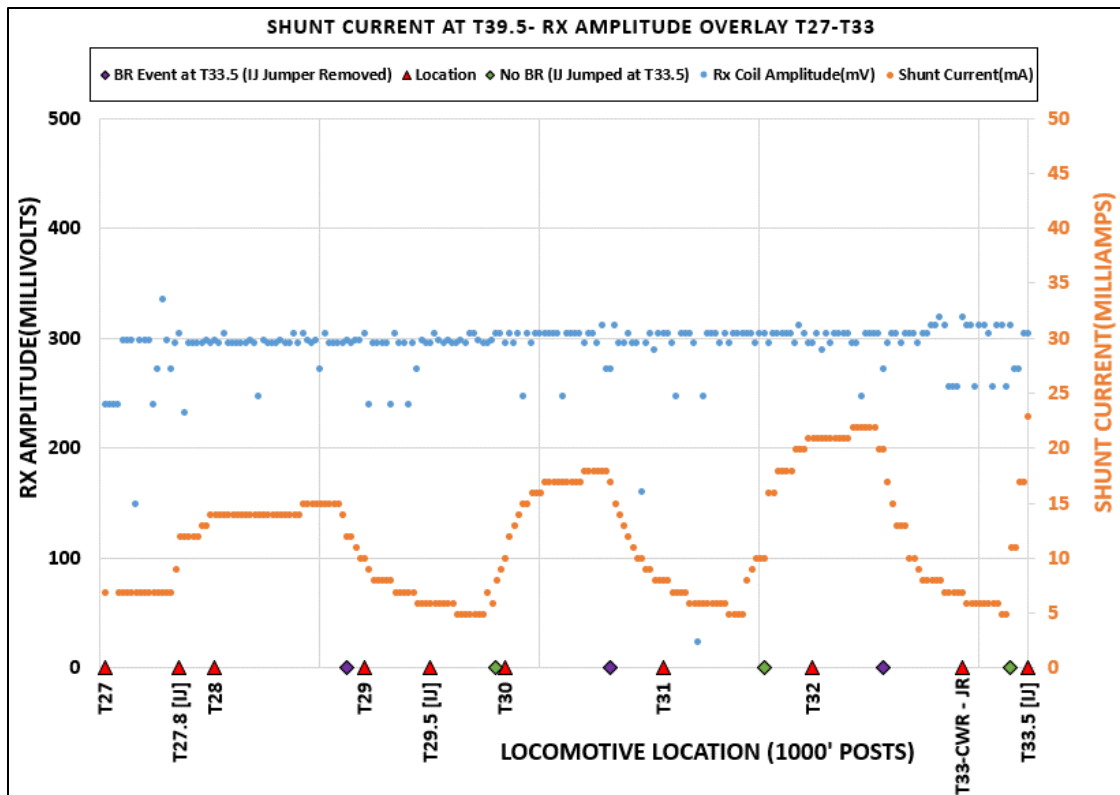


Figure 81. Dynamic Test Cases 7, 8, and 9 Tx and Rx Overlay vs. Locomotive Location from T27–T33.5

The induced shunt currents at the end of the test block for test cases 7, 8, and 9 (Configuration A) and test cases 4, 5, and 6 (Configuration B) were observed to behave as follows. The current increases noticeably from the noise floor/open shunt current (5–7 mA) as the train enters the test track at T27.8 with a shunt at the far end. As the train traverses the track section from T27.8 to T33.5 and gets closer to the shunt, the decrease in track resistance and the increase in ballast resistance within the loop led to the increases in the detected current at the shunt. The current appeared to increase logarithmically as it approached the shunt. For instances where the rail was broken, the induced signal dropped to the noise floor/open shunt value (5–7 mA). When the train stopped 100 feet from IJ at T33.5, the induced current leveled off at the peak. For tests where the locomotive went past the IJ at T39.5, the induced signal dropped off to the noise floor/open loop current (5–7 mA).

The measured Rx coil current shows a very slight monotonic increase as the train moves most of the way from T27 toward the T39 shunt. This increase is slight because the desired signal is being masked by crosstalk from the Tx coil on the same locomotive. Due to the resistance of the jumpers across the IJs at T33 no longer being in the circuit, a noticeable increase in the Rx coil current is seen when the train reaches this location. The other noticeable increase in the Rx coil current is seen when the train is very close to T39, where the desired signal detected becomes large enough to overcome the crosstalk masking.

Test cases 6 and 9 show the system can induce a signal from which a broken rail within a shunted track is discernable. [Figure 82](#) shows an overlay of the induced shunt current and the Rx amplitude for test case 6.

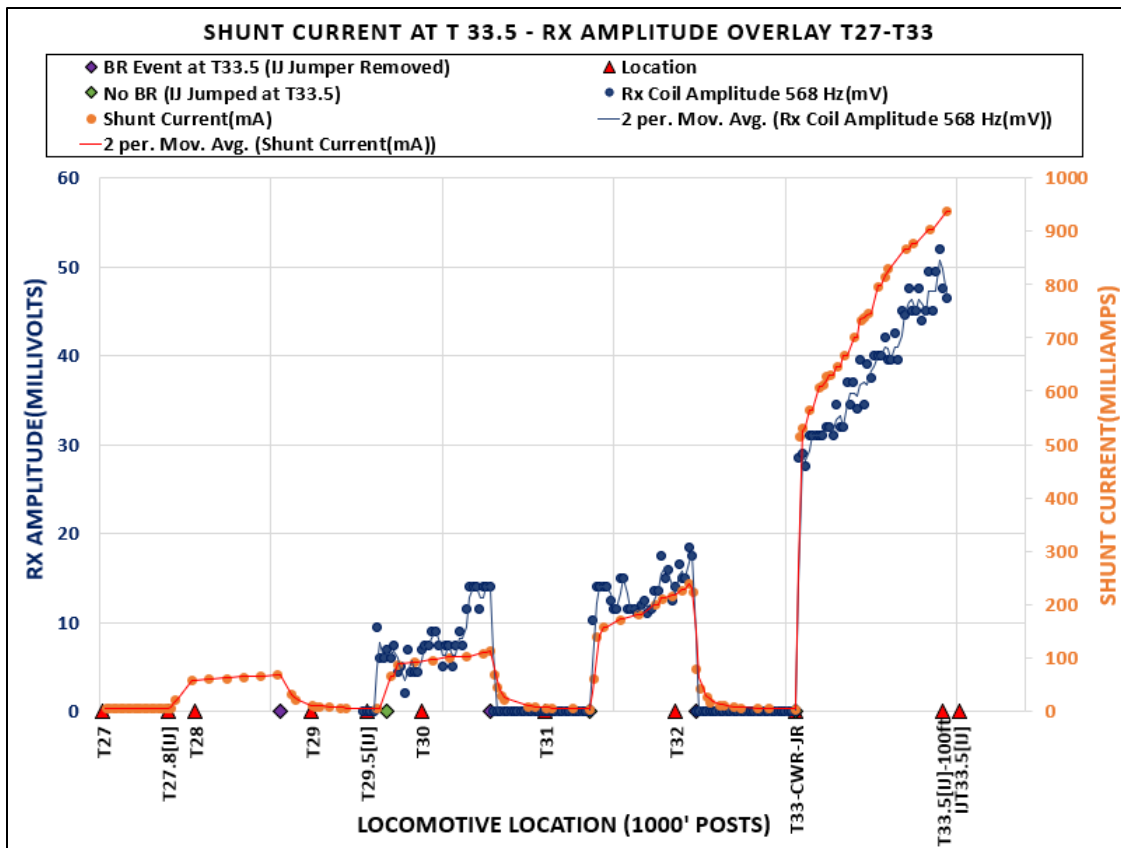


Figure 82. Dynamic Test Case 6 Tx and Rx Overlay vs. Locomotive Location

As the train enters the track section at T27.8, the current starts to rise as the train approaches the shunt. A rail break is simulated by removing the shunt from the IJ terminals at T33. After approximately 30 seconds, the shunt is reapplied. This cycle is repeated every 60 seconds (i.e., shunted for 30 seconds, then not shunted for 30 seconds) so that the difference in signal levels can be seen between the simulated cases of intact rail versus broken rail. The induced shunt current has been seen to drop and increase as the simulated rail break is made and removed. A similar behavior is observed with the Rx coil amplitude at approximately 3,000 feet from the shunt. Around this point, the induced signal in the rail increases in magnitude to the Rx coil signal pick up threshold with the approaching locomotive.

By comparing the similar data between test cases 5 and 6, a distinct difference between detected normal and broken rail status can be observed. This difference can be used to set the system to trigger a broken rail warning to the train control system on board the locomotive.

As soon as the simulated rail break condition was initiated, the detected shunt current decayed with a time constant before settling at the electrical noise floor (6 mA). The signal decay time constant on rail breaking decreased as the locomotive moved closer to the broken rail section and shunt.

4.2.5.10 Transmit Range

In test case 9, it was observed that the detected current at the shunt at T33.5 increases from the noise floor (6 mA) to approximately 12 mA when the train enters the shunted test block at T27.8

with the shunt. This result indicates an induced signal can be detected up to at least 12,000 feet in advance of the locomotive.

4.2.5.11 Signal Reception

By analyzing the recorded data, the signal received by the Rx coil was observed to have different characteristics with different system configurations. When the Tx and Rx coils are located on the same locomotive (test cases 8 and 9), the Rx coil signal amplitude remains relatively steady for Configuration A and slowly increases as the train gets closer to the shunt because the signal detected by the Rx coil is dominated by crosstalk from the nearby Tx coil. Because the desired signal is much smaller, it only has a small effect on the total signal level at the Rx coil.

The Rx coil is more effective at detecting the desired signal (not overwhelmed by crosstalk) when the Rx coil is located at the far end of the track block (Configuration B), particularly when the locomotive is within approximately 3,000 feet from the shunt. As the train approaches the shunt, the Rx signal amplitude noticeably decreases on initiation of a broken rail event (test cases 5, 6, and 11). In Configuration A, the level of coupling (Tx-to-Rx coil crosstalk) is evident during the dynamic testing with the Rx coil signal ranging between 248 and 300 mV. In contrast, the Rx amplitude in Configuration B ranged from 14 to 60 mV when the rail had no break.

4.2.5.12 System Performance with Wet Ballast

Test case 11 shows the system performance under wet track conditions. When comparing the data from test cases 5 and 11 ([Figure 80](#)), the system shows similar induced-current propagation characteristics. The detected signal is attenuated but not to a significant extent. Therefore, this system, as currently configured, continues to display an acceptable performance when the ballast is moderately wet, albeit with a slightly attenuated signal that can be picked up by an appropriate Rx. However, under heavy rain conditions, the results may be less acceptable. Further testing or modeling with ballast conditions representative of heavy rain as well as snow is recommended.

4.2.5.13 Conclusions

The following conclusions can be made from the dynamic test results:

- The test system can induce a signal that varies between normal clear track, broken rail, and occupied track. However, with the Tx and Rx coils collocated on the same locomotive, the signal picked up at the Rx coil is masked due to electromagnetic coupling with the nearby Tx coil and other environmental electrical noise. To meet the objectives of a production OBRD system, a method to mitigate the crosstalk will need to be devised, e.g., during a follow-on project.
- The Rx signal characteristics are affected by different system configurations, especially when the Tx and Rx coils are located at different locations, with the separation distance between coils in Configuration B highlighting the importance of reducing the coupling between Tx and Rx coils.
- At the tested settings, the current system has a well detectable signal propagation range of more than 12,000 feet.
- There was no significant induced signal attenuation from the wet track and ballast

conditions. However, applying more water and/or a longer period between track wetting and testing to allow the water to sufficiently foul the ballast and create real world heavy rain conditions (or modeling thereof) may be needed to observe significant signal attenuation.

To determine its viability, the described baseline OBRD system will need to induce, propagate, and detect a usable signal via a receiver on the same locomotive. The detected signal levels must be sufficiently different from each other to be distinguished by the system and ensure a clear, occupied, and broken rail track status. The signal induction and propagation from the dynamic test results have shown the system to be viable if the crosstalk problem can be solved. The research indicates that induction functionality is viable, but crosstalk mitigation is a lagging factor that will need to be further addressed for better system signal reception. Based on the field testing, analysis, and conclusions stated in this section, several research topics present themselves for further investigation to not only mitigate crosstalk but to enhance the overall OBRD system ([Section 7](#)).

5. Model Development

To assist with the development and testing of an optimal OBRD system, a helpful tool for further research would be models that incorporate empirical data to simulate the system's performance when certain track and environmental variables are changed. The data collected from the track characterization and dynamic testing data aided in the development of models that can be used to predict how the track characteristic impedance varies with changing weather conditions and track length, as well as how these variations would in turn affect the OBRD system transfer function and signal propagation capabilities. These models will be instrumental in defining the operational envelope parameters of a fully functional OBRD system.

The proposed models presented included:

- Track Impedance Model
 - Variation with length
 - Variation with temperature
 - Variation with moisture
- Signal Propagation Model
- OBRD system transfer function

5.1 Track Impedance Model

The OBRD system can be modeled as a Tx and Rx coil affected by track characteristic impedance. The input impedance for any length of track section can vary up to the track characteristic impedance, and the component parameters are affected by weather conditions, subsequently affecting the magnitude and phase of the input impedance. The following two models from [Equations \(12\) and \(13\)](#) can be derived by taking the empirical data and the transmission line equation into account:

- Variation with length
- Variation with temperature
- Variation with moisture

5.1.1 Impedance Variation with Length

The frequency-dependent maximum and minimum track characteristic impedance can be used to develop the operational envelope for the OBRD system. The data collected from the track impedance characterization effort described in [Section 3](#) provided a framework for determining the edges of the operational system boundary. The proposed model used the standard transmission line from [Equation \(5\)](#) as shown [Equation \(11\)](#) ([Section 2.4](#)):

$$Z(x) = Z_o \frac{Z_L + Z_o \tanh(\gamma x)}{Z_o + Z_L \tanh(\gamma x)} \quad (11)$$

Using the data from the track impedance characterization effort and applying the standard Tx line from [Equation \(5\)](#), a sample family ([Appendix H](#)) of 30 input impedances over the range of 30 frequencies, and the distance is shown in [Figure 83](#).



Figure 83. Sample Closed Loop Track Input Impedances at Different Frequencies and Distance to a Shunt

The track input impedance at a given distance from the shunt will be bound by the shunt impedance and the characteristic track impedance at a given frequency. This range of impedances and the propagation constant are affected by track and ballast conditions and type that, in turn, are affected by weather conditions. Therefore, the input impedance plot curvature given by the propagation constant and upper impedance bound defined by the track characteristic's impedance at a given frequency will be vary with changes in weather conditions, particularly moisture and temperature.

The input impedance when the system is an open circuit, i.e., the load/shunt impedance is infinite, can be derived from the standard Tx line from [Equation \(5\)](#) and can be expressed as the following equation.

$$Z(x) = Z_o \coth(\gamma x) \quad (12)$$

Using the data from the track impedance characterization effort and by applying [Equation \(12\)](#), a sample family ([Appendix H](#)) of 30 input impedances over the range of 30 frequencies and distance is shown in [Figure 84](#).

For both open loop and closed loop cases for a very long track circuit, the input impedance tends toward the characteristic impedance of the track. The input impedance of a short or open-circuited lossless Tx line alternates between open- ($Z(x) \rightarrow \infty$) and short-circuit $Z(x) = 0$) conditions with each $\lambda/4$ increase in length(x) (Ellingson, S. W., 2018).

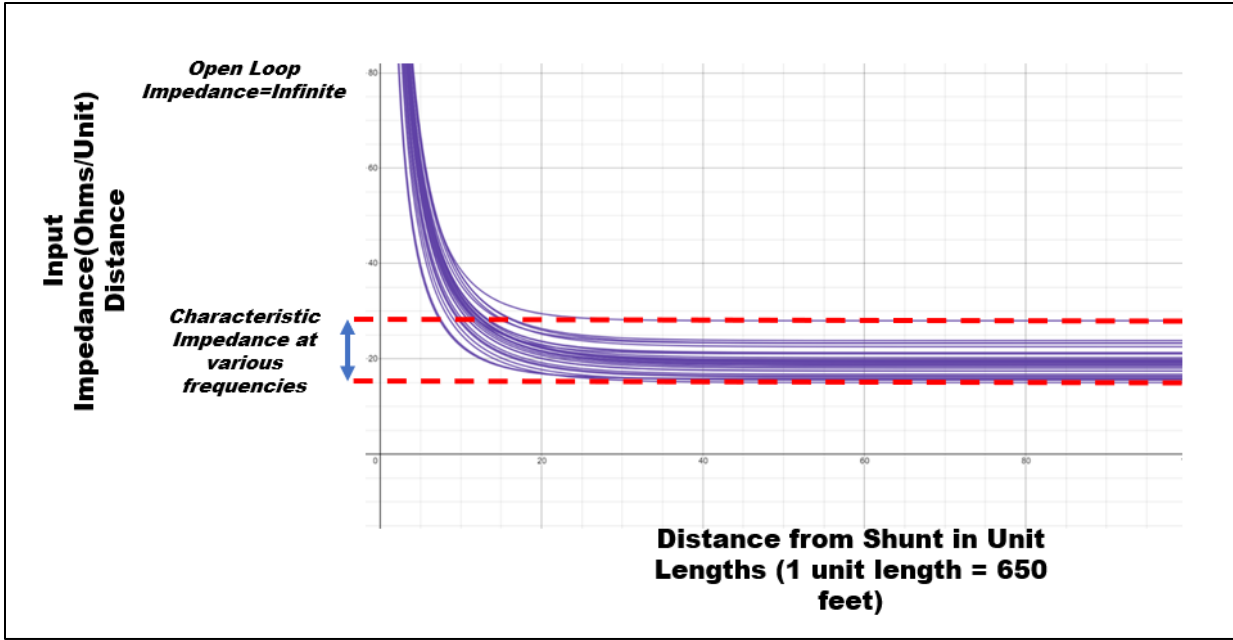


Figure 84. Sample Open Loop Track Input Impedances at Different Frequencies

5.1.2 Impedance variation with Temperature Model

It was observed that the rail temperature varied cyclically with the ambient temperature (Figure 17) over a period of 24 hours, in particular temperature and moisture, affected the environmental conditions. Temperature had the greatest impact on the resistance component while moisture had the greatest impact on the ballast conductance. Therefore, rail resistance and ballast conductance are the primary drivers of the relationship between temperature and moisture variance.

For a conductive material, resistance varies with temperature as follows:

$$R(T) = R_0(1 + \alpha(T - T_0)) \quad (13)$$

Where:

R = Resistance after temperature change (Ohms)

R₀ = Original resistance (Ohms)

α = Temperature coefficient of resistance for the conducting material (Rail/Ballast)

T = Conductor (Rail/Ballast) temperature

T₀ = Reference temperature that alpha is specified for the conducting material (Rail/Ballast)

In addition to temperature, the resistivity of the ballast is inversely proportional to the moisture content. Using the data collected and previous research (Parsons, R. L., Rahman, A. J., Han, J., Glavinich, T. E., 2014), the model relating conductance and moisture can thus be given using the following Equation (14):

$$G(p) = G_0 + G_{max}(1 - e^{-p}) \quad (14)$$

Where:

G = Conductance in Siemens per unit length as a function of ballast moisture content

G_0 = Conductance in Siemens per unit length with 0 percent ballast moisture

G_{max} = Conductance in Siemens per unit length at maximum ballast moisture saturation

p = ballast moisture content as a percentage

The R and G values can then be applied to the characteristic impedance formula and modify it as follows:

$$\gamma(T, p) = \sqrt{(R(T) + j\omega L)(G(p) + j\omega C)} \quad (15)$$

and:

$$Z_o(T, p) = \sqrt{\frac{R(T) + j\omega L}{G(p) + j\omega C}} \quad (16)$$

modifying the input impedance formula as follows:

$$Z_{in}(x, T, p) = Z_o(t, p) \frac{Z_L + Z_o(T, p) \tanh(\gamma(T, p)x)}{Z_o(T, p) + Z_L \tanh(\gamma(T, p)x)} \quad (17)$$

Equation (17) can be used to derive the relationships between the track temperature and ballast moisture content and the characteristic and input impedance of a given track section.

5.2 Signal Propagation Model

Per Section 5, the system can be simplified to define the operational boundaries of an OBRD system. The system operational envelope will be bound by the minimum and maximum characteristic impedance values for a given unit distance of track. This operational envelope can be used to define the fail-safe parameters of an OBRD system.

For the empirical data collected, the current appears to vary logarithmically with distance. Since the emf is nearly constant, the track impedance is inversely proportional to the current. Therefore, an operational envelope of various impedances could be used to approximate the expected impedance and signal propagation limits and determine the operational boundary so the system became a fail-safe once the predefined boundary of the system operational envelope is breached.

Given the following Equation (17):

$$emf = I_r Z_{in}(x) \quad (18)$$

Where:

I_r = Current in rail due to induced emf and track impedance loop (Wb/m²)

emf = Induced electromotive force in rail due to the varying magnetic field of the Tx coil (Volts)

$Z_{in}(x)$ = Input impedance as a function of distance from a shunt (Ohms/per unit distance)

Then:

$$I_r = \frac{emf}{Z_{in}(x)} \quad (19)$$

The current propagation is the reciprocal of the input impedance that can be given by the reciprocal of the input impedance and varies accordingly with the propagation constant as shown in Equation (20).

$$I_r = \left(\frac{1}{Z_{in}(x)} \right) \quad (20)$$

The above Equation (20) can be enhanced to account for dynamic changes in impedance due to temperature and moisture by using $Z_{in}(x, T, p)$ as opposed to $Z_{in}(x)$.

5.3 Proposed System Model

The proposed system model is derived from an ideal transformer model where the transformer coil intermediates between the input and output signals. The model replaces the primary input coil of the transformer with the Tx coil and the secondary output coil with the Rx coil. The transformer core is replaced with a characteristic impedance in the track circuit loop. Figure 85 illustrates the functional diagram of the system model.

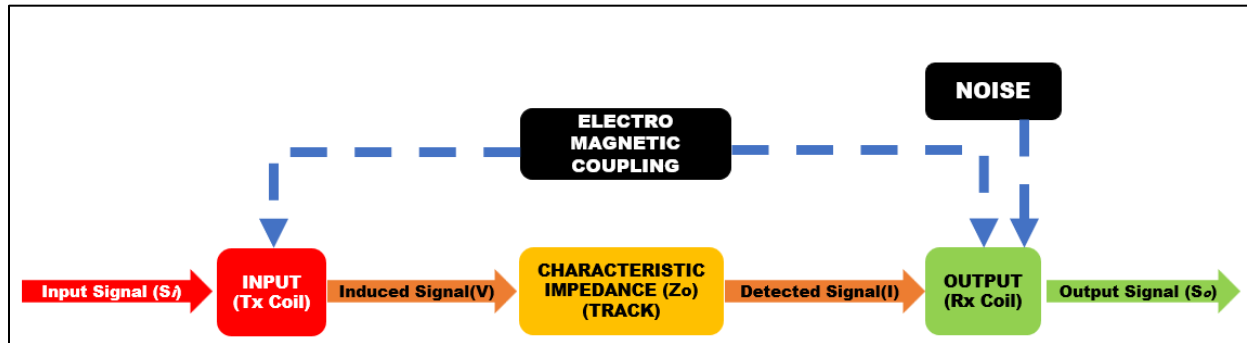


Figure 85. Functional Block Diagram of System Model

The functional diagram shows the system model signal flow from initial signal generation, then propagation, and finally detection. Each block diagram part can be mathematically or electrically represented to produce a highly generalized model. The signal flow and interaction with each section can be explained as follows:

- Input signal: A signal generator creates the AC input signal that is then amplified to drive the Tx coil. The model is not concerned with how the magnetic field is generated but with how the magnetic field is used to induce a voltage and resultant current in the rail.
- Input Tx coil: The Tx coil produces a changing magnetic field that induces an emf in the rail. The equation to determine the induced emf can be found in [Section 2.2](#).
- Characteristic impedance: The characteristic impedance determines the magnitude and phase of the resultant current induced by the emf. The propagation characteristics of the signal at a given distance are a function of the characteristic impedance and propagation constant of the transmission line model. The relationship between the voltage and current is given by ohms law.
- Output Rx coil: The output Rx coil detects the changing magnetic field due to the induced current in the rail and generates voltage in the Rx coil. The characteristics of the coil will determine the output voltage.

- Output signal: The output signal is an AC voltage that drives a signal detection circuit. The detection circuit could present a high input impedance to a signal detection/processing unit.
- Magnetic coupling: Magnetic coupling over the air will occur due to the interplay of the magnetic field generation function of the Tx coil and the magnetic detection function of the Rx coil. This coupling is defined by the same equation that defines emf induction, but it could also be reduced to a coupling constant that would vary with the strength of the magnetic field.
- Electromagnetic noise: There are several sources of both internal and external electromagnetic noise. These sources include, but are not limited to, the system self-induced noise, particularly from the RNB, locomotive electric motor noise, overhead electric power lines, catenary power lines, etc. The noise can be reduced to a signal constant for simplicity.
- Transfer function: The functional block equations combine all the identified flows that are then used to develop a transfer function for the system. The transfer function can then be used to simulate the expected performance of a system given certain variable inputs.

5.4 Transfer Function Model

A transformer offers an analogy (i.e., two coils intermediated by a circuit) for developing the system model transfer function with the Tx coil modeled as the primary coil, the Rx coil modeled as the secondary coil, and the track modeled as the transformer core. Using a transformer analogy as the starting point, a transfer function can be developed based on the input (at the Tx coil) and output (at the Rx coil) magnetic fields.

The transfer function can be used to simulate the propagation characteristics of an induced signal given certain track conditions represented by the input impedance of the track circuit at a given distance. A transfer function that relates the input magnetic field from the Tx coil in the rail (B_{tx}) and the induced magnetic field at the Rx coil (B_{rx}) can be derived as follows.

Where:

B_{tx} = Generated magnetic flux at Tx coil (Wb/m^2)

B_{rx} = Induced magnetic flux at Rx coil due to current in the rail (Wb/m^2)

I_r = Current in Rail due to Induced emf and track Impedance Loop (A)

r = Distance of Rx coil from rail (m)

S = Cross section areal of active area (m^2)

emf = Induced electromotive force in rail due to B_{tx} (V)

x = Distance from shunt (unit distance)

$Z_{in}(x)$ = Input impedance as a function of distance from a shunt (ohms/unit distance)

f = Frequency of B_{tx} (Hz)

μ = Permeability of a medium (H/m)

μ_o = Permeability of free space = $4\pi \times 10^{-7}$ (H/m)

The Transfer Function (T(s)) is computed using Equation (21):

$$T(s) = - \frac{\text{Input magnetic flux density}}{\text{Output magnetic flux density}} = \frac{B_{rx}}{B_{tx}} \quad (21)$$

Combined with the equations from Section 2.2:

$$B_{rx} = \mu_o \frac{I_r}{2\pi r} \quad (22)$$

$$B_{tx} = \frac{\text{emf}}{Sf} \quad (23)$$

Applying Ohms law:

$$\text{emf} = I_r Z_{in}(x) \quad (24)$$

Implies:

$$B_{tx} = \frac{I_r Z_{in}(x)}{Sf} \quad (24)$$

Since:

$$T(s) = \frac{B_{rx}}{B_{tx}} \quad (25)$$

By substitution:

$$T(s) = \frac{B_{rx}}{B_{tx}} = \mu_o \frac{I_r}{2\pi r} \div \frac{I_r Z_{in}(x)}{Sf} \quad (26)$$

Simplifying to:

$$T(s) = \frac{B_{rx}}{B_{tx}} = \frac{\mu_o Sf}{2\pi r Z_{in}(x)} \quad (27)$$

The value of Z_{in} tends toward the characteristic impedance of the track as “x” tends to infinity and reduces to the shunt impedance when $x = 0$. When the shunt impedance is equal to the characteristic impedance of the track circuit, conditions for maximum power transfer are established, and the system appears to be purely resistive.

The system transfer function (T(s)) derived above can be used to determine the propagation potential of a signal under various track conditions (Z_{in}) including the following:

- The average magnitude of the time-varying magnetic flux of the Tx coil.
- The characteristic track impedance of a given section of track.

The following assumptions are made:

- The Tx coil is positioned 3 inches above the rail with the generated magnetic flux perpendicular to the rail. However, the equation can be modified with the B_{tx} varying inversely with the distance from the rail.
- The crosstalk due to magnetic coupling is zero (assumed to be mitigated by effective shielding and filtering).

The transfer function is only concerned with the properties of the generated signal (i.e., magnitude, phase, amplitude, and frequency) and does not consider how the inducing magnetic field is generated by the Tx coil nor how the magnetic field is picked up by the Rx coil. These functions would be design specific to the respective coils. However, the equation can be used to determine 1) the desired design magnetic field generation of the Tx coil and 2) the desired signal pick-up sensitivity of an Rx coil for a given signal under certain track conditions.

The transfer function presented is a highly generalized ideal function, but this function does not limit its usefulness. For example, this function can be used to estimate initial system behavior and can be improved upon to accommodate the impact of noise, “crosstalk,” and design characteristics of different types of Tx and Rx coils.

5.5 Summary

At the core of each model is the track input impedance at distance “x” from the shunt that is bound by the shunt impedance and the characteristic track impedance. The input impedance will vary with characteristic track impedance, changes in environmental conditions and track conditions, both of which will subsequently affect the OBRD system performance. [Table 22](#) provides a summary of the models.

Table 22. Summary of Proposed Models

Model	Mathematical Representation
Track Impedance Model Variation with Length of Track	$Z_{in}(x) = Z_o \frac{Z_L + Z_o \tanh(\gamma x)}{Z_o + Z_L \tanh(\gamma x)}$
Track Impedance Model Variation with Temperature and Moisture	<p>Given that the system resistance is given by:</p> $R(T) = R_0(1 + \alpha(T - T_0))$ <p>and system conductance as a function of ballast moisture content is given by:</p> $G(p) = G_0 + G_{max}(1 - e^{-p})$ <p>Then, Z_{in} as function of distance, system temperature and system conductance:</p> $= Z_o(T, p) \frac{Z_{in}(x, T, p)}{Z_o(T, p) + Z_L \tanh(\gamma(T, p)x)}$
Signal Propagation Model	$I_r = \frac{emf}{Z_{in}(x)}$
System Transfer Function Model	$T(s) = \frac{B_{rx}}{B_{tx}} = \frac{\mu_o S f}{2\pi r Z_{in}(x)}$

Although anchored in theoretical and empirical data, the proposed foundational models will need to be continuously back tested under various scenarios and assumptions that capture as many of the real-world variances as possible. It is expected that the models will continue to evolve and incorporate more variables, such as noise due to the locomotive electric motor and other noise, the addition of tuned shunts, etc., to become more robust as further research on the topic is carried out.

In addition, although a function-based approach in developing the model is presented, there is an opportunity for the collected track impedance data to be used in further research with a big data, model-based approach.

6. Preliminary Development and Migration Plan

The OBRD research project focuses on adopting and incorporating the technology into an enhanced version of the Overlay-Positive Train Control (O-PTC)/Quasi-Moving Block (QMB) train control system to enable the adoption of FMB operations. Since the project concept is still in the early stages of development, a preliminary development and subsequent migration plan are presented. Therefore, this section is divided into two main categories:

1. A development plan for transforming the research into a fully functional viable technology capable of integrating with a train control system
2. The migration plan for the wide-scale deployment of the system in support of FMB operation

6.1 OBRD Development Plan

Several phases would be expected to evolve the system into a highly reliable OBRD system that would replace conventional track circuits and enable FMB operations. [Figure 86](#) illustrates the proposed subsequent phases of the OBRD development with this research project as Phase 1.

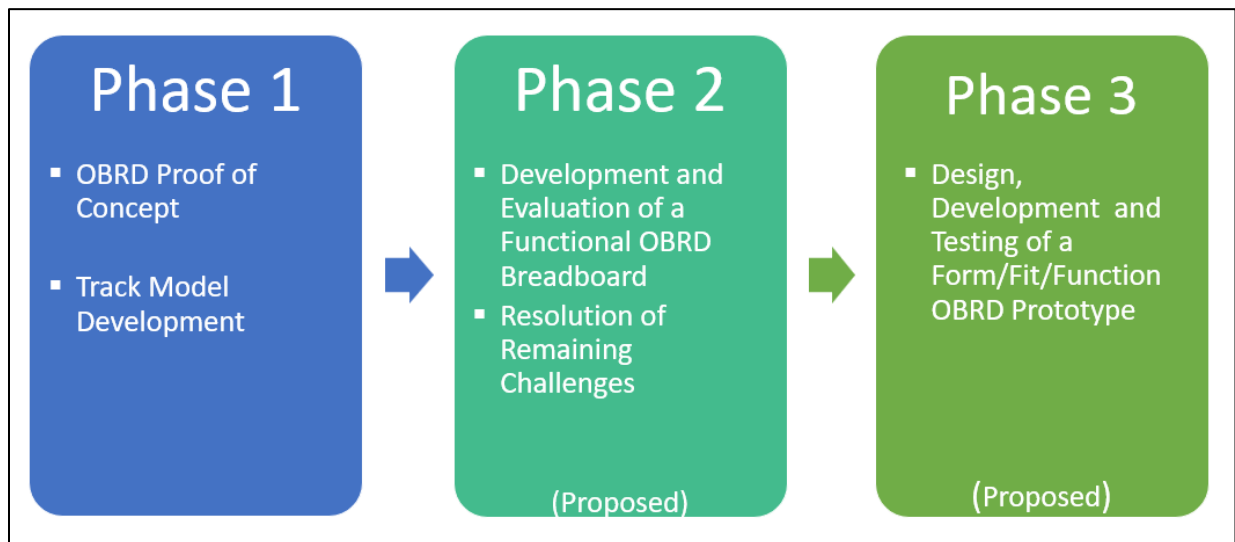


Figure 86. Development Phases of the OBRD Concept

The objectives of Phase 2 include:

- Demonstrating the OBRD concept as a complete breadboard design
- Evaluating using the models developed in this project, analyzing and comparing other potential alternative architectures and configurations to potentially improve performance
- Identifying issues with the potential solution(s) and proposing practical mitigations

The scope of Phase 2 consists of:

- Using the models developed in Phase 1 to analyze and compare other potential alternative variants, architectures, and configurations that could improve system performance

- Developing a minimum viable, functional breadboard design that incorporates the identified mitigations
- Evaluating and testing the breadboard in the lab and field environments
- Developing technical specifications for the proposed solution

Phase 3 will be the development of a form/fit/function demonstrator system capable of interfacing with O-PTC/QMB in support of a FMB that will be the final step in the development of the OBRD concept. After developing a functional demonstrator prototype with definitive specifications for use by vendors to design fully operational OBRD systems, the following proposed deployment migration plan can be initiated.

6.2 Deployment Migration Plan

Once integrated with O-PTC, the OBRD concept will set the stage for the widescale adoption and deployment of FMB. Therefore, changes must be made to the functionality of O-PTC to accommodate interfacing with the OBRD concept. The required changes have been captured in the FMB concept of operations (ConOps) and companion system and segment requirements developed in a parallel FMB (TTCI, Pending) project. In addition to the ConOps and required specifications, a migration plan for several alternatives of the Alternative Broken Rail and Rollout Detection/Alternative Broken Rail Detection (ABRRD/ABRD) was developed, and this plan details the proposed deployment approach. The FMB ConOps details the three alternative ABRRD/ABRD variants as follows:

- **Head-of-Train (HOT)-ABRRD:** Onboard broken rail and rollout detection interrogates the track ahead of the train
- **End-of-Train (EOT) ABRD:** Onboard broken rail detection interrogates the track behind the train
- **Wayside ABRRD:** Alternative wayside broken rail and rollout detection, i.e., wayside-based but without the limitations of fixed block track circuit-based detection

Since the OBRD system detailed in this project falls primarily under the category of a HOT-ABRRD, this section will summarize only the proposed migration path for the HOT-ABRRD/ABRD.

6.3 HOT OBRD Migration Plan

The FMB Migration Consideration document describes migration considerations, including cost drivers, potential implementation paths, and steps for the FMB train control method and ABRRD/ABRD alternatives. In addition, this document provides a high-level cost driver analysis for each path.

The FMB migration plan for the HOT-ABRRD technologies is shown in [Figure 87](#). This plan consists of 3 initial territory stages and 10 potential paths to FMB implementation. The three stages include:

- **Stage a:** FMB active with all track circuits and Wayside Status Messages (WSMs)
- **Stage b:** FMB active without conventional track circuits. This stage has two possibilities depending on the infrastructure at two control points.

- Field interlocking (b.1)
- Switches status awareness (b.2)
- **Stage c: FMB with alternative IXL**

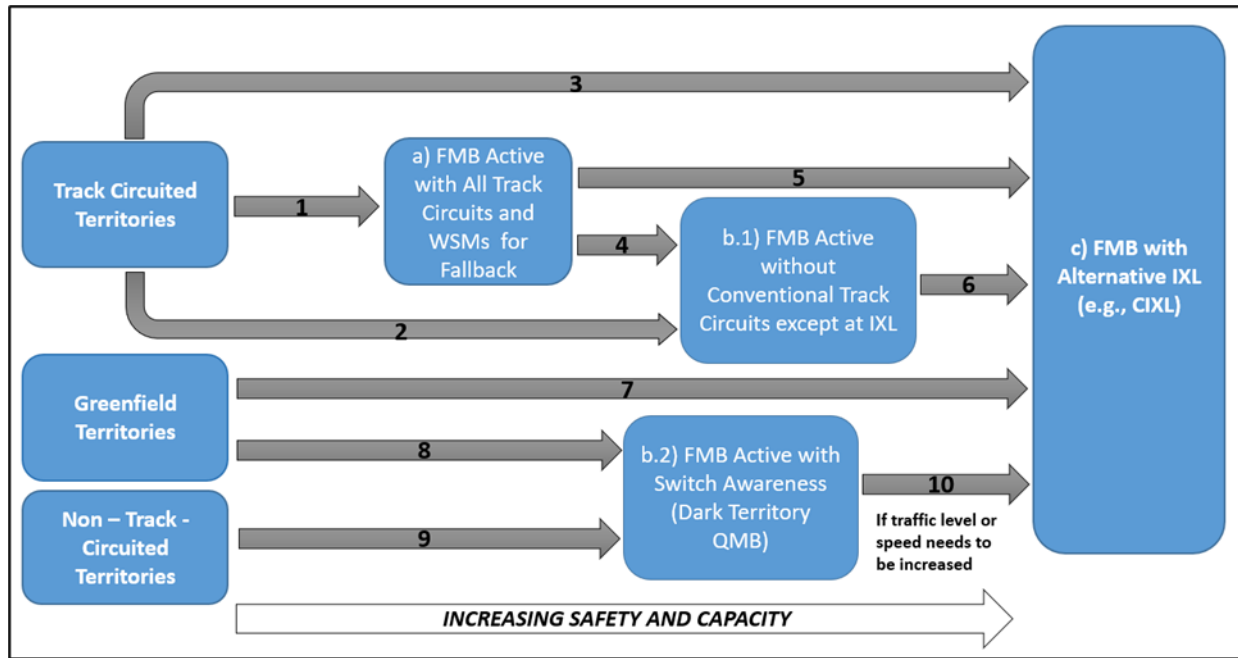


Figure 87. HOT-ABRRD Migration path

Further enumeration on the identified paths, cost drivers, and high-level migration steps is beyond this project’s scope but can be found in the FMB Migration Considerations document (TTCI, Pending).

7. Conclusion

From October 2019 to May 2022, the team researched a concept for an OBRD system that sends and receives AC electrical signals generated on board the locomotive transmitted to the rail via electromagnetic induction with the resultant current propagating through a track section, and back to the locomotive via (tuned) shunts. This research used the long-term data collection of track electrical parameters for use in track impedance characterization. The collected data was used to 1) determine the relationships between track impedance and weather conditions (e.g., temperature, ballast moisture content, etc.), 2) develop foundational models to further research, and 3) develop an OBRD system and framework OBRD operational envelope. The three fundamental challenges included:

1. Strong mutual inductance between the Tx and Rx coils
2. Weak mutual inductance between the rail and the induction coils
3. Track impedance variability

Through the R&D efforts, significant progress was made in the area of inducing a usable signal in the track and reliably propagating the signal over a range up to 2 miles (4 miles round trip). However, there still remains many railroad scenarios where propagation needs to be greater than that (e.g., a heavy train on a downgrade). In addition, the dynamic testing was carried out using one frequency (568 Hz) and track condition. Therefore, the performance reliability will have to be investigated under different frequencies and various track conditions to ascertain a signal can be reliably induced, propagated, and detected at ranges of 2 miles or more for multiple signal frequencies and various track conditions (i.e., weather and types of ballast).

The induced signal also varied appreciably with a change in track state (i.e., broken rail, shunted rail or open rail) indicating a suitable Rx coil would be able to detect these changes in the return signal. Although using passive means (shielding) reduced its effect, crosstalk still masked Rx coil detection sensitivity. The noise and crosstalk detected by the receiver made discerning the induced signal state uncertain, requiring the need for more work in active crosstalk mitigation and signal detection.

The track impedance data collection effort collected several million data points at the rate of 2 MB per day of RLCG, Open Loop Impedance, Closed Loop Impedance, weather, and sensor data per day. This data was used to 1) understand the relationships between track impedance and weather conditions and 2) develop track impedance-based signal propagation models. These models will be useful in developing theoretically plausible signal propagation outcomes due to variable track impedance conditions and improving the overall system performance.

The result of this research confirms the possibility of the general concept of an OBRD system based on an induced signal generated by an onboard transceiver and propagated through the rail with the return signal picked up by the same onboard transceiver. Making the system more reliable in picking up and inferring the signal and integrating it to an onboard train control (i.e., PTC) system would be the final step in enabling FMB functionality.

Recommendations for further improvement of the results of this project and the enhancements of the concept are:

- Interference canceling techniques: Signal canceling technology has been in use for

decades to attenuate interferers based on the direction of arrival or recognizable signal characteristics. This technique involves producing a signal identical to the received interference but 180 degrees out of phase. This signal, when added to the received signal, cancels the interference. In situations where the interferer does not have significant frequency separation from the desired signal, interference cancelers provide far greater attenuation (e.g., 60 dB) than is achievable by filtering. OBRD is particularly well suited for interference canceling since the interfering signal is readily available onboard for subtraction from the received signal.

- Tx and Rx coil R&D to explore different types of Tx and Rx coils and configurations: This research focused primarily on the use of cab signal pick up coils. Other magnetic field detection receivers could be used but have not been tested (e.g., a Transceiver coil) (i.e., a Tx and Rx coil on the same coil).

8. References

- Al-Nazer, L. (2008). [*Development of Rail Temperature Prediction Model*](#). Research Results No. RR08-06, Washington, DC: U.S. Department of Transportation, Federal Railroad Administration.
- B&K Precision. (2020). [*B&K Precision LCR Meter Guide*](#). Yorba Linda, CA: B&K Precision.
- Dorf, R. C. (2000). The Electrical Engineering Handbook. In C. Dorf Richard, *The Electrical Engineering Handbook* (pp. 803–879). Boca Raton, FL: CRC Press Inc.
- Ellingson, S. W. (2018). [*Electromagnetics, Vol. 1. In E. S. W, Electromagnetics, Vol. 1.*](#) Blacksburg, VA, Blacksburg, VA: Virginia Tech University Libraries.
- Liu, C., Yang, S., Cui, Y., et al. (2020). Quantitative analysis on coupling of traction current into cab signaling in electrified railways. *Railway Engineering Science*, 28, pp. 275–289.
- National Weather Service Weather Forecast Office. (2021). [*Climatological Report \(Annual\) Pueblo, CO.*](#) Retrieved from NWS.
- Parsons, R. L., Rahman, A. J., Han, J., Glavinich, T. E. (2014). Track Ballast Fouling and Permeability Characterization by Using Resistivity. *Transportation Research Record: Journal of the Transportation Research Board*, 2448(-1), 133–141.
- The Association of American Railroads, (AAR). (n.d.). AAR standard S-9101, Locomotive Electronics System Architecture. *Locomotive Electronics System Architecture*.
- Transportation Technology Center, I., Polivka, A. L., Malone, J. J., Smith, B. E., & Renfrow, S. M. (2013). *USA Patent No. 9,162,691*.
- Transportation Technology Center, Inc. (2013). *Internal Research and Development Report: Track Impedance Research for Onboard Broken Rail Detection Project*. Pueblo, CO: TTCI.
- Transportation Technology Center, Inc., Malone, Jr., J. L., & Polivka, A. L. (2013). *USA Patent No. 9,102,341*.
- Transportation Technology Center, Inc. (Pending). *Full Moving Block Requirements for Railroad Operations*. Washington, DC: Federal Railroad Administration (FRA).
- Zhang, Y. J., Clemenzi, J., Kesler, K. & Lee, S. (2007). [*Real Time Prediction of Rail Temperature*](#). *Proceedings of the AREMA 2007 Annual Conference*. Chicago, IL: American Railway Engineering and Maintenance-of-Way Association.

Appendix A. Resonance Signal Generator Equipment Setup Instructions

Purpose:

This guide is designed to familiarize the user of the magnet system with setting up and using the high-power magnet system safely and effectively.

Safety Concerns:

The resonant capacitor network can produce above 2,000 V even with a low input voltage. Therefore, no modifications can be made to the jumpers or connections while the network is in operation, but the capacitor network can hold several seconds of charge after power has been removed.

Before modifications are made to the system, both high-voltage terminals should be shorted to ground. The transmission (Tx) coil electromagnet can produce high fields and high temperatures. Care should be taken to monitor the magnet's temperature with a temperature sensor when operating at high fields. The hot spots of the magnet are the two faces closest to the target. The Resonant Network Box (RNB) box can produce four resonant frequencies set by selecting jumpers. The RNB and jumper locations are shown in [Figure A1](#).

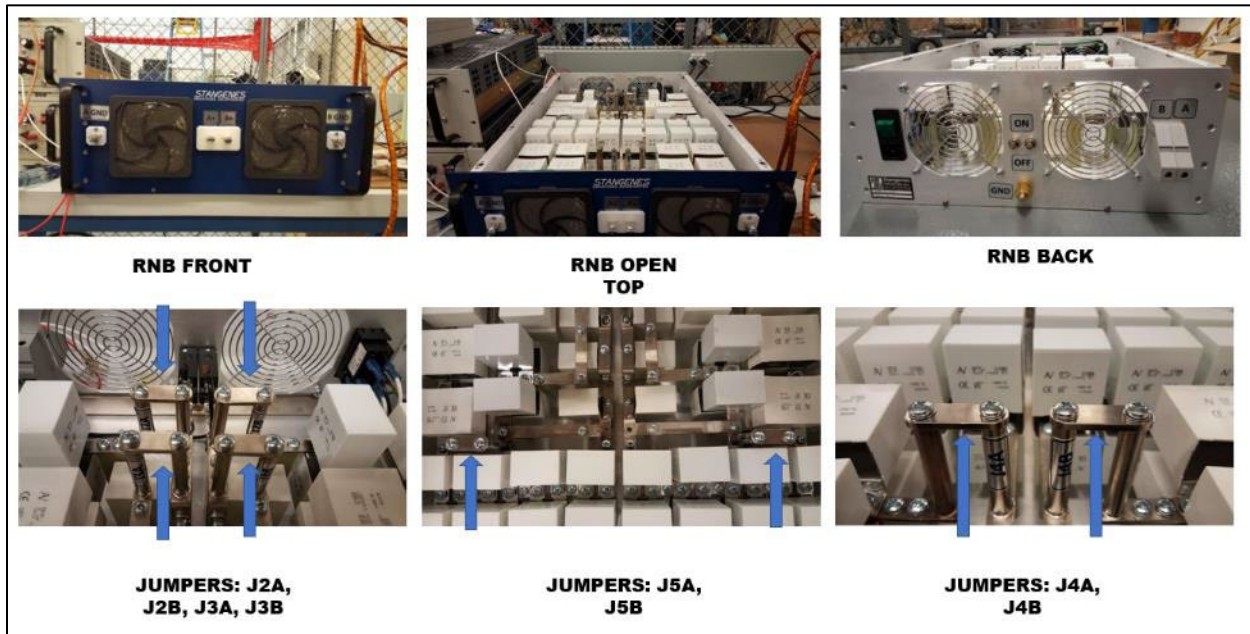


Figure A1. RNB Showing Jumper Locations

[Figure A2](#) shows the circuit diagram showing the amplifier, Resonant Network, and Tx coil.

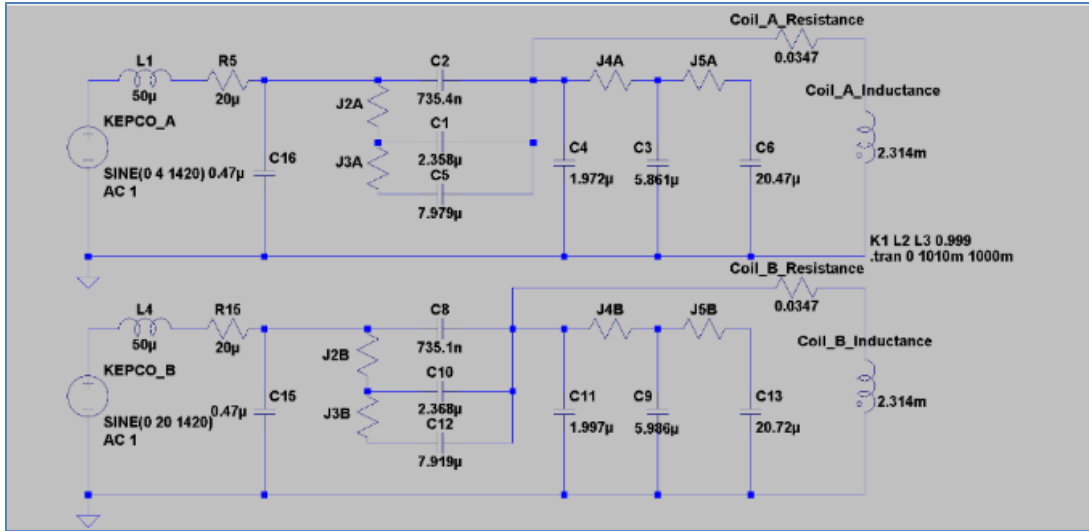


Figure A2. RNB Circuit Diagram

The manufacturer expected resonance frequencies, jumper settings, and RNB output terminal currents that are shown in [Table A1](#).

Table A1. RNB Vendor Defined Jumper Settings

Resonance Frequency (Hz)	Jumper Settings	Current at A and B Terminals
1,420	All Jumpers Open	18 A
707	J2A J2B J4A J4B Jumped	30 A
419	J3A J3B J4A J4B Jumped	42 A
373	All Jumpers Jumped (Default)	48 A

The Tx coil generates a magnetic field at a given resonance frequency setting.

Setup

The signal generation setup block diagram is shown in [Figure A3](#).

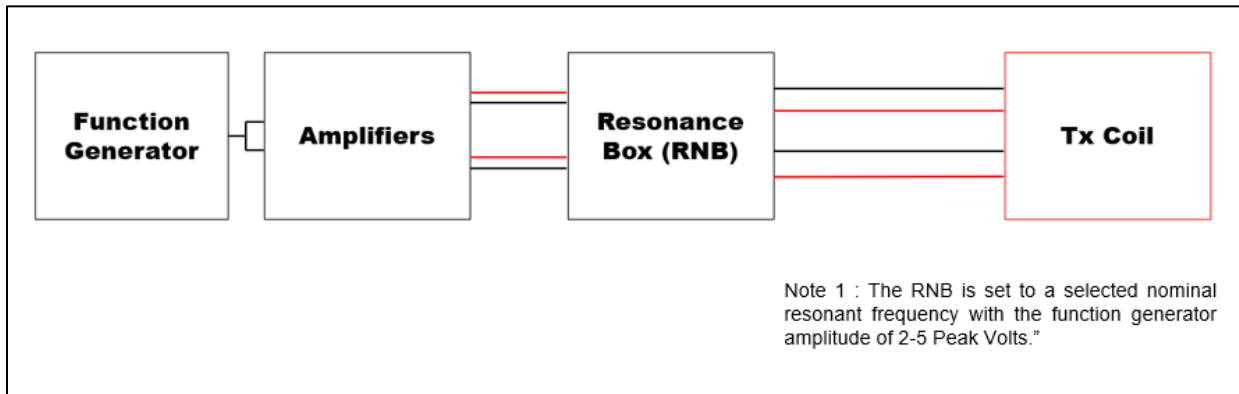


Figure A3. Flow Diagram of RNB Setup

Power Supply Setup

- Connect both power supplies to 120 V AC sources
- Each power supply must receive the same 10 V peak signal from the signal generator to ensure that each coil current is in phase with the other. Connect this across both “Voltage Programming Inputs.”
- Connect “Common” to “Ground” to ensure everything is grounded at this point
- Connect any voltage or current diagnostics to monitor the power supply output

Resonant Network Setup

- Connect the RNB to 120 V AC. This only serves to power the fans to cool the capacitors that are switched on at the connector. The fans should always be on during operation.
- On the back of the RNB, connect from the “A” terminal to the “Output” of one of the supplies. Connect the “B” terminal to the “Output” of the other supply. Both power supplies “Common” will connect to the “GND” terminal on the back of the RNB.
- On the back of the RNB, both power supplies “Common” will connect to the “GND” terminal.
- Ensure that the wires used to connect the power supplies to the RNB are rated for at least 20A/20 V.

The signal generator’s output is split into the input of both power supply amplifiers to ensure the phase of the output of both amplifiers is in sync. One of the power supply amplifiers goes to the “A” side of the RNB, and the other goes to the “B” side of the RNB. The “A” side and “B” side outputs are connected to the four inputs of the Tx coil.

Tx Coil Setup

1. The polarity of the connections is important. If the polarity is incorrect, then the magnetic fields will buck, the circuit will not work, and no field will be output.
2. From the front of the RNB, the “A+” terminal on the RNB Front Panel should be wired to the “A+” terminal on the magnet. Likewise, the “AGND” terminal on the RNB Front Panel should be wired to the “A-” terminal on the magnet.
3. From the front of the RNB, the “B+” terminal on the RNB Front Panel should be wired to the “B+” terminal on the magnet. Likewise, the “BGND” terminal on the RNB Front Panel should be wired to the “B-” terminal on the magnet.
4. If a wire extension needs to be made, ensure that the extension used is rated 100A/2,000 V at the utilized frequency. Keep in mind that these terminals are the most electrically dangerous of the circuit.

Energizing the Signal Generation Setup

The following steps are to be carried out to configure and energize the resonant signal generator equipment setup.

- Configure RNB jumpers to the desired test frequency: The RNB operates at high voltages. Be sure to short each capacitor bank to ground across a resistor prior to

touching anything in the RNB.

- Power on the signal generator, both power supplies, and the fans on the RNB.
- Select the desired frequency and input voltage on the signal generator: All tests were run with $3\text{ V} \pm 0.5$ output from a signal generator to ensure consistent power to the amplifiers.
- Close the A and B side switches on the RNB: The system is fully energized at this point. Do not touch the RNB, the coil, or any other part of the system.
- Using the High Voltage A and High Voltage B values, find the resonant frequency for the system: The highest value corresponds to the resonant point, and resonant points vary based upon test setup.
- Vary frequencies around resonant points as needed and record the desired data.
- Open the A and B side switches on the RNB.
- Turn off the signal generator, amplifiers, and fans on the RNB.

Appendix B. Tx Coil Specifications

Throughout OBRD testing, the Tx coil is a custom-designed coil procured from Stangenes® shown in [Figure B1](#).



Figure B1. Profiles of Tx Coil

Specifications

- Frequency range: 373 Hz–2,000 Hz
- Number of coils: Two coils (A and B)
- Cross section dimensions of each coil: 1.77 inches x 3.5 inches
- Total core dimensions: 1.77 inches x 7.08 inches
- Core material: Nanocrystalline

Tx Coil external dimensions

- 12 inches x 15 inches x 8.5 inches

Design Notes

- The windings are composed of eight #10 gauge independently insulated wires running in parallel to make a sort of “thick wire litz.” There are 68 turns per winding.
- The cores are to be driven separately by two 20-20 amplifiers at selected resonant frequencies.
- Theoretically, running the Tx coil at 80A peak/136 turns (68x2 windings) will give you 10,880 amp-turns on the magnet, allowing the nanocrystalline to run just below the saturation bend of the material with cross section of the 1.5 inches x 3 inches.
- The magnet is epoxy cast and includes provisioning for water cooling.

Theory of Operation

With a magnetic field at 3 inches from the rail, the magnetic field at 80A at a point in the center of the magnet plane located 3 inches from the magnet is 300 Gauss (G). The field at that point at any other current is shown in [Equation \(1\)](#):

$$\text{Peak Flux (G)} = 300 \times \frac{\text{Current}}{80} \quad (1)$$

A simulation of the Tx coil electromagnet is shown in [Figure B2](#).

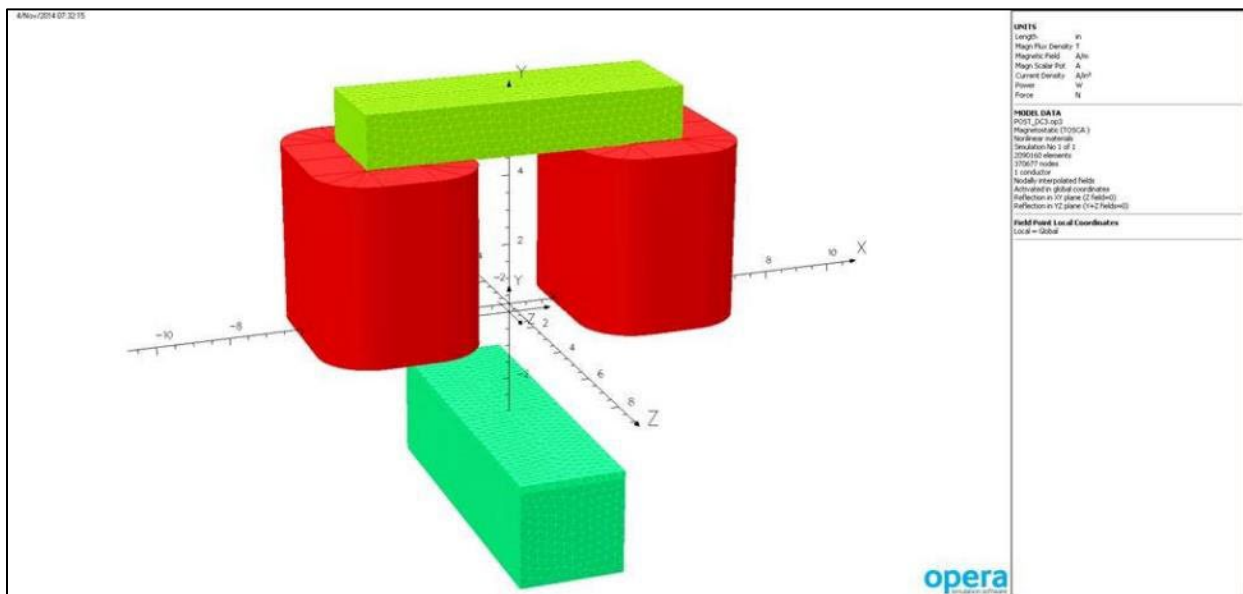


Figure B2. Simulation of Tx Electromagnetic Coils

However, the most critical measure of the magnet would be the field's flux over an area. Therefore, if it can be assumed that the rail is 3 inches x 3 inches x 20 inches, the integral of the flux over that area @80A is 6,800G-in². This would be an average flux of 113 G in the rail. The average flux is used to calculate the expected induced electromotive force (emf).

Appendix C. Rx Coil Specifications

The Rx coil used for testing was an Alstom Automatic Train Protection (ATP) Rx coil (Figure C1) with the specifications listed below. The receiver has two coils, the larger of which is predominantly used for testing shown in Figure C2.

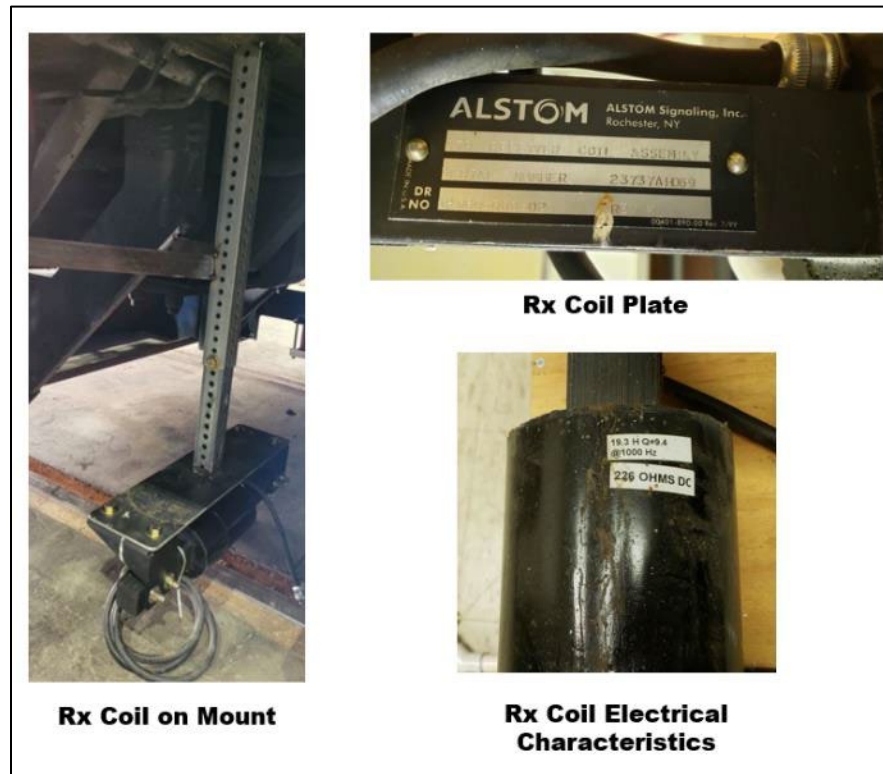


Figure C1. Rx Coil Assembly

Specifications

Electrical Specifications of Large Coil

- Resistance = 226 Ohms (DC)
- Inductance = 19.3 Henries
- Q = 9.4 at 1,000 Hz
- Serial number: 23727AH069

Dimensions

- Length of Rx coil: 24 Inches
- Large coil: 11 inches
- Small coil: 4 inches
- Diameter(s) of coil(s): 6 inches

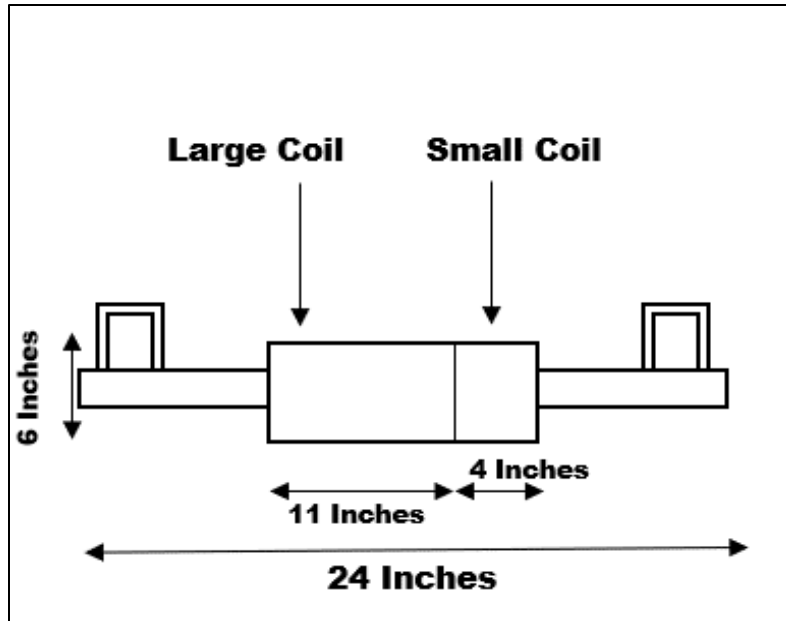


Figure C2. Illustration of Rx Coil Dimensions

Theory of Operation

The ATP Rx coil is mounted on the locomotive between 3 and 8 inches above the rail. The receiver detects an AC signal that is transmitted through the rail. Upon detection, the coil converts the detected signal to an AC voltage.

Appendix D. Supplementary Tx Coil Test Data

Coil Location	Distance to Center of Rail Head	Circuit Configuration	Frequency (Hz)	V Amp A	V Amp B	HV A (V)	HV B (V)	HVCA (A)	HVCB (A)	V Beta (mV)	Current Beta (mA)	Current Omega (mA)
Table	3.75"	Open	355	20.22	20.22	62.2	62.4	5.85	5.89	8.5	10.47	N/A
			365	20.3	20.3	167.8	167.8	15.37	15.38	22.3	27.53	N/A
			370	20.21	20.21	267.5	269.2	20.52	20.55	38.4	44.6	N/A
			380	20.2	20.2	393.2	393.5	39.92	39.9	54.3	63.65	N/A
			386	20.2	20.2	68.2	68.4	5.93	5.92	9.8	11.35	N/A
			560	20.8	20.8	227.2	228.5	23.38	23.38	42.4	50.95	N/A
			569	20.8	20.8	391	394	22.8	22.8	75.3	81.94	N/A
			673	20.8	20.8	474.9	478.5	27.48	27.58	93.7	114.8	N/A
			582	20.5	20.5	278.5	280.5	15.78	15.8	53.9	62.8	N/A
			595	20.6	20.6	160.4	161.2	7.75	7.75	27.8	31.52	N/A
			685	21	21.9	103.8	103.5	5.06	4.85	23.3	15.73	N/A
			698	21	21	237.2	237.2	12.2	12.3	57.4	63.3	N/A
			703	20.9	21	316.8	317.1	15.03	14.48	71.3	47.33	N/A
			712	20.8	20.9	190.9	190.9	9.1	8.58	43.4	38.38	N/A
			720	20.9	20.8	122.1	121.8	5.75	5.43	28.3	18.3	N/A
			1890	21.4	21.4	141.9	141.1	7.72	7.72	50.1	35.97	N/A
			1900	21.4	21.4	298.3	298	9.9	9.9	72.8	51.85	N/A
			1417	21.3	21.3	345.3	345.4	8.41	6.47	121.7	40.86	N/A
			1430	21.3	21.3	244.8	244.6	4.48	4.52	87.3	29.02	N/A
			1450	21.2	21.2	132	132.6	2.47	2.4	48.5	15.9	N/A
			355	20.2	20.2	63.4	63.6	5.97	5.99	9.9	11.18	2.8
			365	20.2	20.2	172.3	173.2	15.85	15.85	27.8	6.89	10.15
			370	20.2	20.2	268.5	270.4	24.43	24.42	37.8	45.93	3.75
			380	20.2	20.2	393.5	393.8	39.8	39.8	58.7	68.52	2.83
			386	20.6	20.6	67.9	67.2	5.81	5.8	10.2	11.88	6.89
			560	20.9	20.8	226.5	228.4	13.34	13.42	43.8	56.12	7.09
			568	20.9	20.9	393.8	397	22.97	23.02	89.2	63.7	12.54
			573	20.7	20.7	474.3	478.6	27.43	27.6	95.8	77.4	15.4
			682	20.5	20.5	278.4	280.4	15.8	15.8	62.8	49.52	8.72
			595	20.6	20.6	139.4	140.1	7.66	7.68	28.5	22.08	4.41
			685	20.92	21.04	103.8	103.7	5.11	4.87	23.7	15.74	3.91
			688	21	21	258	258.1	12.46	11.94	58.3	38.27	9.52
			703	21	20.94	316.8	316.8	14.44	14.4	71.2	47.02	11.67
			712	20.8	20.9	190.6	190.5	8.97	8.58	43.6	38.09	6.92
			720	20.9	20.8	122.2	121.9	5.68	5.4	28.5	18.11	4.46
			1890	21.4	21.4	138.5	138.3	7.74	7.67	52.2	36.47	3.01
			1418	21.4	21.4	205.3	205.2	4.02	3.91	71.4	24.18	4.17
			1417	21.3	21.3	345.3	345	8.58	6.45	128.3	39.3	6.84
			1430	21.2	21.2	239.8	239.8	4.53	4.43	85	28.14	4.82
			1450	21.24	21.24	132.9	132.5	2.47	2.4	47.7	15.63	2.74
			355	20.2	20.2	62	62.2	5.88	5.88	12	15.04	N/A
			365	20.3	20.3	167.9	168.5	15.02	14.98	20	25.02	N/A
			371	20.2	20.2	300	301.2	27.36	27.25	57.4	38.3	N/A
			380	20.2	20.2	398.5	398.7	39.3	39.5	20	33.89	N/A
			238	20.2	20.2	71	71.1	6.2	6.15	14	9.38	N/A
			560	20.8	20.8	272.7	275.4	9.8	10.12	41.6	28.8	N/A
			568	20.8	21	400	401.2	23.7	23.3	77.6	51.42	N/A
			574	20.8	20.8	518.7	520	30.65	30.65	104.2	68.4	N/A
			582	20.4	20.5	368.4	369.8	17.55	17.52	60.4	39.43	N/A
			606	20.6	20.6	145.8	145.4	8.13	8.08	33.2	18.73	N/A
			685	21	21	107.4	107.4	5.21	5.04	21.7	13.82	N/A
			693	21	21	279.8	279.8	13.26	12.83	55.8	35.42	N/A
			704	21	21	166.6	166.5	17.27	16.7	73.7	46.54	N/A
			712	21	21	205.4	205.4	9.8	9.3	41.8	25.13	N/A
			720	21	21	124.7	124.2	5.72	5.52	28.8	16.03	N/A
			1890	21	21	143.9	143.4	2.89	2.75	44.5	15	N/A
			1400	21.4	21.4	211.8	211.2	4.21	4.05	65.9	22.08	N/A
			1418	21.3	21.3	423.8	423.8	8.07	7.78	127.8	42.32	N/A
			1430	21.2	21.2	234.4	233.6	5.26	5.09	58	28.22	N/A
			1450	21.2	21.2	134.8	134.3	2.53	2.44	43.2	13.97	N/A
			355	20.2	20.2	61.4	61.6	5.84	5.51	12.8	8.28	1.86
			365	20.3	20.3	162	163.8	14.89	14.82	12.6	21.22	4.78
			371	20.2	20.2	298.8	300.9	27.36	27.26	60.5	39.72	8.85
			380	20.1	20.1	268.8	269.1	9.63	9.59	21.9	14.46	3.21
			386	20.3	20.2	71.1	71.2	6.2	6.18	14.6	9.54	2.12
			560	20.8	20.9	223.8	224.4	13.2	13.15	43.8	29.54	5.59
			568	20.9	21	401.6	402.3	15.13	15.11	10	15.89	10.09
			574	20.7	20.7	518.5	519.5	30.8	30.65	108.3	70.1	13.53
			582	20.6	20.5	283.7	284.8	16.15	16.08	56.9	37.07	7.6
			595	20.6	20.5	146	146.4	8.24	8.07	29.9	19.17	3.59
			684	21	21	105.1	105.7	5.11	4.93	21.6	13.8	2.83
			688	21	21	278.2	277.5	13.2	12.9	56.4	36.85	7.51
			704	21	21	166.8	166.5	17.25	16.7	74.6	47.15	9.8
			712	21	21	205.4	204.8	9.52	9.22	42.3	26.42	5.43
			720	21	21	124.8	124.2	5.72	5.52	28.2	16.2	3.84
			1890	21.4	21.4	142.7	142.2	3.84	3.78	43.7	14.73	2.46
			1400	21.4	21.4	212.6	212.5	4.2	4.07	64.8	21.72	3.65
			1418	21.3	21.3	413.2	413.8	7.99	7.77	125.2	41.37	6.85
			1430	21.2	21.2	233.2	232.5	5.22	5.07	83.8	27.45	4.48
			1450	21.2	21.2	134.7	134.3	2.43	2.42	43.6	15.22	2.51
			355	20.2	20.2	43	42.8	4.24	4.18	9.5	6.06	N/A
			365	20.2	20.3	77.2	76.9	7.33	7.3	16.8	10.74	N/A
			377	20.2	20.2	191.7	192.8	17.76	17.65	41.2	26.13	N/A
			380	20.2	20.2	170.8	170.3	15.7	15.49	17	28.86	N/A
			386	20.2	20.2	304.5	304	9.48	9.35	22.8	14.35	N/A
			560	20.7	20.7	121.7	121.4	7.45	7.41	21.6	16.04	N/A
			568	20.7	20.9	181.6	184.4	12.27	11.2	18.2	24.41	N/A
			684	20.7	20.7	174.6	172.2	22.02	21.8	68.2	47.85	N/A
			592	20.5	20.5	276.2	275.3	16.01	15.87	48.9	34.85	N/A
			605	20.5	20.6	146.7	146.3	8.28	8.23	28.5	18.44	N/A
			685	20.9	20.9	58.1	57.8	2.9	2.84	15.1	7.55	N/A
			698	21	21	95.1	94.5	4.84	4.53	21.4	12.23	N/A
			719	20.9	21	232.2	230	11.02	10.74	59.3	29.24	N/A
			725	20.8	20.6	185.4	184.4	8.7	8.48	47.6	23.86	N/A
			719	20.9	20.9	134.8	134.2	5.32	5.18	10	14.58	N/A
			1890	21.3	21.3	67.6	67.2	4.12	3.88	13.3	7.13	N/A
			1400	21.3	21.3	80.8	80.4	1.68	1.63	37.9	5.51	N/A
			1448	21.3	21.3	272.6	271.3	5.38	5.23	93.6	27.74	N/A
			1480	21.2	21.2	223.8	222.6	4.86	4.23	77.4	22.79	N/A
			1480	21.2	21.2	138.9	138.8	2.5	2.47	45.7	13.55	N/A
355	20.2	20.2	43.3	43.2	4.28	4.22	10.1	6.97	2.76			
365	20.2	20.3	78.3	78.1	7.49	7.41	17.8	11.33	4.89			
377	20.2	20.2	190.7	189.4	17.68	17.45	42.8	12.09	10.75			
380	20.2	20.2	189.4	188.6	15.58	15.37	18.1	20.02	10.75			
386	20.2	20.2	304.2	303.8	9.43	9.3	23.6	14.82	6.42			
560	20.8	20.7	133.2	132.7	7.6	7.51	19.9	13.96	3.03			
568	20.7	20.9	180	179.3	10.95	10.8	29	20.37	7.13			
584	20.7	20.8	194.5	192.5	23.85	23.01	64.3	41.25	15.46			
682	20.5	20.6	28.8	28.9	16.4	16.4	16.8	11.27	11.27			
605	20.5	20.6	148.5	147.5	8.6	8.33	24.9	16.63	3.84			
685	21	21	58.6	58.2	2.92	2.86	15.4	7.76	2.7			
688	20.9	21	96.7	96.2	4.88	4.67	15	12.53	4.33			
719	20.9	21	213.6	210.1	10.96	10.69	59.9	25.61	10.16			
725	20.9	20.88	184.4	183.2	8.66	8.43	47.9	23.52	8.27			
735	20.9	20.9	134.6	133.9	5.3	5.16	30.2	14.72	4.99			
1890	21.3	21.3	87.4	87.1	1.42	1.37	22.6	6.87	2.08			
1400	21.3	21.3	81.1	80.9	2.69	1.64	27.2	2.24	24.9			
1448	21.3	21.3	272.4	271.2	5.97	5.23	90.9	36.87	7.78			
1460	21.2	21.2	233.2	231.8	4.35	4.23	75	22.01	6.21			
1480	21.2	21.2	130.4	129.8	2.5	2.43	44.6	13.94	3.62			
355	20.2	20.2	42.8	42.87	4.21	4.18	9	5.24	N/A			
365	20.2	20.3	78.6	78.5	7.83	7.68	8.7	9.3	N/A			

Figure D1. Tx Coil Measurements 1

Coil Location	Distance to Center of Rail Head	Circuit Configuration	Frequency (Hz)	V Amp A	V Amp B	HV A (V)	HV B (V)	HVCA (A)	HVCB (A)	V Beta (mV)	Current Beta (mA)	Current Omega (mA)
Aluminum Stand	4.5"	Open	378	20.2	20.2	206.9	206.4	19.1	18.9	23.2	24.53	N/A
			380	20.2	20.2	188.9	188.4	17.38	17.22	21.3	22.43	N/A
			386	20.2	20.2	110.3	110.2	9.99	9.87	12.8	13.23	N/A
			560	20.7	20.7	122.7	122.8	7.56	7.51	18.4	13.42	N/A
			568	20.9	20.9	178.7	178.4	11.2	10.86	10.72	19.28	N/A
			585	20.6	20.7	406.4	406.1	24.14	23.84	60.7	43.29	N/A
			592	20.5	20.5	297.8	297.2	17.36	17.15	44.6	31.47	N/A
			605	20.5	20.7	150.6	150.3	8.58	8.49	23.3	16.05	N/A
			685	20.9	20.9	99.3	99.1	2.95	2.89	10.5	6.45	N/A
			698	21	20.9	97.1	96.5	4.73	4.64	17.2	10.47	N/A
			719	20.9	21.01	260.2	259.8	12.33	12.06	45.9	27.55	N/A
			725	20.8	20.9	204.2	203.2	9.59	9.37	36.4	21.68	N/A
			735	20.9	20.9	119.2	118.6	5.52	5.38	21.7	12.75	N/A
			1390	21.3	21.3	89.6	89.4	1.52	1.41	18.8	6.13	N/A
			1400	21.3	21.3	84.3	84.1	1.83	1.69	22.8	7.4	N/A
		1449	21.3	21.3	311.8	310.8	6.45	5.95	84.3	26.57	N/A	
		1460	21.2	21.2	238.2	237.7	4.88	4.49	65	20.33	N/A	
		1480	21.3	21.3	129	128.6	2.59	2.38	35.8	11.01	N/A	
		355	20.2	20.2	42.9	42.8	4.22	4.19	5.7	6.02	2.47	
		365	20.2	20.2	77.1	77	7.38	7.32	9.9	10.65	4.49	
		378	20.2	20.23	206.1	205.2	19.02	18.85	26	27.6	11.64	
		380	20.2	20.2	188.3	187.9	17.34	17.15	23.8	25.23	10.53	
		386	20.2	20.2	110.2	109.8	9.98	9.87	14.3	14.89	6.2	
		560	20.7	20.78	123.8	123.8	7.64	7.57	19.5	14.36	5.9	
		568	20.7	20.9	181.7	181.8	11.09	10.95	28.5	20.84	8.61	
		585	20.6	20.6	403.7	403.4	23.94	23.66	63.7	45.57	18.56	
		592	20.57	20.52	295.7	295.5	17.23	17.06	46.6	33.01	13.11	
		605	20.5	20.7	150.2	150.2	8.56	8.47	24.3	16.87	6.73	
		685	20.9	20.9	98.4	98.1	2.91	2.85	10.6	6.53	2.16	
		698	21	20.9	95.3	94.8	4.66	4.56	17.2	10.53	3.68	
719	20.9	21	260.7	259.3	12.34	12.07	46.4	27.95	9.74			
725	20.8	20.9	205.2	204.3	9.68	9.42	36.9	22.07	7.91			
735	20.9	20.9	119.4	119	5.53	5.41	21.9	12.94	4.64			
1390	21.3	21.3	70.6	70.3	1.54	1.43	18.2	5.91	1.73			
1400	21.3	21.3	85.5	85.3	1.85	1.72	21.8	7.13	2.1			
1449	21.3	21.3	310.6	309.8	6.42	5.93	79.9	25.14	7.22			
1460	21.2	21.2	236.7	235.8	4.84	4.45	61.2	19.13	5.39			
1480	21.2	21.2	128.7	128.2	2.59	2.37	33.8	10.43	2.92			
685	20.9	21	60.9	60.3	3.02	2.95	6.8	3.99	N/A			
698	20.9	20.9	101.2	100.4	4.94	4.82	11	6.62	N/A			
718	20.9	21	297.2	293.4	14.08	13.72	32.4	19.32	N/A			
725	20.8	20.9	213.2	211.2	10	9.72	23.5	13.84	N/A			
735	20.9	20.9	117.2	115.1	5.4	5.25	13.1	7.58	N/A			
685	20.9	20.9	61.23	60.7	3.04	2.97	6.9	4.14	1.56			
698	20.9	20.9	102.3	101.5	4.99	4.86	11.4	6.88	2.6			
718	21	21	296.3	294.7	14.06	13.78	33	19.73	7.41			
725	20.8	20.8	212.6	210.5	9.95	9.68	23.8	14.07	5.21			
735	20.9	20.9	117.2	116	5.4	5.25	13.2	7.72	2.85			
355	20.2	20.2	77.6	79.5	7.25	7.3	14.6	16.62	N/A			
365	20.2	20.2	146.6	150.6	13.26	13.4	28.7	32.33	N/A			
370	20.15	20.19	123.2	126.9	11.01	11.16	24.1	26.92	N/A			
380	20.19	20.24	67.7	69.5	5.92	5.96	13.4	14.55	N/A			
386	20.26	20.2	52.8	54	4.55	4.58	10.7	11.38	N/A			
355	20.22	20.22	81.3	83.4	7.56	7.65	16.2	18.53	4.67			
365	20.19	20.24	147.1	151.6	13.33	13.51	30.5	34.4	8.67			
370	20.14	20.19	121.7	125.4	10.87	11.01	25.1	28.03	7.02			
380	20.2	20.24	67.4	69.1	5.88	5.93	14.1	15.24	3.82			
386	20.25	20.3	52.7	53.9	4.55	4.57	11.3	11.96	3			

Figure D2. Tx Coil Test Measurements 2

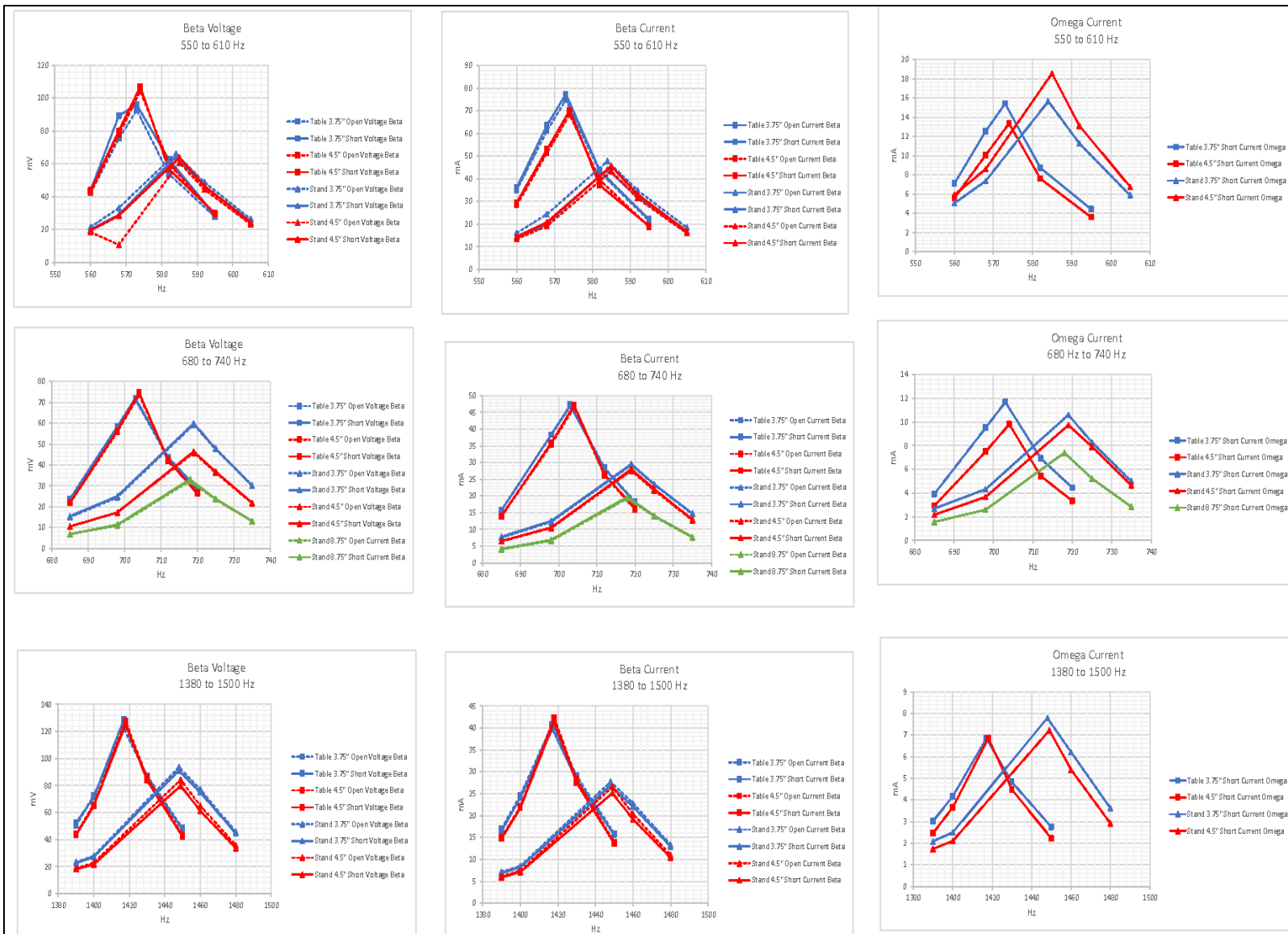


Figure D3. Graphs of Tx Coil Measurements

Appendix E. Insulated Joints Measurements

Tables E1 through E2 include the insulated joint (IJ) measurements on the Transit Test Track (TTT) test areas prior to field testing.

Table E1. TTT IJ Measurements from September 2020

Location	Test Type	Rail	Voltage	Amps	Ohms
T27.5	AC	Inside	7.46	0.022	339.0909091
T27.5	AC	Outside	7.46	0.029	257.2413793
T29.5	AC	Inside	7.58	0.01	758
T29.5	AC	Outside	7.58	0.004	1,895
T33.5	AC	Inside	7.14	0.09	79.33333333
T33.5	SMU/DC	Inside	7.6	0.085	89.41176471
T33.5	AC	Outside	7.49	0.023	325.6521739
T33.5	SMU/DC	Outside	7.6	0.019	400
T39.5	AC	Inside	7.56	0.009	840
T39.5	SMU/DC	Inside	7.6	0.005	1,520
T39.5	AC	Outside	7.6	0.005	1,520
T39.5	SMU/DC	Outside	7.6	0.00003	253333.3333
T45	AC	Inside	7.58	0.06	126.3333333
T45	SMU/DC	Inside	7.6	0.004	1,900
T45	AC	Outside	7.56	0.005	1,512
T45	SMU/DC	Outside	7.6	0.002	3,800
T51	AC	Inside	7.57	0.009	841.1111111
T51	SMU/DC	Inside	7.57	0.001	7,570
T51	AC	Outside	7.59	0.008	948.75
T51	SMU/DC	Outside	7.59	0.0019	3994.736842

Table E2. TTT IJ Measurements from September 2021

Location	Test Type	Rail	Voltage	Amps	Ohms
T33.5	AC	Inside	6.87	0.077	89.2207792
T33.5	DC	Inside	7.08	0	∞
T33.5	AC	Outside	6.14	0.175	35.0857143
T33.5	DC	Outside	7.25	0.003	2416.66667
T39.5	AC	Inside	7.12	0.031	229.677419
T39.5	DC	Inside	6.87	0.003	2290
T39.5	AC	Outside	7.26	0	∞
T39.5	DC	Outside	6.14	0	∞

Precision Test Track (PTT) Track Impedance Measurements

Measurements with the negative probe on A and positive probe on B are labeled AB, while measurements labeled BA have the negative probe on the south side and the positive probe on the north, shown in [Table E3](#). All measurements were made using a Fluke multimeter. All pictures were taken for the joint bars and insulated joints as is. Ballast/sand was removed from underneath the joint prior to measurements being taken.

Table E3. PTT IJ and Bond Wire Measurements from April 2021

Location	Measurements		
IJW1	AB 714K Ω	BA -714K Ω	
IJ1E	AB 138.5 Ω	BA 308.4 Ω	
IJE1 TO IJW1	AD 594K Ω	B+C- 407 Ω	B-C+ 216 Ω
IJW2	AB -1.3M Ω	BA 1.3M Ω	
JBE1	AB 1.8 Ω	BA 2 Ω	
JBW1	AB .8 Ω	BA 1.2 Ω	
JBW2	AB .3 Ω	BA .4 Ω	
IJE2	AB -2.159M Ω	BA 2.159M Ω	
JBE2	AB 1.2 Ω	BA 1.2 Ω	
JBE3	AB 1.4 Ω	BA.6 Ω	
JBW3	AB.9 Ω	BA .9 Ω	
IJE3 TO IJW3	AD1.3M Ω	BC2.1M Ω	
IJE3	AB -.828M Ω	BA .828M Ω	
IJw3	AB -2.748M Ω	BA 2.752M Ω	
IJW4	AB.6 Ω	BA1.3 Ω	
JBW5	AB 1	BA .7	
JBW4	AB 1.3 Ω	BA 1.3 Ω	
IJW5	AB .9 Ω	BA.7 Ω	
JBW7	AB .7 Ω	BA .7 Ω	
IJE4	AB 405 Ω	BA 368 Ω	
IJW6	AB 1.376M Ω	BA 1.376M Ω	
IJE4 TO IJW6	AD 1.36M Ω	BC 263 Ω	
JBW6	AB .6 Ω	BA .6 Ω	

Appendix F. Measurement Equipment

The following recording and measurement tools were used in the course of this research:

- Multimeters
 - Fluke® 87/89 with true RMS AC voltmeter with an input impedance greater than 100 K Ohms
 - BT Clamp Meters BT Meter BT-570C
- 5100 Series Meggit® Gauss METERS
- B&K precision 891 LCR Meter
- Oscilloscopes
 - SIGLENT SDS1000X-E®
 - Compocket Minis® Portable Oscilloscope
- Rogowski Loop
- Garmin® GPS Receiver
- Data Collection Computers
- National Instruments® Data Acquisition System (DAQ)
- DEWEsoft® software
- Portable Cab Signal Tester
- Raspberry Pi® Single board computer
- Arduino® Microcontroller

Appendix G. Characteristic Impedance Calculations from Sample Track Impedance Data

According to the Transmission Line Model equations in [Section 2.4](#), the characteristic impedance can be measured using two ways. One way is to use the Resistance, Inductance, Capacitance and Conductance (RLCG) variables to calculate the characteristic impedance and propagation constant. Another way is to use the closed and open loop circuit impedance magnitude and phase angle as shown by Equation (7). In this section, an example for calculating the characteristic impedance and propagation constant is shown as well as the input impedance at a given track length.

Table G1 shows a sample of measurement values for the impedance variables used to calculate the corresponding characteristic impedance, propagation constant, and the input impedance with a shunt at a distance of 198 meters. [Tables G1](#) and [G2](#) show the results of the characteristic and input impedances using the following two methods, respectively:

- The first method uses RLCG variables.
- The second method uses open and closed loop impedance measurements.

Table G1. Sample of Measurements for Track Impedance Variables at 20 Hz

Frequency (Hz)	R (ohm)	L (H)	C (F)	G (S)	CL-Z (ohm)	CL-Z Phase (deg)	OL-Z (ohm)	OL-Z Phase (deg)
20.3	2.31E-01	-9.50E-03	-8.99E-06	2.99E-03	1.23	-78.9	308	20.9

Method 1

1. Applying the characteristic impedance [Equation \(4\)](#) from [Section 2.4](#) to RLCG measurements at the measured frequency to obtain the circuit characteristic impedance
2. Using the RLCG measurements at the measured frequency as inputs, the propagation constant is calculated by applying the propagation constant from [Equation \(6\)](#) from [Section 2.4](#).
3. The propagation constant is normalized to per meter unit by dividing the results from step 2 by the unit measurement distance in meters (198 meters/~650 feet).
4. Using the obtained characteristic impedances as propagation constants and applying the input impedance [Equation \(5\)](#) from [Section 2.4](#), the input impedance with the load (shunting axle of 0.06 ohm) is calculated at a specific distance (e.g., 190 meters) from the source. The sample data results for each frequency data are tabulated in [Table G1](#).

The calculations show that the estimated impedance seen from a source that includes track impedance and train shunt has a magnitude of 1.24 ohms. Comparing this value to the impedance measured with a short circuit condition (closed loop impedance) shows credibility in the results where the closed loop impedance has a magnitude of 1.23 ohms, a magnitude that is slightly lower than when the circuit has a shunt.

**Table G2. Characteristic and Input Impedance Calculations for
RLCG Sample Measurements**

Frequency (Hz)	R (Ω)	L (H)	C (F)	G (S)	$ Z_0 $ (Ω)	Z_0 Phase (degrees)	Z_{in} (198) (Ω)	Z_{in} (198) Phase (degrees)	CL_Z (Ω)	CL_Z Phase (degrees)
20.3	0.21	-0.01029	-1E-05	0.0033	19.47	-29.8	1.34	-78.2	1.25	-80.3
23.7	0.21	-0.00868	-8E-06	0.0033	19.31	-30.0	1.32	-78.0	1.25	-79.9
27.6	0.21	-0.00750	-7E-06	0.0033	19.40	-30.1	1.33	-78.1	1.24	-80.4
32.2	0.21	-0.00608	-6E-06	0.0033	18.88	-29.9	1.26	-77.6	1.24	-79.9
37.5	0.21	-0.00526	-6E-06	0.0033	18.76	-28.6	1.27	-77.8	1.24	-79.7
43.8	0.21	-0.00426	-6E-06	0.0033	18.01	-26.5	1.20	-76.7	1.24	-79.5
51.0	0.22	-0.00392	-6E-06	0.0033	18.36	-25.2	1.29	-77.5	1.23	-79.7
59.5	0.24	-0.00373	-5E-06	0.0033	19.42	-25.5	1.43	-77.7	1.23	-79.3
69.3	0.18	-0.00308	-5E-06	0.0033	18.67	-25.0	1.36	-79.9	1.22	-78.5
80.9	0.22	-0.00239	-5E-06	0.0033	17.42	-21.5	1.25	-76.8	1.22	-79.4
94.3	0.23	-0.00220	-5E-06	0.0033	17.46	-19.7	1.33	-77.5	1.23	-79.3
109.9	0.24	-0.00185	-5E-06	0.0033	16.73	-17.1	1.32	-76.7	1.24	-79.2
128.1	0.24	-0.00165	-5E-06	0.0033	16.37	-15.2	1.37	-77.3	1.26	-79.0
149.4	0.24	-0.00150	-5E-06	0.0033	16.17	-13.6	1.44	-77.7	1.27	-78.6
174.2	0.26	-0.00128	-5E-06	0.0033	15.51	-11.6	1.44	-77.2	1.28	-78.5
203.1	0.26	-0.00109	-4E-06	0.0033	15.00	-10.6	1.43	-77.1	1.32	-78.7
236.8	0.26	-0.00090	-1E-06	0.0033	19.12	-25.2	1.38	-76.4	1.32	-78.5
276.1	0.27	-0.00081	-1E-06	0.0031	19.70	-23.8	1.44	-76.7	1.33	-78.3
321.9	0.27	-0.00067	-9E-07	0.0030	19.83	-23.5	1.39	-76.1	1.34	-78.2
375.3	0.28	-0.00059	-8E-07	0.0029	20.22	-22.9	1.44	-76.3	1.34	-77.9
437.6	0.29	-0.00054	-7E-07	0.0028	21.12	-22.5	1.54	-76.6	1.52	-78.5
510.1	0.30	-0.00048	-7E-07	0.0027	21.29	-20.3	1.59	-76.8	1.53	-78.5
594.8	0.30	-0.00043	-6E-07	0.0025	22.54	-20.0	1.66	-77.3	1.58	-78.5
693.5	0.31	-0.00038	-4E-07	0.0024	23.30	-20.5	1.69	-77.1	1.65	-75.8
808.5	0.33	-0.00031	-3E-07	0.0023	23.83	-20.4	1.64	-76.2	1.85	-67.9
942.7	0.33	-0.00024	-3E-07	0.0022	23.26	-20.3	1.46	-74.3	2.00	-54.9
1,099.1	0.36	-0.00015	-2E-07	0.0021	21.04	-18.4	1.13	-68.3	2.17	-36.8
1,281.4	0.37	-0.00006	-2E-07	0.0020	15.74	-9.0	0.63	-47.4	2.41	-13.5
1,494.0	0.38	0.00005	-1E-07	0.0019	15.84	42.1	0.63	45.6	2.70	14.9
1,741.9	0.40	0.00016	-1E-07	0.0018	27.98	58.3	1.84	75.6	3.06	48.5

The calculations for the second method of figuring the characteristic impedance using closed and open loop values are shown below.

Method 2

1. Applying the characteristic impedance [Equation \(7\)](#) from [Section 2.4](#) to open loop (OL-Z) and closed loop (CL-Z) measurements at the measured frequency to obtain the circuit characteristic impedance.
2. The propagation constant at different measurements is derived using the open loop (OL-Z) and closed loop (CL-Z) measurements at the measured frequency as inputs for the propagation constant [Equation \(8\)](#).
3. The propagation constant is normalized to per meter unit by dividing the results from step 2 above by the unit measurement distance in meters (198 meters/~650 feet).
4. Using the obtained characteristic impedance propagation constants and applying the input impedance [Equation \(5\)](#) from [Section 2.4](#), the input impedance is calculated with the load (shunting axle of 0.06 ohm) at a specific distance (e.g., 190 meters) from the source. The results for each frequency from the sample data are tabulated in [Table G3](#).

Table G3. Characteristic and Input Impedance Calculations for Closed and Open Loop Impedance Sample Measurements

Frequency (Hz)	R (Ω)	L (H)	C (F)	G (S)	Z ₀ (Ω)	Z ₀ Phase (degrees)	Z _{in} (198) (Ω)	Z _{in} (198) Phase (degrees)
20.3	1.25	-80.3	280.0	20.0	18.68	-30.1	1.26	-77.6
23.7	1.25	-79.9	280.9	19.8	18.71	-30.1	1.26	-77.2
27.6	1.24	-80.4	279.0	19.8	18.64	-30.3	1.26	-77.7
32.2	1.24	-79.9	276.4	19.7	18.53	-30.1	1.25	-77.2
37.5	1.24	-79.7	276.4	19.5	18.52	-30.1	1.25	-77.0
43.8	1.24	-79.5	276.8	19.5	18.51	-30.0	1.25	-76.8
51.0	1.23	-79.7	276.8	19.6	18.48	-30.1	1.25	-77.0
59.5	1.23	-79.3	276.9	19.8	18.46	-29.8	1.24	-76.5
69.3	1.22	-78.5	277.0	19.7	18.40	-29.4	1.24	-75.8
80.9	1.22	-79.4	277.1	19.6	18.39	-29.9	1.23	-76.6
94.3	1.23	-79.3	277.3	19.6	18.43	-29.9	1.24	-76.6
109.9	1.24	-79.2	277.6	19.6	18.56	-29.8	1.25	-76.5
128.1	1.26	-79.0	277.9	19.6	18.68	-29.7	1.27	-76.3
149.4	1.27	-78.6	278.2	19.8	18.77	-29.4	1.28	-76.0
174.2	1.28	-78.5	278.6	21.3	18.86	-28.6	1.29	-75.9
203.1	1.32	-78.7	278.7	21.4	19.16	-28.7	1.33	-76.2
236.8	1.32	-78.5	274.9	25.4	19.02	-26.5	1.33	-76.0
276.1	1.33	-78.3	273.6	30.7	19.05	-23.8	1.34	-75.8
321.9	1.34	-78.2	284.4	29.7	19.53	-24.2	1.36	-75.7
375.3	1.34	-77.9	285.5	32.5	19.56	-22.7	1.35	-75.4
437.6	1.52	-78.5	289.4	33.7	20.95	-22.4	1.53	-76.3

Frequency (Hz)	R (Ω)	L (H)	C (F)	G (S)	$ Z_0 $ (Ω)	Z_0 Phase (degrees)	Z_{in} (198) (Ω)	Z_{in} (198) Phase (degrees)
510.1	1.53	-78.5	283.9	36.9	20.86	-20.8	1.55	-76.3
594.8	1.58	-78.5	303.3	38.4	21.88	-20.1	1.59	-76.4
693.5	1.65	-75.8	313.8	39.7	22.75	-18.0	1.66	-73.8
808.5	1.85	-67.9	329.7	40.0	24.72	-14.0	1.88	-66.2
942.7	2.00	-54.9	324.4	40.7	25.44	-7.1	2.03	-53.5
1,099.1	2.17	-36.8	338.5	42.1	27.10	2.7	2.22	-35.8
1,281.4	2.41	-13.5	343.8	44.4	28.76	15.5	2.46	-13.2
1,494.0	2.70	14.9	361.8	47.5	31.26	31.2	2.76	14.6
1,741.9	3.06	48.5	366.6	51.3	33.48	49.9	3.10	47.7

The input impedance results in [Table G3](#), where the characteristic impedance calculations were based on the second method (i.e., using the closed and open loop impedance measurements), show good estimation of the impedance seen by the source that includes track and train shunt impedances. How the estimation closely matches the closed loop impedance can be observed by comparing the input impedance magnitude measurements with the closed loop impedance magnitude measurements. However, the comparison of the input impedance results between [Tables G2](#) and [G3](#) show mismatches at some frequencies. These mismatches can be seen in [Figure G1](#) where the percentage difference between the results of the two methods for calculating the characteristic impedance (Z_0), propagation constant (Γ), and input impedance (Z_{in}) at a distance of 198 meters are shown above. The percentage difference curve in each graph indicates the average percentage difference at each frequency while the wider curves show the standard deviation of the average percentage difference. The results of checking the real and imaginary components of the closed loop impedance measurements and comparing them to the corresponding resistance and inductance measurements showed that those values do not align at the frequency entries that mismatch with the input impedance calculations. These results give an indication that the input values for these entries have a margin of error either in the closed loop circuit measurement or the resistance and inductance measurements, while the general impedance trend and impedance are closely matched. It should be noted that component RLCG measurements are prone to parasitic interference that can cause some data points to vary between 4 percent at lower frequencies to up to 10 percent at higher frequencies when compared to the open loop/closed loop method (B&K Precision, 2020).

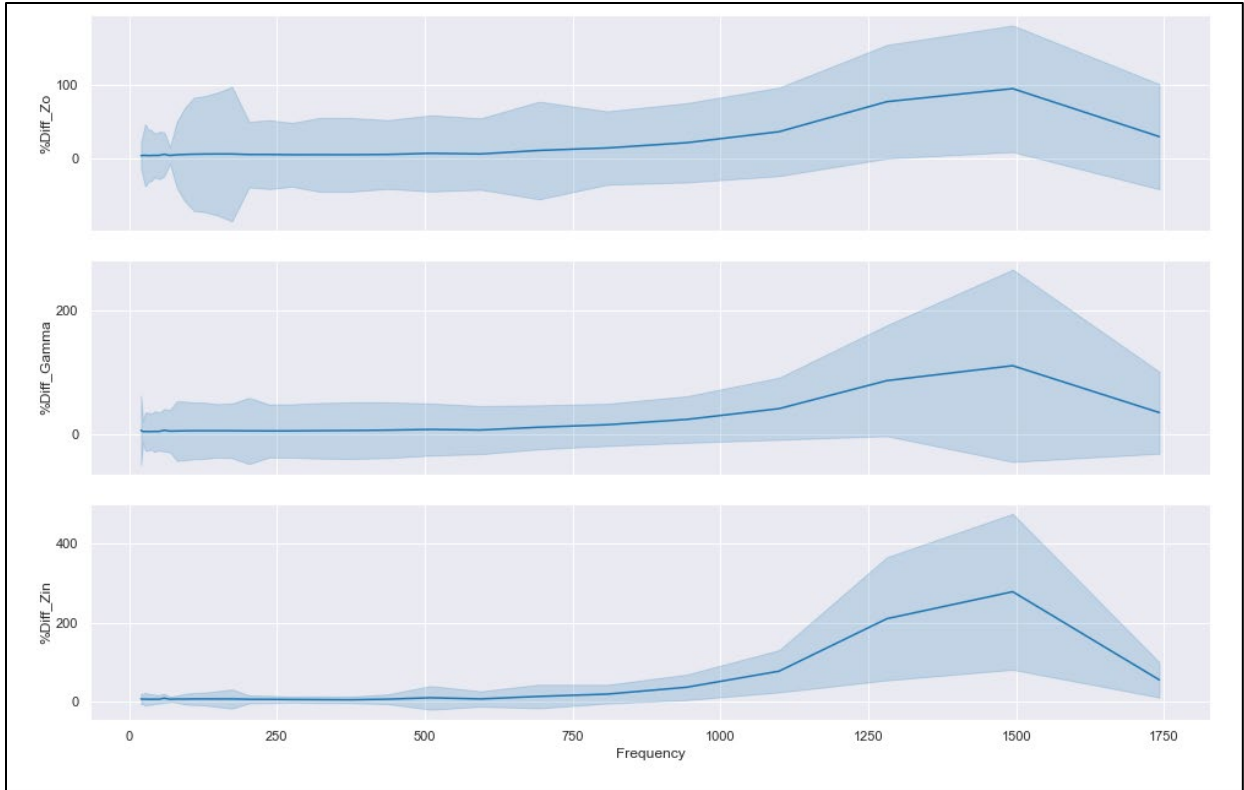


Figure G1. Percentage Difference and the Corresponding Standard Deviation Between the Results of the Two Methods of Calculating Zo, Gamma, and Zin with the Transmission Line Equations

Appendix H. Portable Cab Signal Tester

The portable cab signal tester (model number: D3005H15-A01) is a microprocessor-based test system designed to test cab signal equipment in railroad locomotives and cars. This tester generates signals to drive the on-board signal receivers and speed detection equipment to test for proper receiver operation. The main function of the portable cab signal tester is to generate CAB and SPEED signals as required to test the functionality and sensitivity of the on-board receiver equipment.



Figure H1. Image of Portable Cabs Signal Tester Utilized

System Components

- Portable cab signal tester
- 0.8 Ohm wire loop (housed in a PVC) pipe and connector
- DC Power Input Cable

Quick Instructions Guide

- Connect the power cable to the POWER input connector
- Connect the portable cab tester and turn the unit “ON”
- Connect the test loop to the “LOOP OUTPUT”
- Select the test frequency and adjust “LOOP CURRENT” to the desired setting

Abbreviations and Acronyms

ACRONYM	EXPLANATION
A GND	A Ground Terminal on RNB
ABRRD	Alternative Broken Rail and Rollout Detection
ABRD	Alternative Broken Rail Detection
AC	Alternating Current
AWG	American Wire Gauge
AAR	Association of American Railroads
ATP	Automatic Train Protection
B GND	B Ground Terminal on RNB
BT	Bluetooth
CBTC	Communications-Based Train Control
DAQ	Data Acquisition
DC	Direct Current
emf	Electromotive Force
EOT	End-of-Train
XML	Extensible Markup Language
FRA	Federal Railroad Administration
FMB	Full Moving Block
GPIO	General Purpose Input/Output
GPS	Global Positioning System
GND	Ground
HOT	Head-of-Train
LCR	Inductance (L), Capacitance (C), and Resistance (R)
IJ	Insulated Joint
OBRD	Onboard Broken Rail Detection
O-PTC	Overlay-Positive Train Control
PVC	Polyvinyl Chloride
PTC	Positive Train Control
PTT	Precision Test Track
QMB	Quasi Moving Block
RTT	Railroad Test Track

ACRONYM	EXPLANATION
Rx	Receiver Coil
R&D	Research and Development
RLCG	Resistance (R), Inductance (L), Capacitance (C), Conductance (G)
RNB	Resonant Network Box
RMS	Root Mean Square
SPICE	Simulation Program with Integrated Circuit Emphasis
SMU	Source Measure Unit
TRL	Technology Readiness Level
TIMS	Track Impedance Measurement System
TTT	Transit Test Track
Tx	Transmit (transmission) Coil
TTC	Transportation Technology Center
TTCI	Transportation Technology Center Inc.
UV	Ultraviolet
USPTO	United States Patent and Trademark Office
V	Volts